

# Self-assembly of porphyrin derivatives adsorbed on metal surfaces

## Abstract

*Two different porphyrin derivatives were studied by Scanning Tunnelling Microscopy (STM) in Ultra-High Vacuum (UHV) at room temperature. Both porphyrin derivative molecules self-assemble on the Cu(111) and Ag(111) surfaces respectively. The self-assembly of both molecules was investigated at different coverages mainly below a full monolayer.*

*Molecule 1 containing pentafluoro-groups formed a dominant porous network with hexagonal pores in addition to two other close packed assemblies upon deposition onto Ag(111). This porous network had an intriguing structure because the pentafluoro-groups came quite close together. The porous network remained with nearly no changes even if the sample was annealed up to 300°C. This demonstrated that this porous network was also very stable. Until present, there are no reports of porous networks formed by such highly fluorinated porphyrin derivatives. Sub-Phthalocyanine (SubPc) was deposited onto the formerly prepared porous network on Ag(111). The SubPc molecules were adsorbed into the pores of the network. If more SubPc molecules were added, a new type of close packed assembly formed. Upon deposition onto Cu(111) molecule 1 formed exclusively close packed assemblies. The prevailing assembly on Cu(111) was subject to Low Energy Electron Diffraction (LEED) experiments. This allowed us to determine the unit cell of this assembly with a very high precision.*

*Molecule 2 containing peripheral cyano-groups formed a porous network with triangular pores on Cu(111). It was dominant at a coverage below one monolayer. Subsequently, SubPc molecules were co-deposited onto the porous network. They coordinate to the pores but it remains unclear whether the molecules fit inside the pores. On Ag(111) a close packed assembly was formed.*

## SELF-ASSEMBLY OF PORPHYRIN DERIVATIVES ADSORBED ON METAL SURFACES

ABSTRACT.....	1
1. INTRODUCTION .....	3
2. MATERIALS & METHODS .....	7
2.1. Principles STM, LEED, UHV, molecule deposition .....	7
2.2. Specification UHV-System (Nanolab) .....	9
2.3. Preparation of the crystals (Sputtering/Annealing).....	10
2.4. Deposition of molecules.....	11
2.5. STM/LEED-Measurements .....	11
3. RESULTS .....	12
3.1. Porphyrin derivative 1.....	12
3.1.1. Molecule <b>1</b> on Ag(111).....	12
3.1.2. Hexagonal network of <b>1</b> with SubPc on Ag(111) .....	21
3.1.3. Molecule <b>1</b> on Cu(111).....	28
3.1.4. LEED Results for molecule <b>1</b> .....	33
3.2. Porphyrin derivative 2.....	36
3.2.1. Molecule <b>2</b> on Ag(111).....	36
3.2.2. Molecule <b>2</b> on Cu(111).....	38
3.2.3. Molecule <b>2</b> with SubPc on Cu(111).....	43
4. DISCUSSION .....	44
5. CONCLUSION.....	53
6. ACKNOWLEDGEMENTS.....	54
7. REFERENCES .....	54
APPENDIX .....	57

## 1. Introduction

The first STM which was built in 1981 by Gerd Binnig and Heinrich Rohrer [*refs. 1,2*] opened the door to the world at the nanometre scale. It was the first scanning probe technique which allowed the people to study surfaces directly in real space. It enabled to investigate surfaces locally as opposed to other averaging techniques like electron diffraction or spectroscopy. The local approach has several advantages: it is relatively easy to interpret and it allows e.g. to study the influence of defects on a surface, to name a few. Furthermore, also quantum effects can be studied in a more detailed way. In the beginning, the STM was mostly used to study metal surfaces and the effect of the deposition of metals and salts onto the metal surfaces. Later on, the effect of molecules on conducting surfaces came into focus. The self-assembly which can occur on these surfaces is also very interesting to be investigated with the STM. The assemblies on surfaces are also a bit easier to understand because they are only 2D compared to 3D assemblies that are much more complicated. Findings from the studies on surfaces can be useful in molecular electronics, quantum computing, surface chemistry, etc. Especially in surface chemistry there are new approaches which try to use also the geometrical properties of molecules to catalyze reactions. For instance, the practical sense of well defined reaction rooms is demonstrated by the high efficiency of the biological enzymes. In such environment, reactions which are impossible in free space can take place. Especially reactions with organic molecules result very often into a whole bunch of products and side products. By adapting the reaction room geometry to a specific reaction the main product fraction might be increased very much. But to design such adapted geometries it is very important to understand the different types of molecule-molecule and surface-molecule interactions. For example, the above mentioned porous networks are of particular interest for chemistry since the pores can bind molecules and reduce the number of degrees of freedom of the trapped molecules. Therefore if a reaction with the trapped molecule happens already a lot of binding sites are blocked by the porous network. So the trapped molecule could then react only with other molecules at the free binding sites and the porous network would act as a catalyst. Apart from the experimental side, there is further interplay with simulations and theory that try to quantify and categorize the different types of interactions. New predictions can be made and verified using different experimental techniques. Such methods can be Atomic Force Microscopy (AFM), photoemission techniques like XPS/UPS or Infrared Spectroscopy, electron diffraction techniques like LEED and especially STM which was mainly used for that project.

The usual approach is that new molecules are synthesized which are thought to have some desired properties with respect to their stability and their self-assembly. The molecules are then investigated by different methods. If the results are interesting and reproducible much more time is then invested to explore these molecules extensively. Such molecules can then become model systems like e.g. PTCDA which is a perylene.

In experiments on surfaces like STM two different types of interactions are very important for the self-assembly, namely molecule-molecule and substrate-molecule interactions. In some cases by changing the material or even by changing only the surface orientation e.g. from (111) to (110) the self-assemblies can vary a lot which means that the substrate-molecule interactions are dominating in these cases. By LEED measurements one can relate the molecular superstructure to the substrate. If the molecule-molecule interaction is very strong the self-assembly should be much less affected by changing the substrate. But the exact influence of these two types of interactions onto a distinct molecule is still not very well understood and this makes it hard to predict the influence of the substrate in advance.

Porphyryns are organic dyes which are also very important in biology where e.g. the chlorophyll and the heme-group of haemoglobin have a porphyrin complex in the centre

(figure 1). The porphyrin core itself is a conjugated  $\pi$ -system and therefore also of interest for nano-electronics. For self-assembly studies porphyrins are further interesting because they are chemically and thermally stable. Since it is also possible to vary the side-groups by chemical modifications they are one of the most common group of interest for research of the distinct effect of side-groups onto the self-assembly. Since the  $\pi$ -system interacts quite strongly with the surface [ref. 3] it is very often the case that the surface-molecule interactions dominate over molecule-molecule interactions. Different self-assemblies were found with porphyrins lying on the surface in a simple close packed assembly but also in more complicated formations like porous networks, standing up or chains at low temperatures [refs. 4,5]. In case of porous networks there have been done also some studies with  $C_{60}$  which fits into the pores and hops between the pores which means that one can see the diffusion of  $C_{60}$  on such assemblies [refs. 6-8]. Normally it is not possible to image diffusing particles because they are too fast but if that they can be trapped in a pore for some time they can be observed.

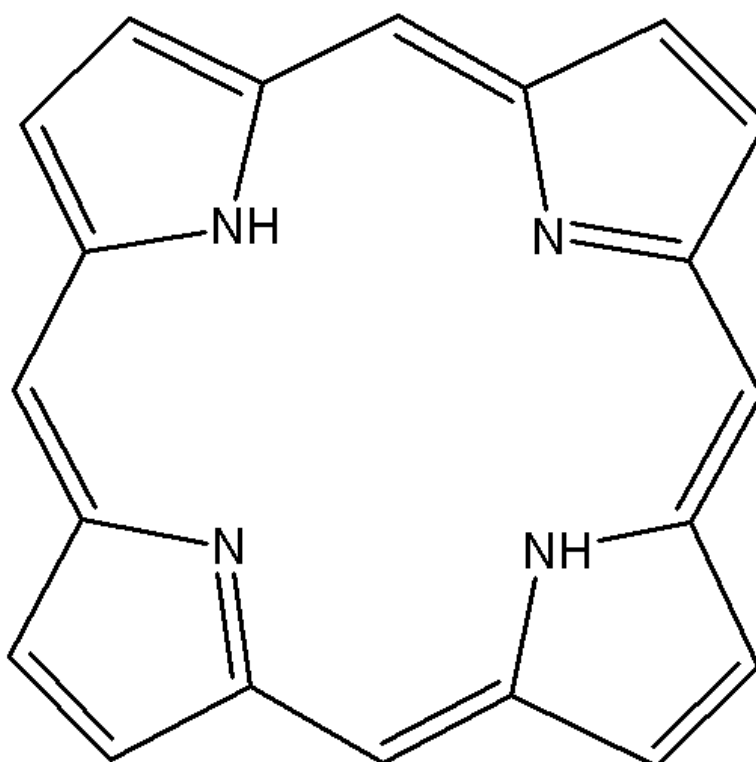


Figure 1: The porphine molecule which is the simplest porphyrin and builds together with a  $Zn^{2+}$  metal centre the core of the molecules investigated in this work.

In this project we focused on two different porphyrin derivatives. The first molecule **1** ( $C_{72}H_{42}F_{10}O_4N_4Zn$ ; Mw=1282.5u) was symmetric with a 2-fold axis. It was quite big (figure 2) and contained two rings in a row attached to the four arms of the porphyrin core. Two of the 4 arms which were opposite to each other had a pentafluoro-group on the end of the arm. The other 2 arms had two methoxy groups to create a steric hindrance. The diameter molecule **1** was  $\sim 2.6$ nm along the methoxy-groups and  $\sim 2.7$ nm between the pentafluoro-groups. The reason for this design was to create larger pores. The arrangement of the fluorine groups onto the assemblies was further of interest since the pentafluoro-phenyl was also predicted to have interesting properties. For example the phenyl ring of a pentafluoro-group should be electron poor because the fluorine residues remove the electrons from the  $\pi$ -system. Therefore a possible interaction with the normal phenyl rings could occur which should be stronger than normal  $\pi$ -stacking [ref. 9]. Molecule **2** ( $C_{48}H_{24}N_8Zn$ ; Mw=778.1u) was

symmetric with a diameter of  $\sim 2.1$  nm and had a 4-fold axis. It contained only 1 phenyl-ring on each arm terminated by a cyano-group (*figure 3a*). In consequence to their structural differences, the molecules formed different assemblies but distinct similarities could also be observed, especially when imaging the porphyrin core. Since we observed a porous network for both molecules, we subsequently deposited SubPc ( $C_{24}H_{12}BCIN_6$ ;  $M_w=430.66u$ , *figure 3b*) onto the porous network assemblies. For molecule **1** it seems that SubPcs adsorbed into the pores, however deposition of a certain amount of SubPc led to the formation of a new assembly which eliminated the porous network. For molecule **2** the SubPcs coordinated to the pores of the network but it is not clear if the molecules fit inside the pores.

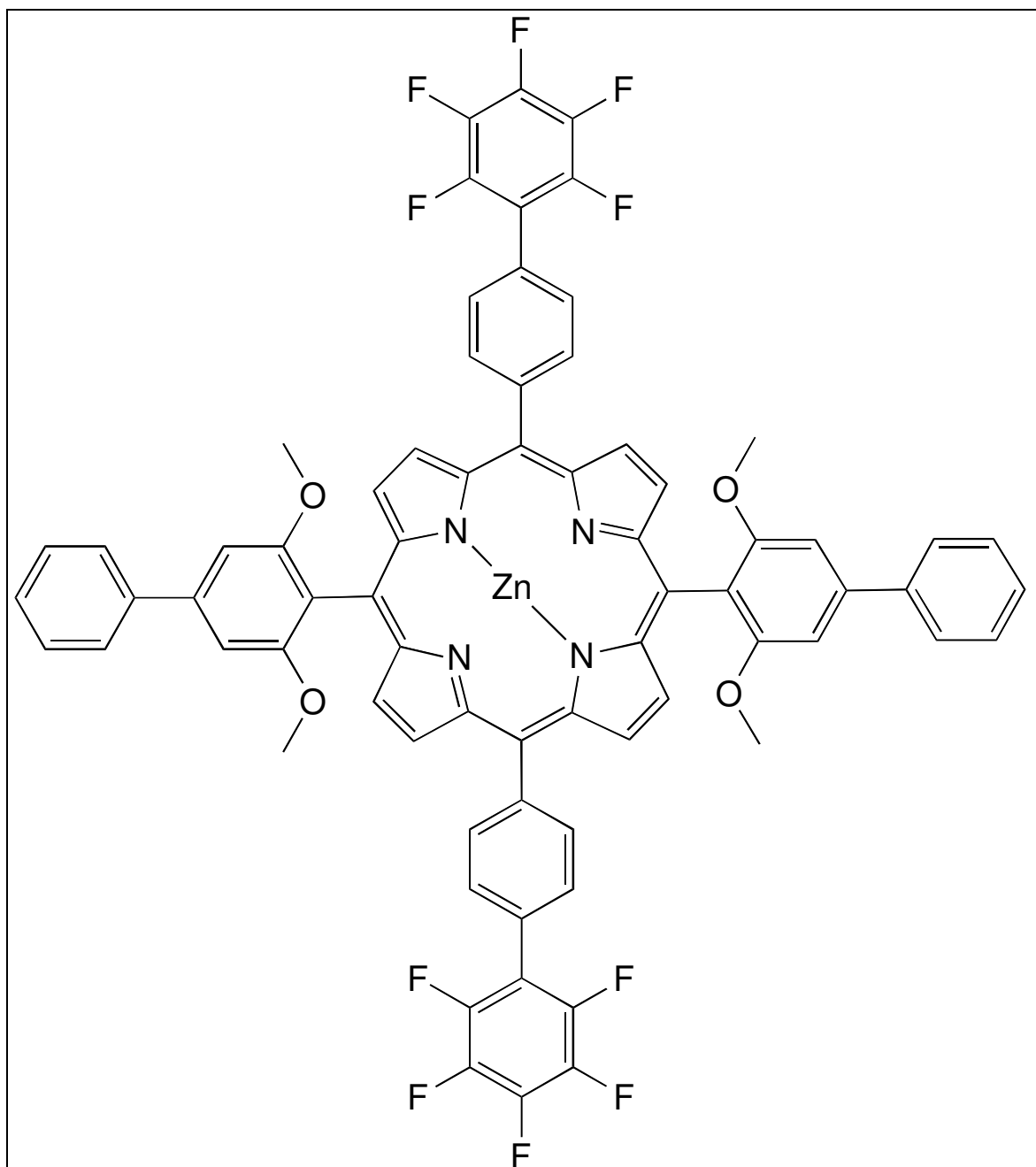


Figure 2: Molecule **1** ( $\{5,15\text{-Bis}(2,6\text{-dimethoxy-4-phenylphenyl})\text{-}10,20\text{-bis}[4\text{-}(2,3,4,5,6\text{-pentafluorophenyl})\text{-phenyl}]\text{porphyrinato}(2\text{-})\text{-}kN^{21},kN^{22},kN^{23},kN^{24}\}\text{zinc(II)}$ ). Diameter:  $\sim 2.6$  nm along methoxy-groups respectively  $\sim 2.7$  nm along pentafluoro-groups.

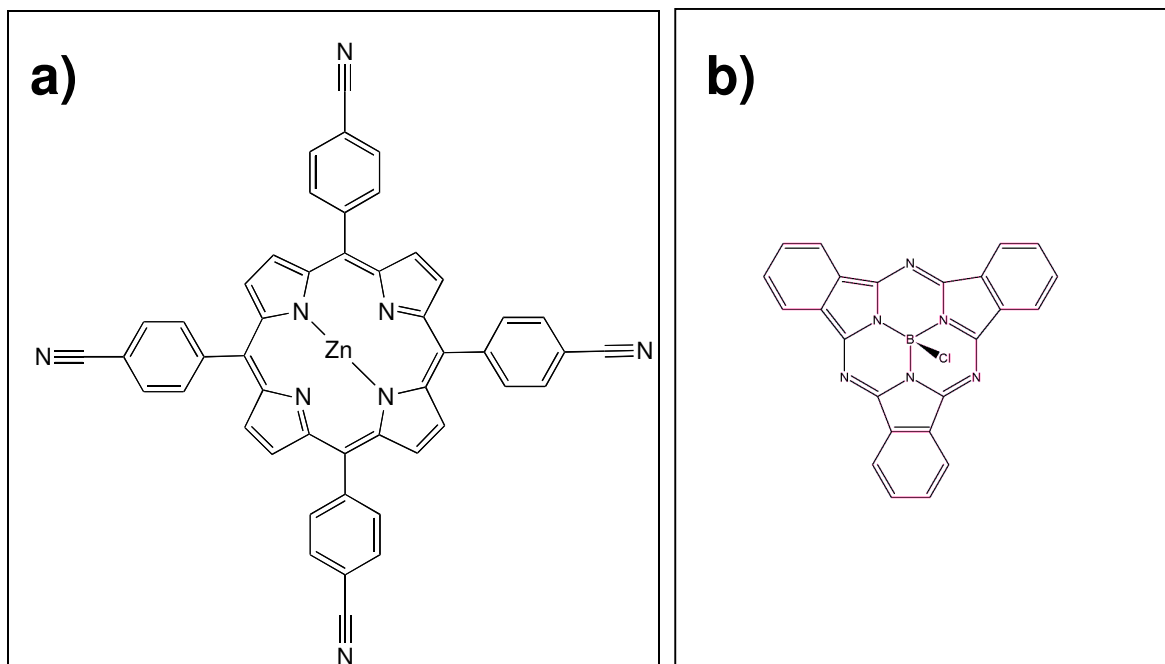


Figure 3: a) Molecule **2** [5,10,15,20-Tetrakis(4-cyanophenyl)porphyrinato(2-)- $kN^{21},kN^{22},kN^{23},kN^{24}$ ]zinc(II)  
Diameter: ~2.1nm. b) Chloro[subphthalocyaninato]boron(III) also called Sub-Phthalocyanine (SubPc).  
Diameter: ~1nm

## 2. Materials & Methods

### 2.1. Principles STM, LEED, UHV, molecule deposition

The STM is very useful for investigating the molecular assemblies on a metal surface with molecular or even submolecular resolution. It was the first type of scanning probe microscopes and uses the quantum-mechanical tunnelling effect which allows small currents to flow if two objects are close enough together even through vacuum. The STM uses a very sharp tip to approach to the surface of the sample and in principle it's the radius of the tip which determines the resolution of the recorded image. Highly sensitive electronics are necessary to measure the extremely small tunnelling current. The distance between the sample and the tip is controlled by piezo-elements which are able to move the tip or the sample with respect to each other with a precision of less than 1Å. The sample is scanned line-wise using the piezo-elements to move. Technically it is possible to move either the sample or the tip with the piezo-elements and it depends on the design of the microscope if the tip or the sample is moved during scanning. In principle, one can measure with the STM in two different modes. In the first mode, a constant height of the tip above the sample is maintained and the changes of the current are recorded. In the other mode, the tunnelling current is kept approximately constant by choosing a set-point for the tunnelling current. In this mode, the movement of the piezo-element in the Z-direction is recorded. Another possibility is to focus onto one point of a sample and to do Scanning Tunnelling Spectroscopy (STS) [ref. 10]. But the STM has also some limitations: it cannot measure on a non-conducting surface. In fact, the tunnelling current occurs there too, but this tunnelling current cannot be measured since one cannot contact the isolating sample. The measured sample also has to be very flat with a maximum inclination of about 50nm per micron. This leads to a surface where one can see distinctively the step-edges and therefore it is also important to have as large islands as possible without step-edges. An island of a metallic substrate should have at least an area of 200 nm<sup>2</sup>. It is also not possible to deposit much more than two or three monolayers (ML) of a molecule onto a metal surface if the molecule itself is an isolator. Because of that most experiments use a molecule coverage which is below two ML. In fact a lot of experiments are done just between zero and one ML of deposited molecules since most interesting effects are observed at such low coverages. Furthermore, it is also important to have a sample which is as clean as possible. Because of that, the STM used in this project was operated under UHV conditions.

Another experimental method used in this work was LEED. It allows to find out the lattice parameters of the deposited molecules and to set them in relation with the metal substrate lattice. LEED uses the matter wave properties of electrons to create diffraction patterns. Electrons coming from an electron gun with energies between 3eV and 200eV are shot onto the sample. Electrostatic apertures are used to focus the electron beam. Electrons reflected from the sample are then visualized on a hemispherical fluorescent screen. The penetration of the electrons into the sample is about 0.5nm-1nm, hence only the surface is investigated by this method. The reason for that are the strong interactions between electrons and the sample compared to the weaker interactions of light with a sample. In X-Ray diffraction techniques the penetration depth is much larger. The strong interactions of the electrons with the surrounding are also the reason why it is necessary to execute LEED-measurements in UHV because the mean free path of the electrons is dramatically increased there. Like in all diffraction methods the observed image shows the surface pattern in the reciprocal k-space. Superstructures on the surface (like e.g. deposited molecules) can then be observed on screen as additional spots between the substrate spots. The reason is that the superstructure has a larger unit cell in real space therefore a smaller unit cell in k-space. One problem recording

the LEED-pattern of a superstructure is the intensity of the additional spots which might be too low. In most cases the substrate allows the creation of domains of the superstructure with different orientation which can be seen as additional spots, too. The reason is that the electron beam normally hits such a large area on the surface that several domains are hit and then seen on the screen. This increases the complexity of the LEED-patterns and can make it difficult to resolve them. However if the pattern is solved the result is very precise and allows to find the exact relation between substrate lattice and superstructure, as mentioned above. This is very important to determine the precise interactions between substrate and superstructure. To record a LEED-image it is important to have one dominant assembly which is stable in the electron beam because otherwise one cannot see the spots because the intensity of them is too low. Therefore, the results of LEED-measurement can be very useful to substantiate the findings of STM-measurements.

UHV conditions mean a pressure between  $10^{-8}$  mbar and  $10^{-11}$  mbar and can be reached by using several different pumping systems. A pre-vacuum pressure of about  $10^{-2}$  mbar or  $10^{-3}$  mbar has to be reached by e.g. rotary pumps. Turbo-Molecular Pumps (TMP) can start pumping under these pre-vacuum conditions to reduce the pressure into the range of about  $10^{-7}$  mbar. A TMP works with several rotors that rotate with a speed up to about 100000 rotations per minute. To reach an even lower pressure it is necessary to get rid of the water film by heating up to 120-200°C. At this temperature water molecules and some organic residuals evaporate nearly completely and after cooling down the pressure can reach a level of  $10^{-10}$  bar. Further Ion Getter Pumps can pump more residual gas molecules and the pressure can then even reach  $10^{-11}$  mbar. The Ion Getter Pumps do that by ionizing residual gas molecules. In the electrical field which is created by them the ions are accelerated in direction of the Getter. The Getter is a material which is capable of binding these ions like e.g. titanium which is very reactive. So the residual gas molecules pumped by an Ion Getter pump are just bound onto the surface of the Getter material and not removed out of the chamber. Small contaminations can usually be removed by giving a shot with a Titanium Sublimation Pump (TSP). Then titanium gas is sublimed into the vacuum chamber increasing the pressure to a level of about  $10^{-8}$  mbar. Because titanium gas is very reactive and binds together with residual gas atoms onto the walls of the vacuum chamber the pressure can be decreased by that procedure.

As already mentioned the STM gives a real image of the surface of a sample with a good resolution. But the sample itself has to be well defined since surface chemistry is also depending very much on the configuration of the surface. For this project, only Cu(111) and Ag(111) single crystals were used as metallic substrates. These crystals are grown in a specific way to have only one type of surface configuration like e.g. (111). The (111) configuration is popular because it is nearly inert and does not interact usually with the deposited molecules in a chemical way. The crystals are cleaned by cycles of sputtering and annealing. Ion beam based sputtering is done by a sputter gun which releases ions of noble gases, usually argon. If the angle between sample and sputter gun is set correctly one can remove atoms and molecules from the surface very efficiently. After sputtering, the crystal is annealed up to a specific temperature to reorganize the surfaces by filling up the holes created by sputtering. Also the inhomogenities of the bulk tend to come to the surface and evaporate during annealing. So by repeating sputtering and annealing the crystals get more pure until they are clean enough for the deposition of molecules. The surface configuration is saved too by this process what is very important because it would affect the results if parts of the crystal surface would transform e.g. from a (111) to a (110) configuration. After sputtering and annealing, it is possible to check by STM if a crystal is clean enough in case there are doubts for some reason. The configuration of the crystals can be always checked with LEED. Crystals prepared by sputtering and annealing can be also used for other techniques of surface analysis like LEED, XPS and so on.

There are several methods of depositing molecules onto surfaces. In this project, only evaporation was used to deposit molecules onto the surface. Because everything should be as clean and as pure as possible this should also be the case for the molecules which are deposited onto the metal surface. So these molecules are always tested before deposition if they are pure enough. In case of enantiomers, one can measure racemic mixtures or the enantiopure molecules but one has to take into account that the obtained results may differ. Therefore it is important to know if the molecules are enantiopure or racemic. To avoid deposition of residual contaminations the molecules are heated up to their evaporation temperature and left to degas for some time, prior to the actual deposition. Any contaminants with a lower evaporating temperature should then disappear by time. The contaminants with a higher evaporation temperature than the desired molecules are irrelevant, because they do not evaporate during the deposition at all. The result is that in general contaminations are negligible and do not play a role for the results of the measurements.

## 2.2. Specification UHV-System (Nanolab)

The UHV-System (“Nanolab”, *figure 4*) in which the room-temperature STM-Measurements were carried out, contained different chambers for scanning, preparation and other experiments (e.g. LEED). STM-Measurements were carried out in the so called “STM-Chamber”. In the “PREP-Chamber” LEED-Measurements could be done. Deposition of molecules onto the metal surface was done in the “Molecule-Chamber” where it was also possible to anneal samples. Further, in the “ESCA-Chamber” sputtering and annealing of the samples were done. There was also a separate chamber which could be used for metal evaporation which was called “EVAP-Chamber”. In this chamber, also the tips that were used in the system were prepared. To introduce samples into the evacuated system there was a load-lock which was connected through a valve with the “PREP-Chamber”.

The different chambers were connected by valves and each chamber could be pumped separately by TMP and Ion Getter Pumps. The valves remained closed during the measurements (except for the valves connecting to the respective pumps for the chambers) and were only opened for the transfer of samples or tips. The pressure in all the chambers was in the range of  $10^{-10}$  mbar except for the load-lock where only high-vacuum conditions could be achieved ( $10^{-6}$  mbar).

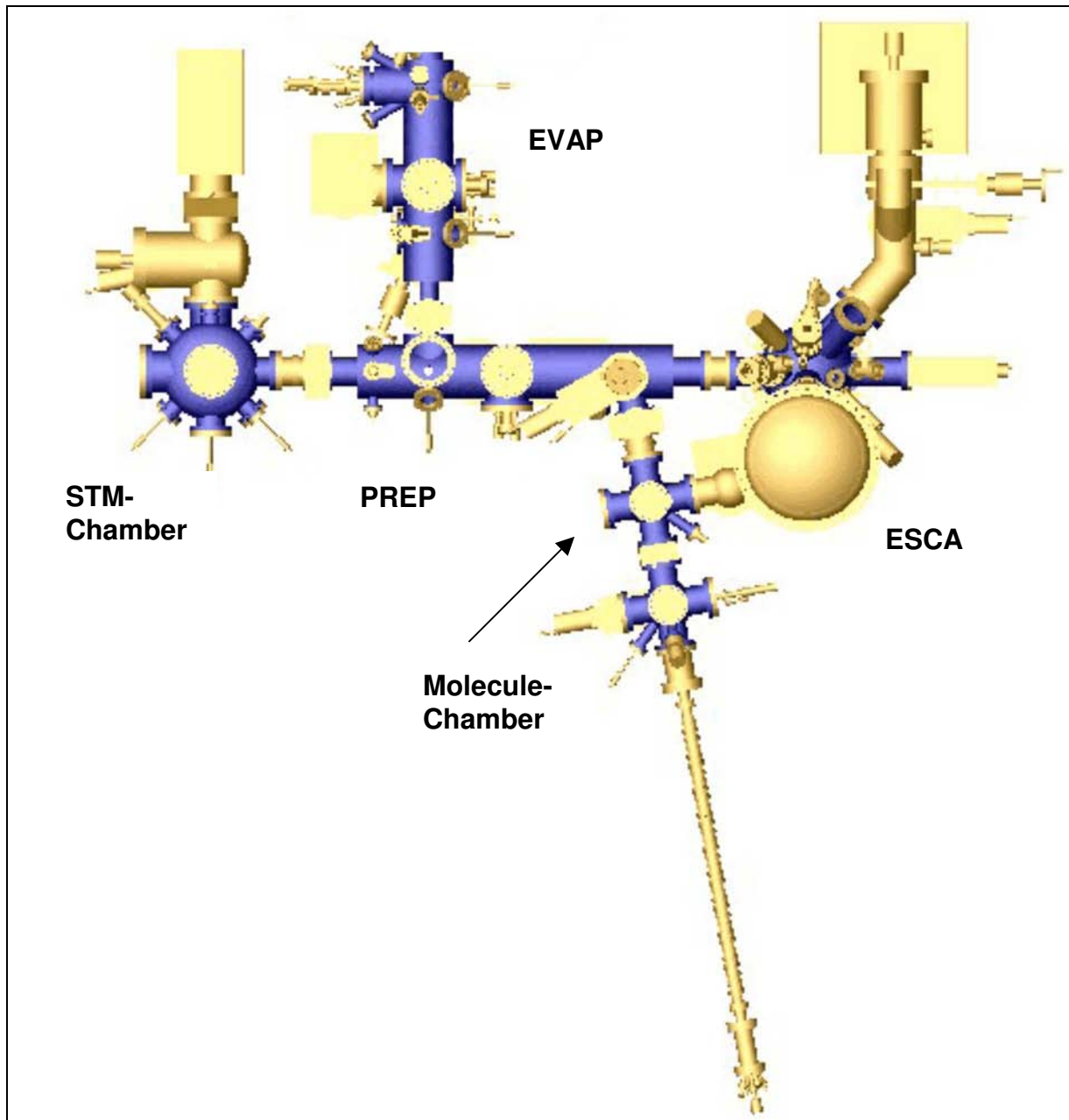


Figure 4: Schematic representation of the “Nanolab”-System

### 2.3. Preparation of the crystals (Sputtering/Annealing)

For the measurements, Cu(111) and Ag(111) single crystals, respectively, were used as substrates for the deposition of molecules. Prior to deposition, these metal surfaces were cleaned by cycles of sputtering and annealing. If the crystals were exposed to ambient conditions before usage 2 cycles of sputtering and annealing were sufficient for cleaning. Sputtering with  $\text{Ar}^+$ -Ions was carried out at a pressure in the range of  $10^{-7}$  mbar in the “ESCA-Chamber”. Successive annealing was done with resistive heating of a filament in contact with the sample. The final annealing temperature was about 800K in case of Cu(111) and about 700K in case of Ag(111). The pressure during annealing was typically in the range of  $10^{-9}$  or  $10^{-10}$  mbar. If necessary and the sample was not clean or exposed to air before usage, more cycles of sputtering and annealing were performed to clean and flatten the crystal surface.

## 2.4. Deposition of molecules

Molecules were deposited in the molecule chamber at a pressure in the range of  $10^{-9}$  mbar or  $10^{-8}$  mbar. The molecule source was a Knudsen cell evaporator with 9 crucibles for different molecules and the temperature could be regulated separately for each crucible. The amount of deposited molecules was measured by a Quartz Microbalance (QMB). The time of molecule deposition onto the metal surfaces was between 30s and 5min. Longer deposition times were undesirable because then the drift of the QMB made the measurement imprecise. Typically we deposited between 0.2 and 1.5 monolayers (ML) of molecules onto the metal surfaces with rates between 0.2 and 1 ML/min.

## 2.5. STM/LEED-Measurements

STM-Measurements were done in the STM-Chamber at a pressure in the range of  $10^{-10}$  mbar using a tungsten-tip at room temperature. The STM-signal was processed using Nanonis software. Usually a tunneling current between 5pA and 50 pA and a bias voltage in the range between -2.5V and +2.5V were used. A short pulse (10ms) of voltage which was in the range between -10V and +10V allowed minor modifications of the tip during scanning. If the tip had to be modified even more the procedure called “field-emission” had to be performed: a high voltage of about 300V was applied between the tip and the sample that were positioned roughly 100nm away from each other, allowing a current of about 25 $\mu$ A to flow. Especially the current couldn't go to high because it was limited by the electronics. The sample which we used for field-emission was a Pd-sample which was not in use anymore for measurements. LEED-measurements were done in the “PREP-Chamber” with a sample that was scanned before in the “STM-Chamber” to check if the desired conditions were fulfilled. Energies in the range between 3eV (for the molecule assembly) and 140eV (second order of the substrate lattice) were used. After LEED-measurements the samples were checked with the STM for possible damages induced by the electron beam.

STM images were processed using WSxM software [*ref. 11*] by doing plane fits (especially also defining local planes), equalizing, flattening, removing lines, if necessary. In some cases pictures were also smoothed using a Gaussian method. Further brightness and contrast were optimized additionally with the help of Corel Draw. In some cases also an unsharp mask was used. All images presented are STM height images. To accentuate structures some STM height images were combined with their respective current image.

Unit cells of the 2D-lattices of the relevant molecular assemblies were also determined with the help of WSxM software. Several images were analyzed and the results averaged to reduce measurement errors. The assemblies were then categorized and a molecular model for every assembly was proposed by comparing the molecular size and structure with the high resolution images.

LEED images were optimized in Corel Draw adjusting brightness and contrast and using the unsharp mask. Simulated LEED-patterns were created using the LEEDpat software.

## 3. Results

### 3.1. Porphyrin derivative 1

Molecule **1** was deposited from two different cells in the evaporator. The deposition temperature was about 600K. The deposition temperature was slightly depending on the amount of molecules in the crucible. But we didn't observe any structural difference between the samples prepared with different deposition temperatures. The deposition rates were between 0.1 and 1.1ML/min.

#### 3.1.1. Molecule **1** on Ag(111)

On Ag(111) seven different samples were prepared and investigated with a coverage between 0.25ML and 0.95ML. With the STM measurements 2 different types of close packed assembly were observed and 1 porous network with hexagonal pores. *Table 1* shows an overview of the assemblies of molecule **1** which were found on Ag(111) stating corresponding unit cell vectors, standard deviations  $\sigma$  and molecular densities of the assemblies.

		Unit cell vectors			$\sigma$		Angle a-b [°]	Molecule Density [molecules/nm <sup>2</sup> ]
		a[nm]	b[nm]	Angle a-b [°]	a [nm]	b [nm]		
Ag1	Porous network (hexagons)	4.20	4.20	60.0	0.20	0.20	-	0.20
Ag2	Alternating close packed assembly	2.02	3.92	80.6	0.15	0.19	1.6	0.26
Ag3	Simple close packed assembly	1.84	2.04	88.5	0.04	0.06	0.5	0.27

Table 1: Assemblies of molecule **1** found on Ag(111) without SubPc. Ag1 vectors were chosen based on STM images and the Van der Waals radii of the molecules.

The hexagonal network (Ag1) was highly dominating and no close packed assemblies were observed when the deposition was done at a rate below 0.2ML/min (*figure 5a*). The assembly covered the whole surface and was in most cases only interrupted by step edges of the substrate. Annealing to 250°C was possible without any observable influence on the hexagonal network (*figure 5b*). Upon further annealing up to a temperature of 300°C we observed that we didn't have a full monolayer of molecules anymore. Additionally to the hexagonal network some very small areas appeared which were covered with a close packed assembly (*figures 6a,7*). The close packed assembly was always found close to a step edge and the hexagonal network was still dominating (*figure 6b*). Further we observed that the molecules near to the close packed assembly were mobile (*figures 7*). This might have been caused by the dynamic assembly and disassembly of the molecules at the hexagonal network borders. The molecules moved from 2D gas phase to positions in the network (similar to [refs. 12,13]). The other possibility would be that the network is not registered by the tip because of a strong movement of gas phase molecules on top of the hexagonal network. Another possibility would be that the tip picked up and lost molecules what would have affected the signal.

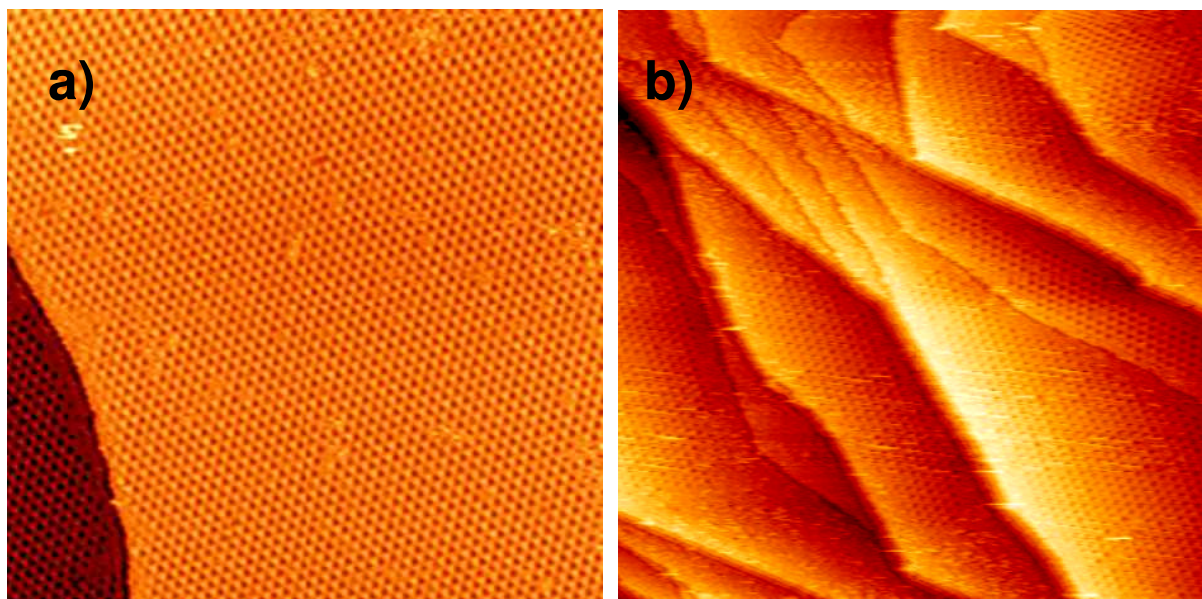


Figure 5: a) Large scale STM-image (190nm\*190nm, I=14pA, U=1.5V, 0.7ML, Sample 9a) demonstrating large scale dominance of the hexagonal network with a very low amount of defects. b) Large scale STM-image (200nm\*200nm, I=20pA, U=1.8V, 0.95ML, Sample 3c) in a region with more step edges. This sample was annealed at 250°C what didn't have any observable effect.

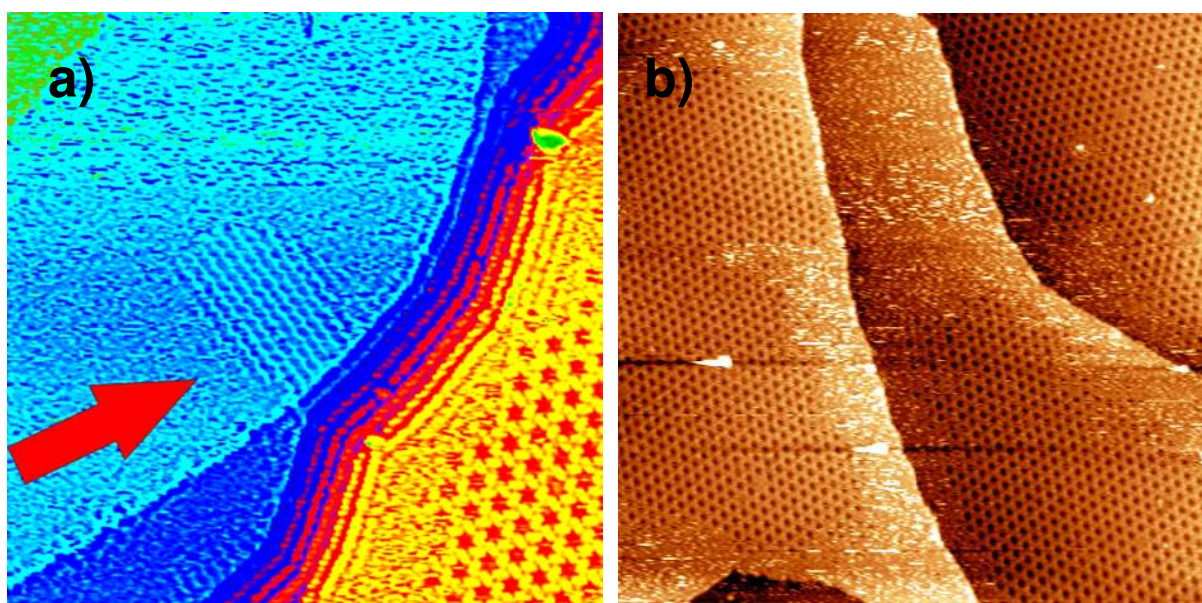


Figure 6: a) STM-image (80nm\*80nm; I=15pA, U=1.6V, 0.95ML, Sample 3d) where the red arrow shows the close packed assembly area close to a step edge after annealing up to 300°C. b) STM-image (200nm\*200nm; I=15pA U=1.6V, 0.95ML, Sample 3d) shows the remaining general dominance of the hexagonal network on the same sample.

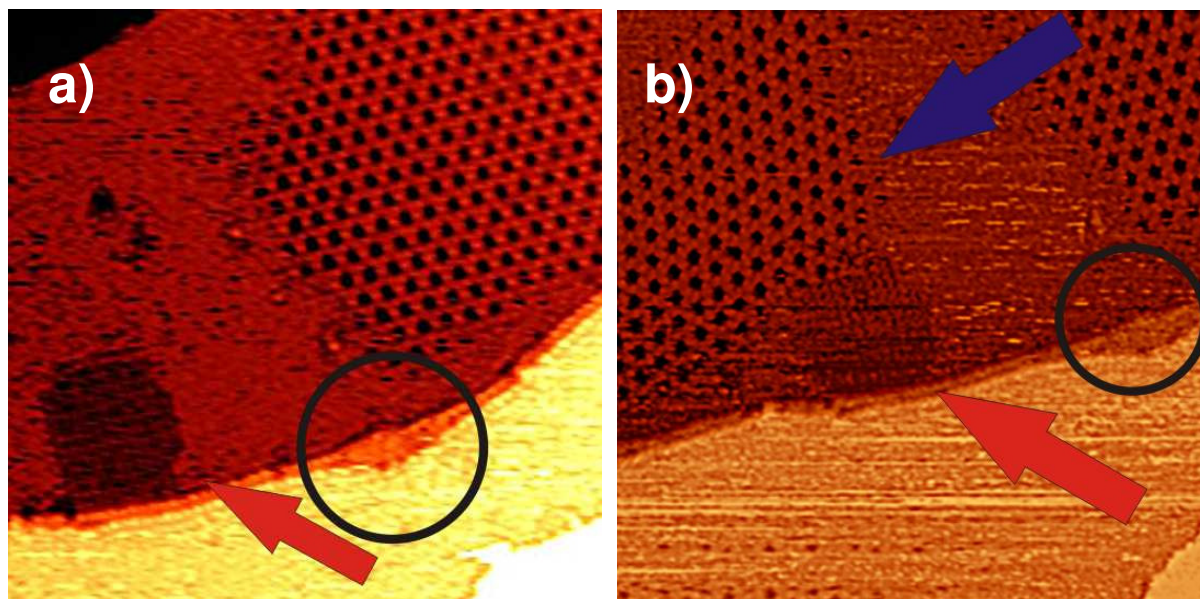


Figure 7: a) STM-image (100nm\*100nm, I=15pA, U=1.6V, 0.95ML, Sample 3d) showing another close packed assembly close to step edge (depicted by red arrow) after annealing up to 300°C. b) STM-image (100nm\*100nm, I=15pA U=1.8V) presenting the situation 74min later. The black circle marks a position on the step edge which can be clearly identified on both pictures. One can see that the close packed assembly (red arrow) was not moving but on the left hexagonal network appeared (blue arrow).

If molecules were deposited with a rate above 0.4ML/min we observed the formation of close packed assemblies simultaneously with the hexagonal network without any annealing in advance (*figure 8*). Two different types of close packed assemblies were then observed. In the simpler one (Ag3) all molecules were oriented the same way. But this assembly did not spread over more than ca. 10 rows while the length of the rows was basically only limited by step edges of the substrate (*figure 9a*). In the other close packed assembly (Ag2) the molecules alternated between two orientations along the same rows. In fact assemblies Ag2 and Ag3 were found to intermix (*figures 9*). However the alternating close packed assembly was also able to exist without the simple close packed assembly (like seen on *figure 8*). The phenomenon that the close packed assemblies appeared in consequence to the high deposition rates was also observed if we deposited only 0.45ML (*figures 10*) which was already an indication that indeed the rate was the determining parameter which led to the formation of close packed assemblies. Further it was observed that Ag2 could be separated from Ag1 with and without a gas phase in between the two assemblies (*figures 8 and 10a*).

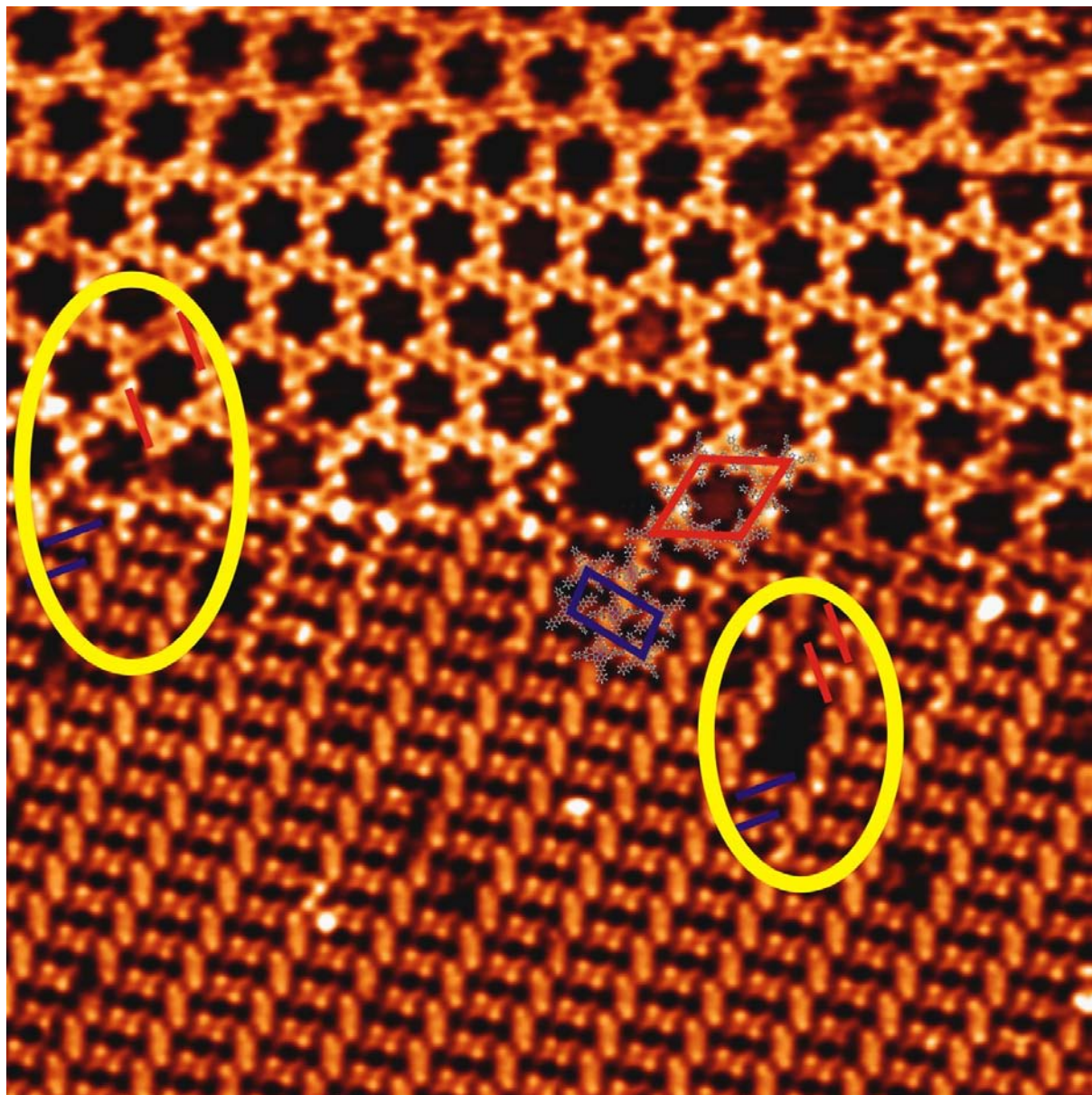


Figure 8: STM-image (50nm\*50nm, I=15pA, U=2.5V, 0.8ML, Sample 6a) of the hexagonal network together with the alternating close packed assembly. The unit cell of the hexagonal network is denoted by the red frame. The unit cell of the alternating assembly has the blue frame. It was interesting in this case to observe that the orientation of the molecules changed from the hexagonal network to the alternating close packed assembly by 90° (denoted by the yellow ellipses). Further one can see in the hexagonal part that some pores are filled by **1** itself (compare *ref. 14*) having a light red colour instead of black for the empty pores.

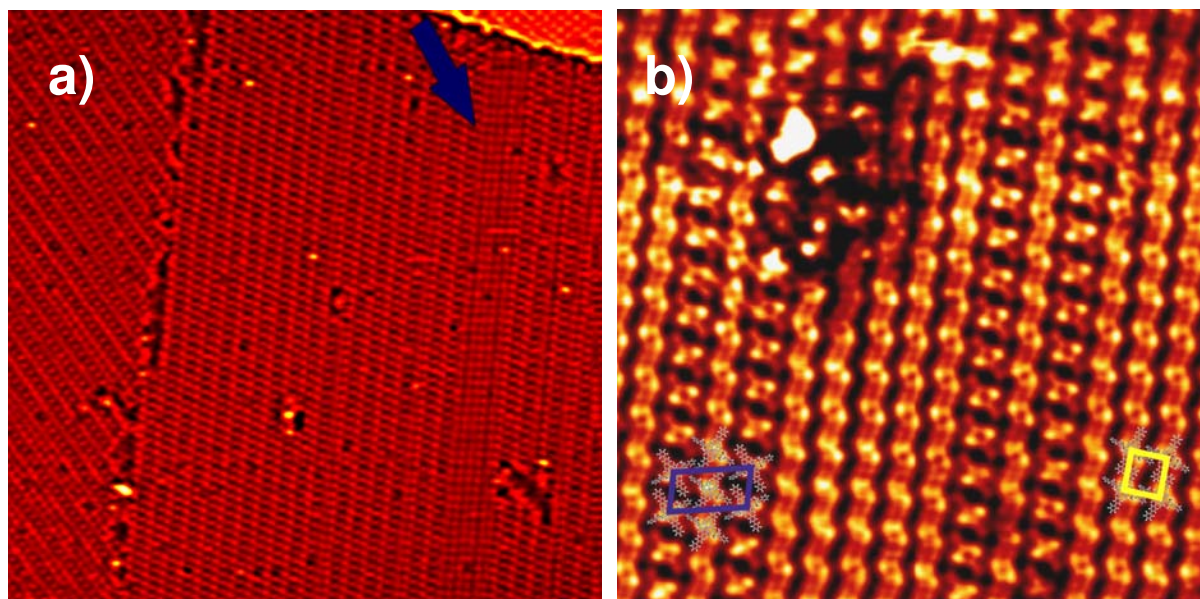


Figure 9: a) STM-image (130nm\*130nm, I=15pA, U=1.4V, 0.8ML, Sample 6a) shows the mix of alternating and simple close packed assembly (denoted with blue arrow). b) STM-image (30nm\*30nm, I=15pA U=1.4V) is a zoom-in on the same region but outside the range of the overview. The unit cells of the two close packed assemblies are denoted in the image.

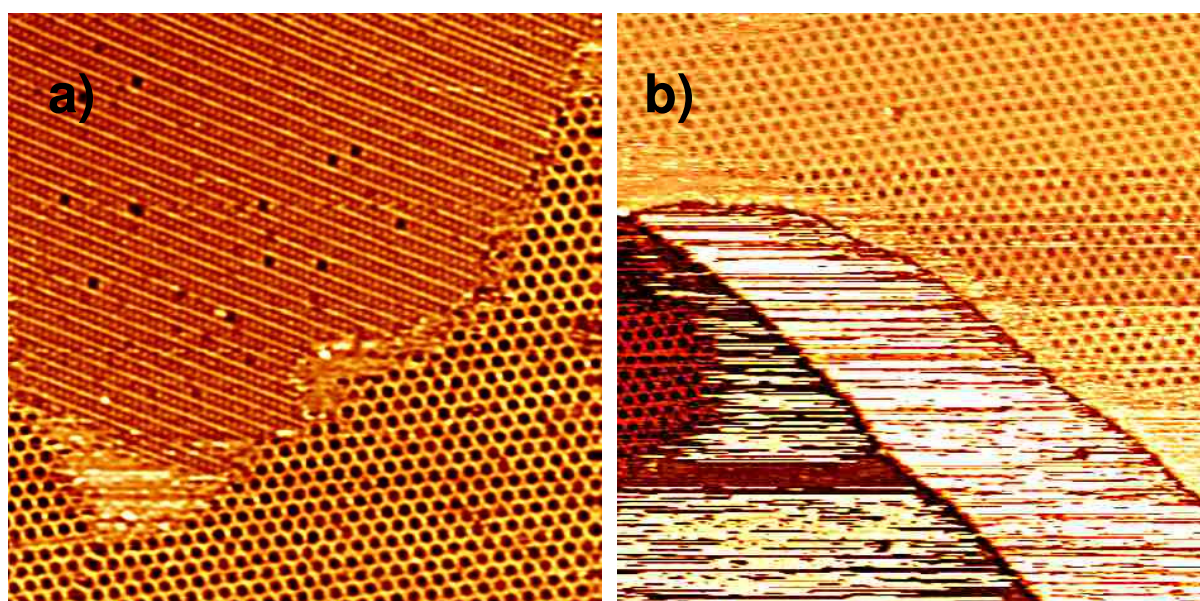


Figure 10: a) STM-image (140nm\*140nm, I=20pA, U=1.1V, 0.45ML, Sample 8b) shows alternating assembly and hexagonal network. It is interesting that this time there was a small gas phase between the two assemblies. b) STM-image (150nm\*150nm, I=20pA, U=1.1V 0.45ML, Sample 8b) demonstrates that the coverage is as low that large regions are only occupied by a 2D gas phase.

The unit cell of the hexagonal network (Ag1) had after statistical analysis the vectors  $a=4.01\pm 0.15\text{nm}$ ,  $b=4.20\pm 0.19\text{nm}$  with an angle of  $60.0\pm 1.5^\circ$ . But from symmetry considerations we took the decision to define  $a=b$ . By applying the models onto the images we decided to choose 4.2nm as a value for the unit cell vectors (*figure 11*) since the molecules in a smaller unit cell seemed to be overlapping. Further this value matched better to the high-resolution images that were taken. The molecules are tilted against each other by  $60^\circ$  and 6 molecules are surrounding one pore. The error for the vectors in this model is in the range of  $\pm 0.2\text{nm}$  according to the statistical results and agrees with the Van der Waals radii of the molecules.

The structure is quite surprising since the pentafluoro-groups come quite close together and maybe there is even an attractive interaction between them. At least there is a possibility for multiple hydrogen bonds between fluorine residues and hydrogen residues. From 5 fluorine residues per pentafluoro-phenyl 3 or 4 can be assigned to create hydrogen bonds. But the distances between the fluorine and the hydrogen residues is with more than  $3\text{\AA}$  quite high for hydrogen bonding. However, since the hydrogen bonding between fluorine and hydrogen can be very strong, such long distances might be possible.

In the first moment one would probably rather think of the same model with every molecule just turned by  $90^\circ$  because of the repulsive forces between the fluorine atoms. But we have three different types of imaging modes which support the model exactly in this orientation (*figures 12*).

One can also clearly see that the molecules do not overlap (*figure 13*). Because of this it is very unlikely that a phenyl-pentafluoro-phenyl interaction occurs (which is mentioned in [*ref. 9*]). Tilting the pentafluoro-phenyl groups does not change the situation since there are 3 pentafluoro-phenyl groups close together from which all should have the same angle with respect to the surface just by symmetric reasons.

The pore of the network has dimensions of  $\sim 2\text{nm}$  at the closest points and  $\sim 3.2\text{nm}$  between the most distant points (measured from STM images). Diffusing molecules of **1** can hop into the pores where they probably rotate at room temperature (*figure 8*, compare [*ref. 14*]). We think that the molecules inside the pores are rotating because usually no clear patterns were observed for the molecule inside the pore. In some cases a 6-fold symmetry was observed which was accurately fitted to the pore dimensions.

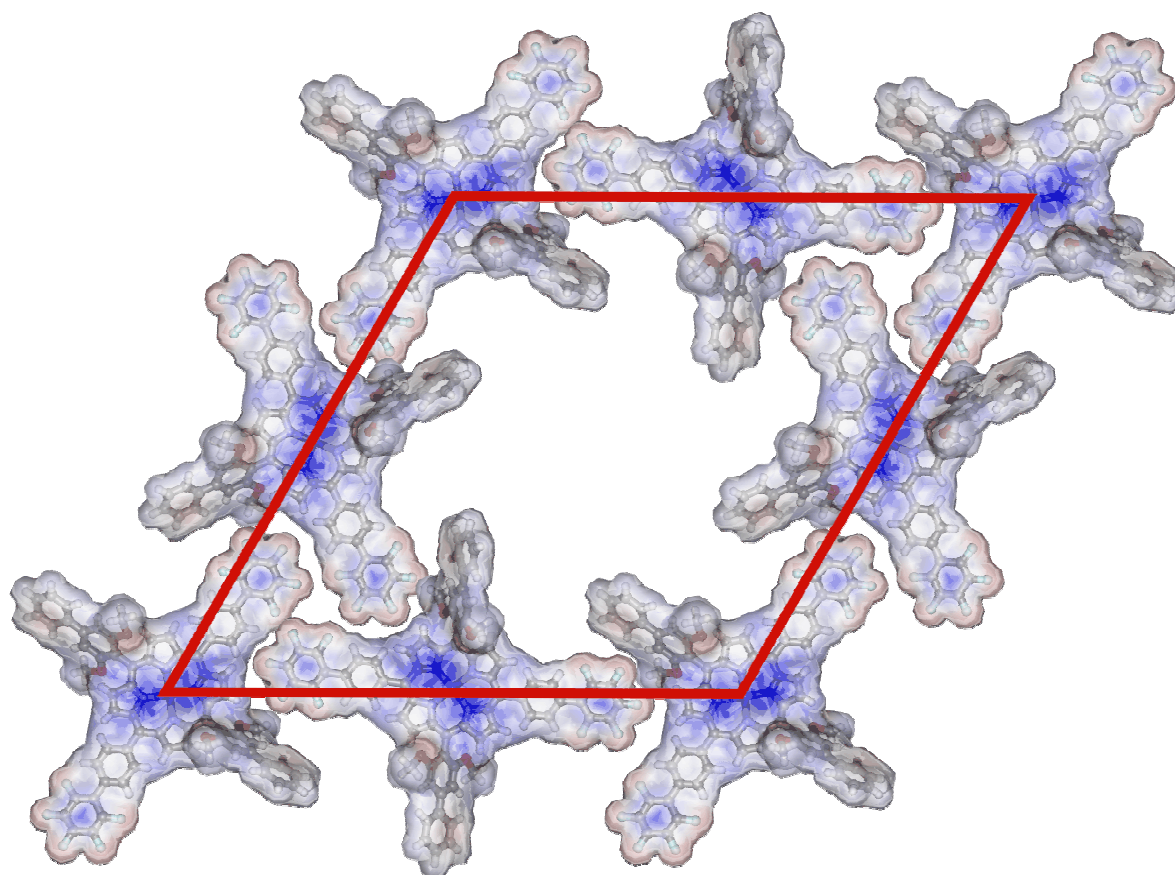


Figure 11: Model of the hexagonal network formed by molecule **1** on Ag(111). Unit Cell vectors:  $a=b=4.2\pm 0.2\text{nm}$ ; Angle= $60^\circ$ . The background shows the Van der Waals-Surface and the electrostatic potential of **1**.

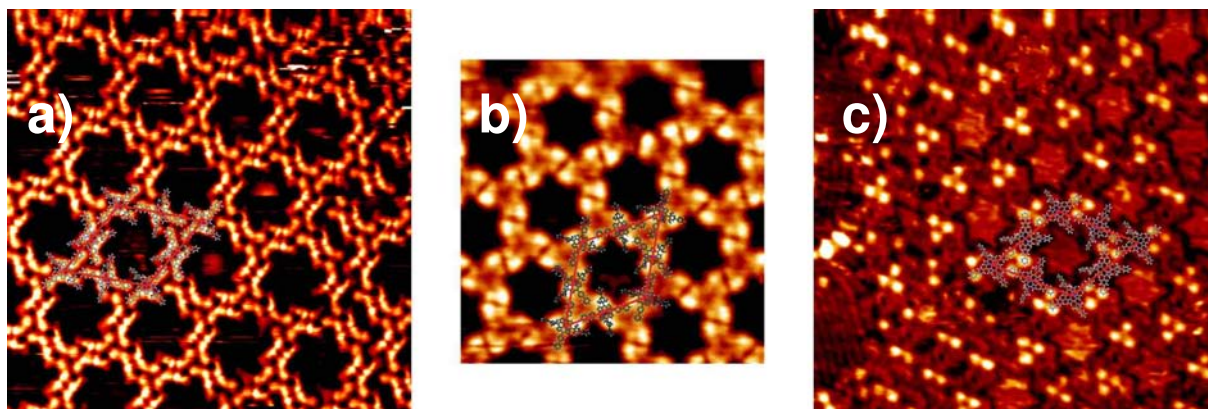


Figure 12: Overview over 3 different STM-imaging modes of the hexagonal network. All 3 pictures have the same scaling. a) STM-image (20nm\*20nm, I=20pA, U=1.8V, 0.6ML of **1**+0.05ML SubPc, Sample 11b) shows precisely the shape of the molecules. One can also clearly see the porphyrin ring. b) STM-image (15nm\*15nm, I=15pA, U=1.6V, 0.95ML, Sample 3d): the methoxy-groups are highlighted and define the positions of the molecules. Further, the porphyrin bending line [refs. 15,16] can be seen. It demonstrates that the porphyrin ring is not planar in this assembly. c) STM-image (20nm\*20nm, I=20pA, U=1V, 0.8ML, Sample 6a): The pentafluoro-rings are highlighted.

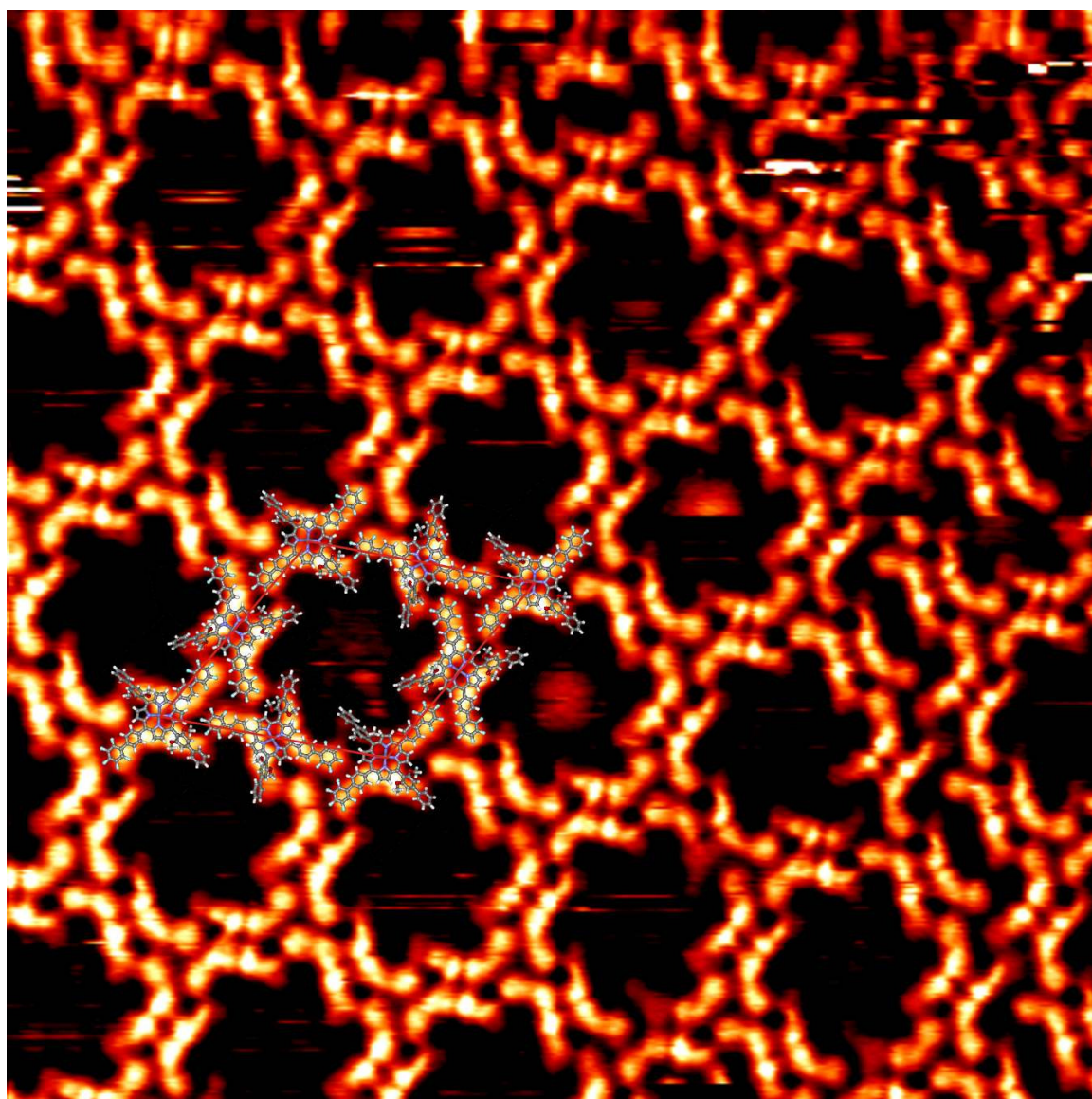


Figure 13: Large version of figure 12a: High-resolution STM-image (20nm\*20nm, I=20pA, U=1.8V, 0.6ML of **1**+0.05ML SubPc, Sample 11b) of the hexagonal network. The shape of the molecule is clearly observed and also some sub-molecular details like e.g. the core.

The close packed assemblies are much easier to understand since the fluorine residues do not come that close together there as in Ag1. On some images the shape of the molecules can clearly be observed. Further we can interpret the imaging modes in the same way as we did for the hexagonal network. In our model the molecules in the alternating close packed assembly (Ag2) have an angle of  $60^\circ$  between each other just like two neighbouring molecules in the hexagonal network. The unit cell vectors of Ag2 are  $a=2.02\pm 0.15\text{nm}$ ,  $b=3.92\pm 0.19\text{nm}$  with an angle of  $80.6\pm 1.6^\circ$  (figure 14a). The unit cell vectors of the simple close packed assembly (Ag3) are  $a=1.84\pm 0.04$ ,  $b=2.04\pm 0.06\text{nm}$  with an angle of  $88.5\pm 0.5^\circ$  (Figure 14b). On high resolution images with both close packed assemblies it was even possible to see small defects (figure 15). The most stabilizing factors are probably again H-bonding interactions between the fluorine residues of the pentafluoro-group and aromatic hydrogen residues. The distances for H-Bonding would fit since they would be below  $3\text{\AA}$  but to determine the number of hydrogen bonds is quite difficult as it is in the case of the hexagonal network.

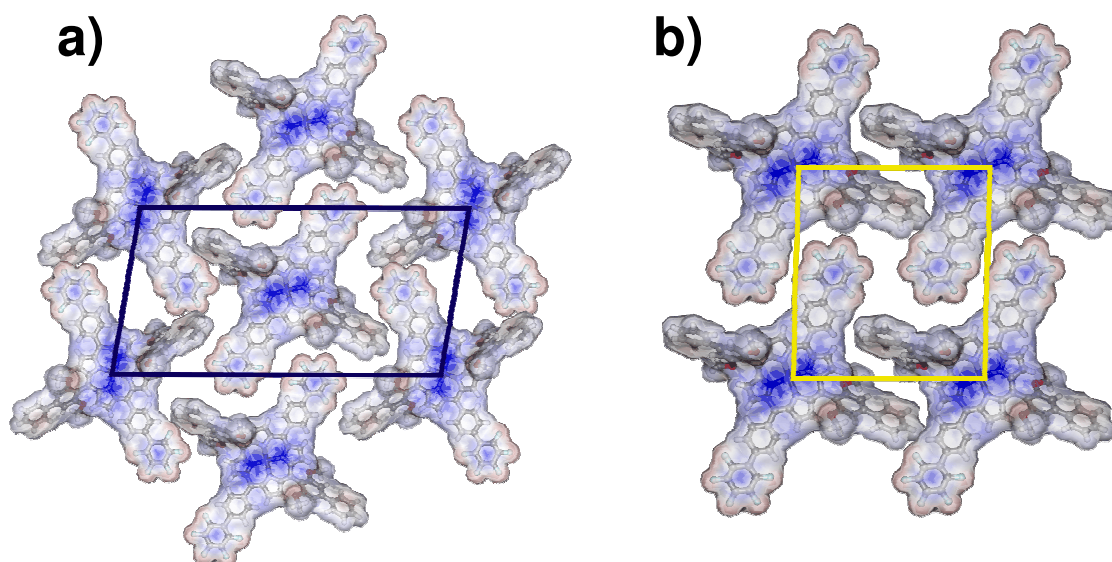


Figure 14: a) Model for the alternating close packed assembly (Ag2). Unit Cell vectors:  $a=2.02\pm 0.15\text{nm}$ ,  $b=3.92\pm 0.19\text{nm}$ ; Angle= $80.6\pm 1.6^\circ$ . b) Simple close packed assembly (Ag3). Unit Cell vectors:  $a=1.84\pm 0.04\text{nm}$ ,  $b=2.04\pm 0.06\text{nm}$ ; Angle= $88.5\pm 0.5^\circ$ . The background on both images shows the Van der Waals-Surface and the electrostatic potential.

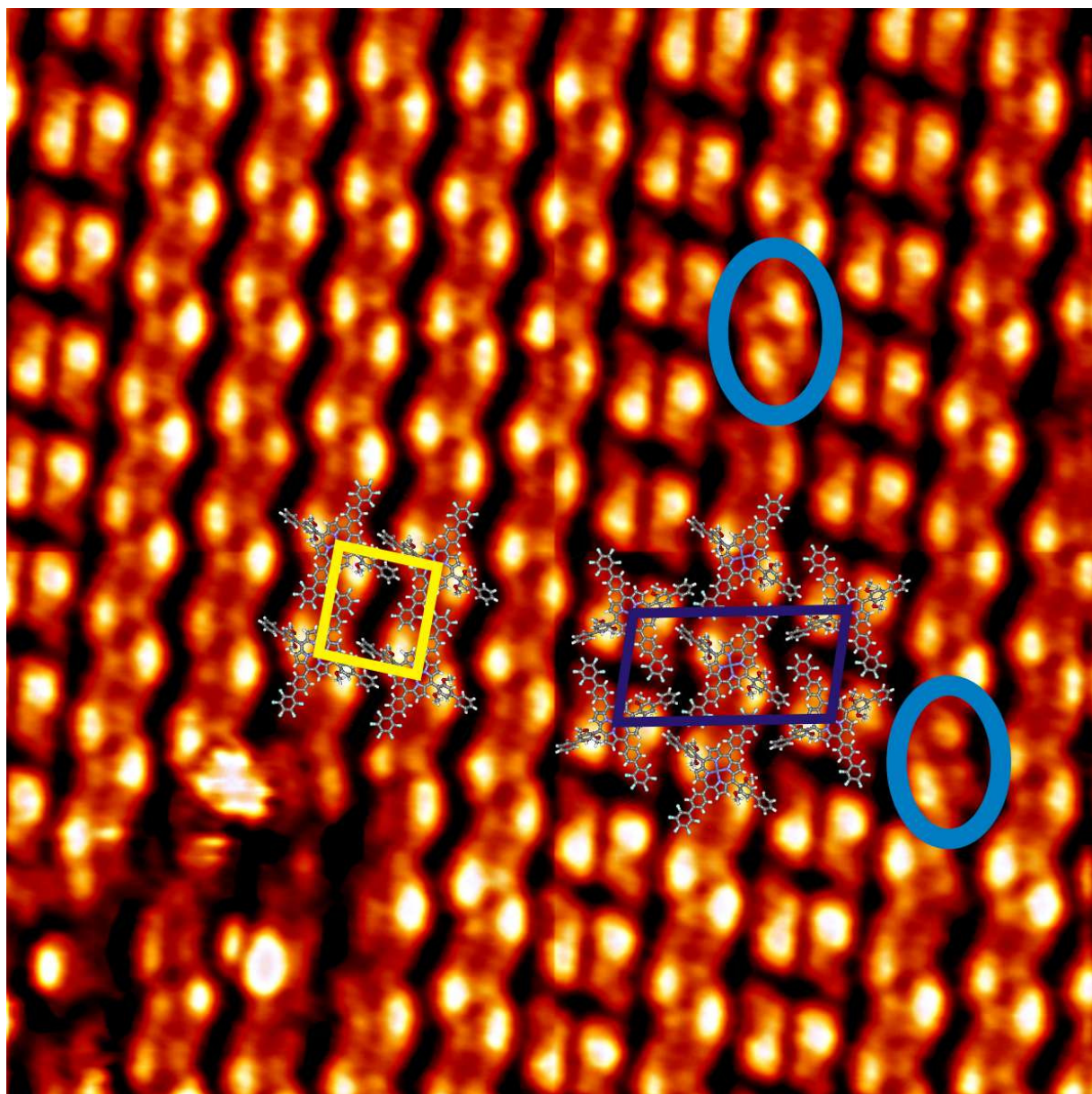


Figure 15: STM-image (20nm\*20nm, I=15pA, U=1.4V, 0.8ML, Sample 6a) showing the simple close packed assembly (Ag3) together with the alternating close packed assembly (Ag2). The tolerance of the assemblies against defects is also demonstrated in this image; the defects are indicated by the light blue ellipses.

### 3.1.2. Hexagonal network of **1** with SubPc on Ag(111)

We were then curious if it would be also possible to fill the porous network with SubPc in a similar manner as various other porous networks can be filled with C<sub>60</sub> [refs. 6-8]. SubPc was evaporated at temperatures of about 500K having a rate between 0.05 and 0.2ML/min onto a predeposited hexagonal network of **1**. Like in the case of molecule **2** there might be an error of the rate of a factor 2 since we didn't make a reference sample to calibrate the monolayer coverage. Instead we used the calibrations coefficient from previous experiments done in this lab. But this calibration coefficient was determined earlier using another QMB that might have been calibrated a bit different.

Upon addition up to ~0.03ML of SubPc onto the hexagonal network there was not too much of a change and the whole surface was still covered by the same network. Only a few SubPc molecules were observed and trapped inside the pores (*figure 16*). However, with ~0.05ML of SubPc on the sample the hexagonal network partially collapsed and a close packed assembly appeared (AgSub, *figure 17a*). Interestingly, it covered much larger areas (see *figure 43*) than the simple close packed assembly Ag3 (*figure 15*) but looked quite similar. The assembly was not completely regular. This is maybe the reason why it can be stable without changing into the alternating close packed assembly. It is also interesting that nearly no SubPc was observed on this close packed assembly areas. However, at the borders of the close packed assembly, a mobile phase was observed (see *figure 17a*) probably consisting of SubPc. On the remaining parts of the hexagonal network, which was still the dominant assembly, the SubPc proportion inside the pores was still quite low. This corresponds to the fact that the total amount of added SubPc was low. There was no further conversion of the hexagonal network into the close packed assembly observed during the next days. With a higher coverage of ~0.08ML on another sample it seemed that only the close packed assembly remained and the entire hexagonal network collapsed (*figure 17b*).

It was further observed that the SubPc molecules were quite dynamic on the surface. As demonstrated in the presented example (*figures 18*) the mobility was so high, that the SubPc molecules were in a different pore with almost every new scan (207s for 1 scan in *figures 18*). But also more static situations were observed where the SubPc molecules did not change the pores so fast like in the presented example. The high mobility of the SubPc molecules also indicates that the binding in the pores is quite weak. One possible reason is that the interaction of the SubPc with Ag is only weak inside the pores. But the SubPc molecules still prefer the pores compared to other binding locations on the hexagonal network since inside the pore the interaction with Ag is for sure the strongest. Further the point where three pentafluoro-groups come together in the hexagonal network is for sure not optimal since that point has probably a negative potential caused by the fluorine residues which should retract SubPc molecules.

A zoom into the filled pores shows that the SubPc molecules inside the pores are rotating since nearly no details are observed except for a 6-fold symmetry coincident with the pore symmetry (*figures 19*). Height differences that were measured agree well with the literature value of ~5Å height for the SubPc molecule [ref. 13]. This supports the notion that the molecules inside the pores are SubPcs. The motion of the molecules trapped in the pore can be described probably with the image of a rotating umbrella with the grip facing downwards. The Cl-residue is the grip in this image pointing to the Ag surface, like already observed in other experiments with SubPc on Ag(111) [ref. 13].

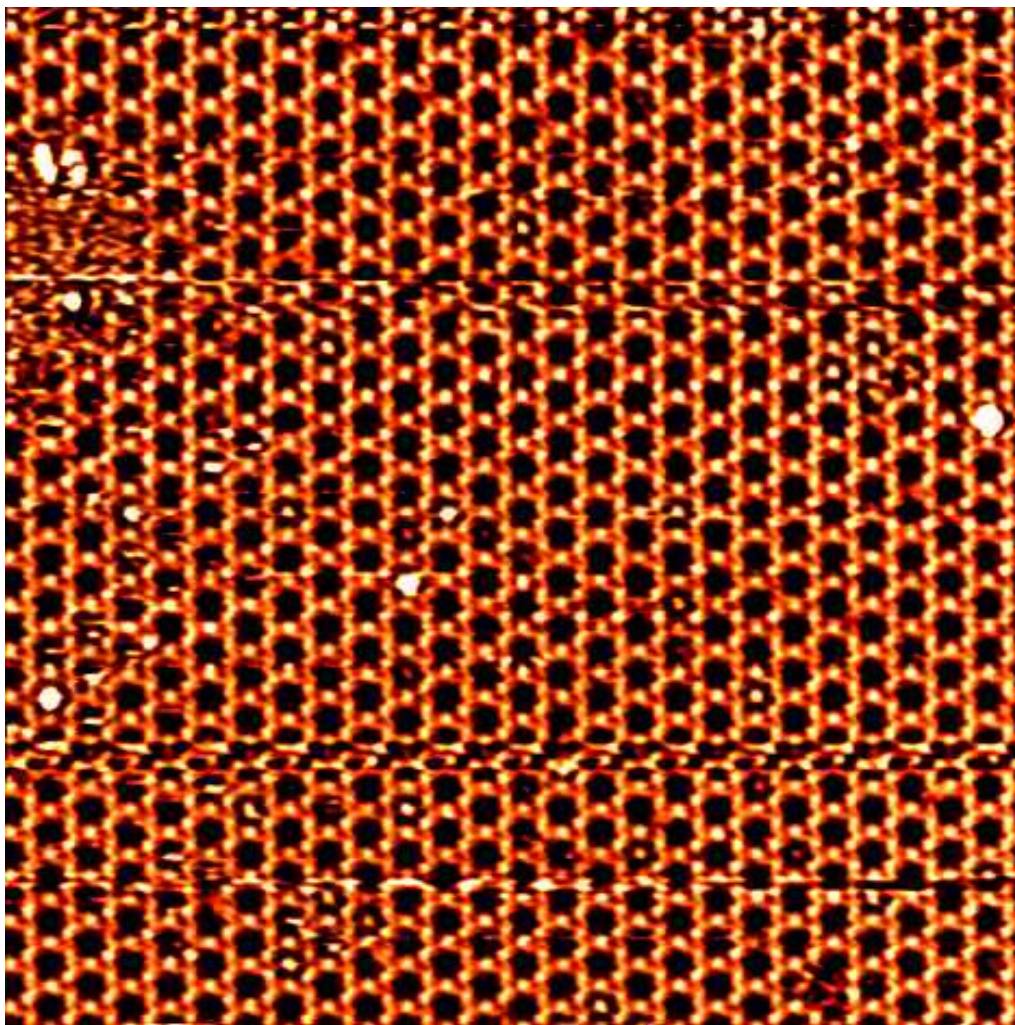


Figure 16: Hexagonal network (90nm\*90nm, I=16pA, U=1.4V, 0.6ML of **1**+0.03ML SubPc, Sample 10c) with 0.03ML of SubPc. Brighter dots are most probably the SubPc molecules trapped in the pores. Darker dots can be molecule **1** itself which can also fit into the pores of its own porous network as single molecule.

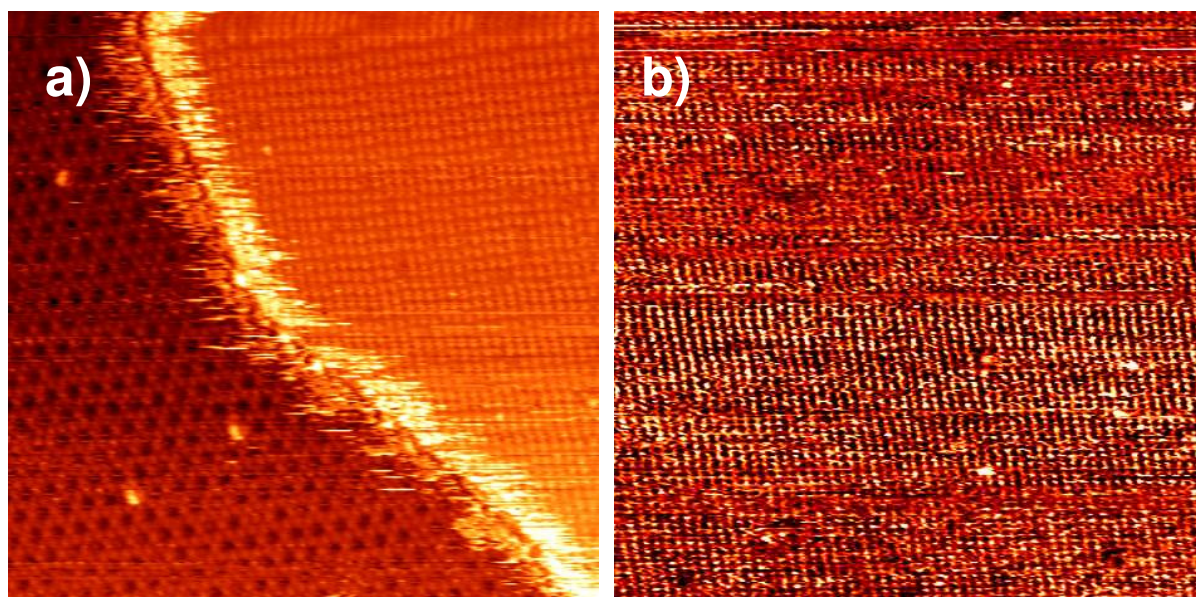


Figure 17: a) STM-image (100nm\*100nm, I=20pA, U=1.2V, 0.6ML of **1**+0.05ML SubPc, Sample 11b): Hexagonal network with ~0.05ML of SubPc. One can see the new type of close packed assembly which is not completely regular and the mobile phase at the borders between the two assemblies. b) STM-image (100\*100nm, I=20pA U=0.8V, 0.45ML of **1**+0.08ML SubPc, Sample 8c): Deposition of 0.08ML of SubPc led to a complete replacement of Ag1 by the SubPc induced close packed assembly phase AgSub.

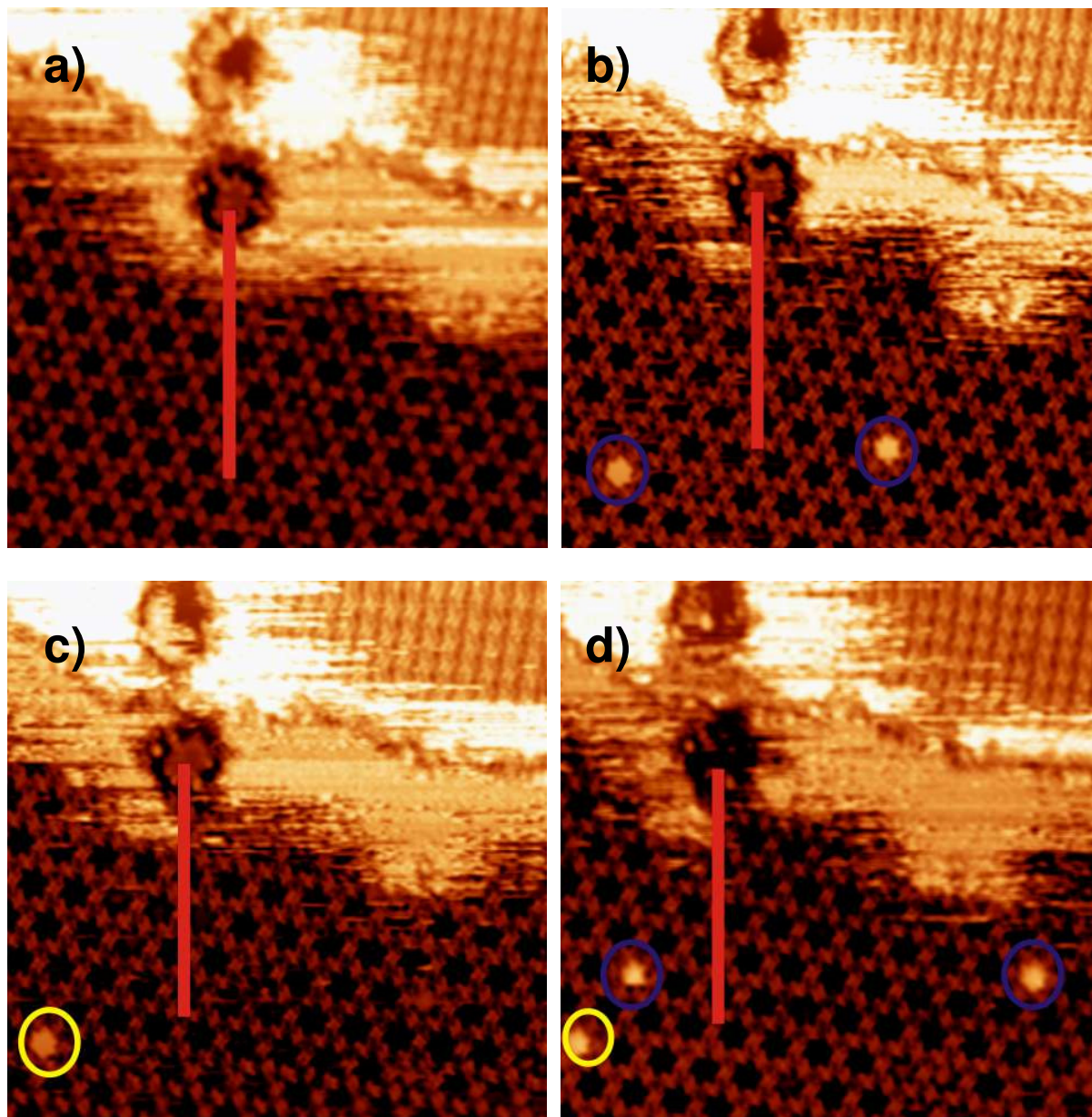


Figure 18: Sequence of STM images (50nm\*50nm,  $I=20\text{pA}$ ,  $U=1.6\text{V}$ , 0.6ML of **1**+0.05ML SubPc, Sample 11b) demonstrating the mobility of SubPc on the hexagonal network of **1**. One can see two defects at the top of the image as orientation marks. The red line has a length of 10nm and is just an additional help for orientation. Blue Circles mark newly appearing SubPc in the pores and yellow circles mark SubPc maintaining the same position. Darker dots might be caused also by **1** filling the pores of its own network. The gas phase between the assemblies serves probably as a reservoir of mobile SubPc molecules. The time between two images was 207 seconds. a) No SubPc molecules observed in the pores. b) Two SubPc molecules fill two pores. c) One SubPc disappeared and one persisted. d) Two new SubPc appeared and the last persisted again.

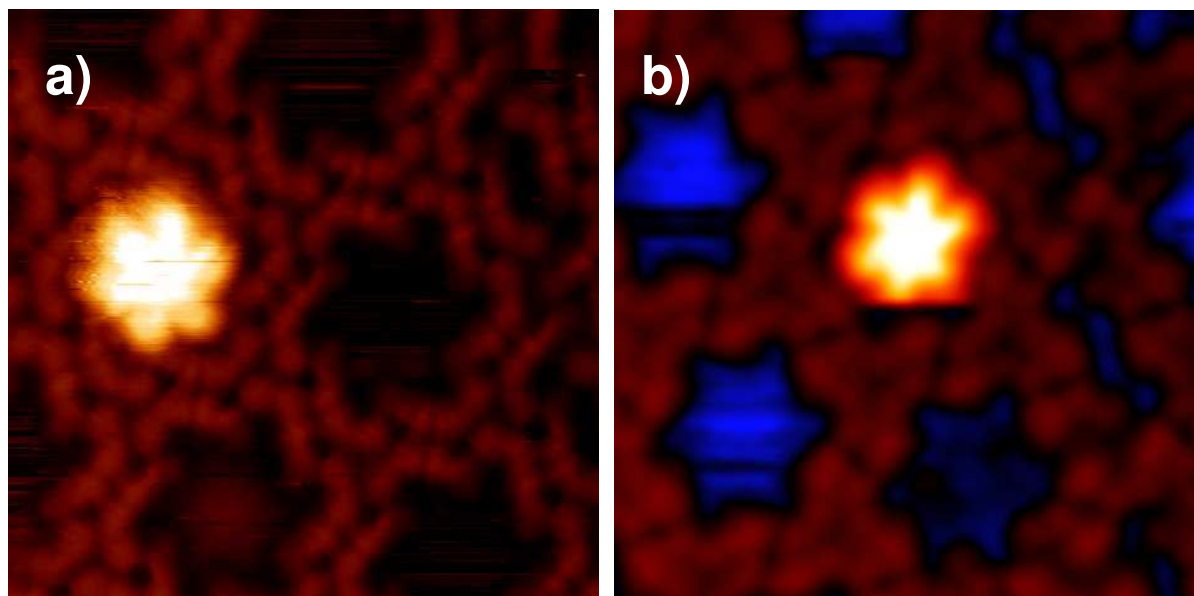


Figure 19: Two high-resolution STM images with different imaging modes (analogue to figures 12a and b). a) High-resolution STM-image (10nm\*10nm, I=20pA, U=1.8V, 0.6ML of 1+0.05ML SubPc, Sample 11b): Hexagonal network with 0.05ML of SubPc. The submolecular structure of the porous network is observed while the SubPc inside does not exhibit such a fine structure except for the 6-fold symmetry which is just observed because the molecule adapts to the space of the pore. b) STM-image (10nm\*10nm, I=20pA U=1.8V, 0.6ML of 1+0.05ML SubPc, Sample 11b): Another imaging mode where the porphyrin bending line [refs. 15,16] is observed again leads also to the conclusion that the SubPc molecule inside the pore is probably rotating.

The close packed assembly which is induced by the presence of a certain amount of SubPc is quite similar to the simple close packed assembly Ag<sub>3</sub>. However it is not restricted to 10 or 15 rows and can form islands that have sizes >100nm\*100nm (as seen on figure 43 where a section of such a large island is shown). The definition of the unit cell for this assembly like we did is not really correct since the assembly is not completely regular. However statistical analysis led us to the conclusion that on a larger scale the irregularities might be distributed in such a way that a unit cell like we defined it still made sense. Since the experiments were done at room temperature it was also not possible to find a more complex unit cell containing more than only one molecule. So the unit cell determined by statistical analysis is not very different from the unit cell of Ag<sub>3</sub> with  $a=1.93\pm 0.02\text{nm}$ ,  $b=2.05\pm 0.07\text{nm}$  and an angle of  $86.6\pm 2.9^\circ$  (figure 20). On a detailed image one can see that this assembly has a lot of defects (figure 21). Along the rows the assembly is quite regular but the rows are not always connected in the same way leading to a non-regular appearance (compare figures 17 and 43). It is quite surprising but it seems that there is probably no SubPc in the unit cell of this assembly. The next remarkable thing is that in our model the rows are opposite to the Ag<sub>3</sub> assembly, connected not via the pentafluoro-groups but with the arms containing the methoxy-group. The reason for this model is that we think that again we observe the methoxy-groups as the brightest spots on the high-resolution images (e.g. in figure 21).

The high number of defects could be explained by lattice mismatches between the close packed assembly and Ag(111). These lattice mismatches could also explain why the simple close packed assembly which was observed without the presence of SubPc was interrupted after about 10 rows or less. Another thing that can be seen clearly is that the arms of the molecule are quite flexible. In this assembly the two arms with the methoxy-group seem to be tilted by coming closer against each other. The force stabilizing this assembly is a bit mysterious since it seems that the rows are connected exactly in the opposite way than observed in all other close packed assemblies on Ag(111) as on Cu(111). The  $\pi$ - $\pi$  interaction between aromatic residues of the arms with the methoxy-group could be the stabilizing factors. The interaction connecting the rows might be the H-Bonding between fluorine and

aromatic hydrogen residues where the different connection types between the rows would correspond to different H-Bonding motives (the same difference as suggested for the difference between Cu1a and Cu1b assembly for the molecule on Cu(111)). Substrate-molecule interactions probably lead to this different behaviour where the H-Bonding seems not to be the assembly determining factor anymore. However, SubPc has an influence for sure since it induces that assembly. The situation is completely different compared to the case of assemblies without SubPc. All in all it seems that the defects are caused by a mismatch of substrate- and molecule-lattices and the observed assembly is a compromise between the molecule-molecule and the substrate-molecule interactions.

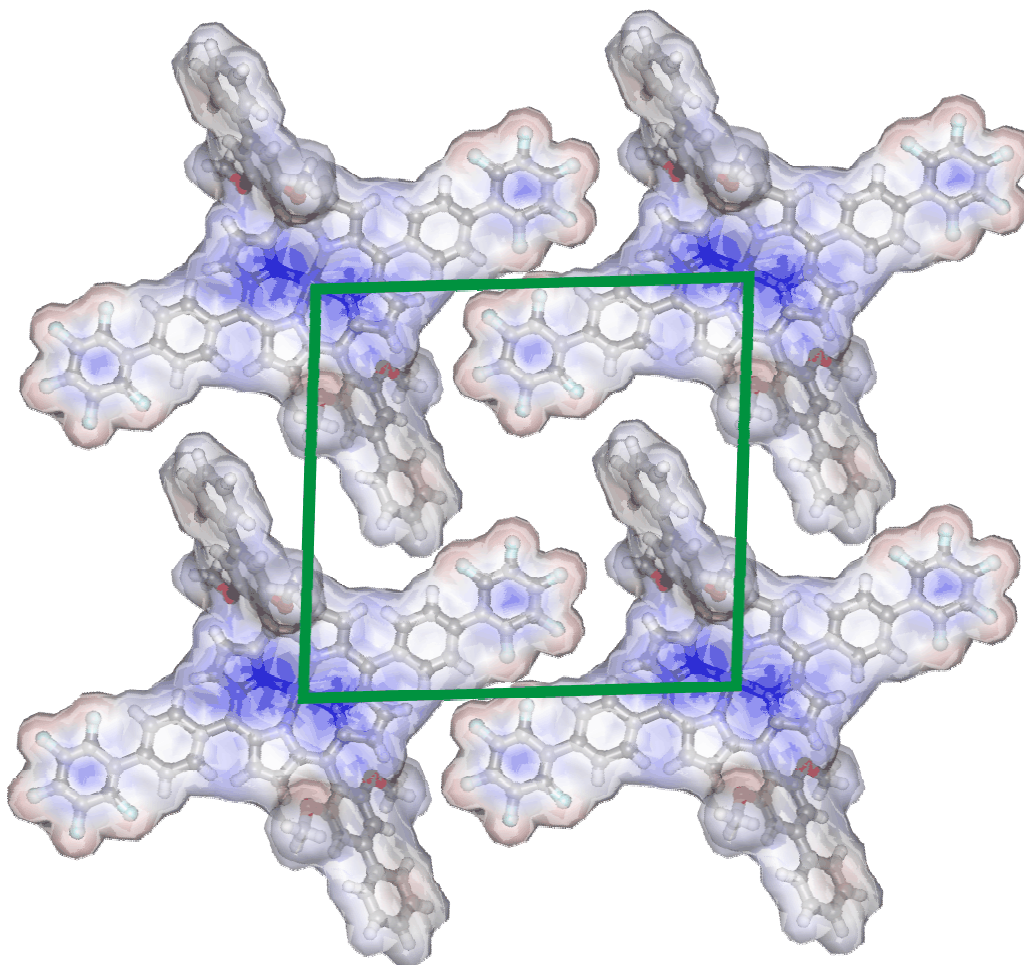


Figure 20: Model of the close packed assembly caused by SubPc influence. Unit Cell vectors:  $a=1.93\pm 0.02\text{nm}$ ,  $b=2.05\pm 0.07\text{nm}$ ; Angle= $86.6\pm 2.9^\circ$ . The arms with the methoxy groups are not tilted in this model, unlike indicated by the high-resolution STM-images.

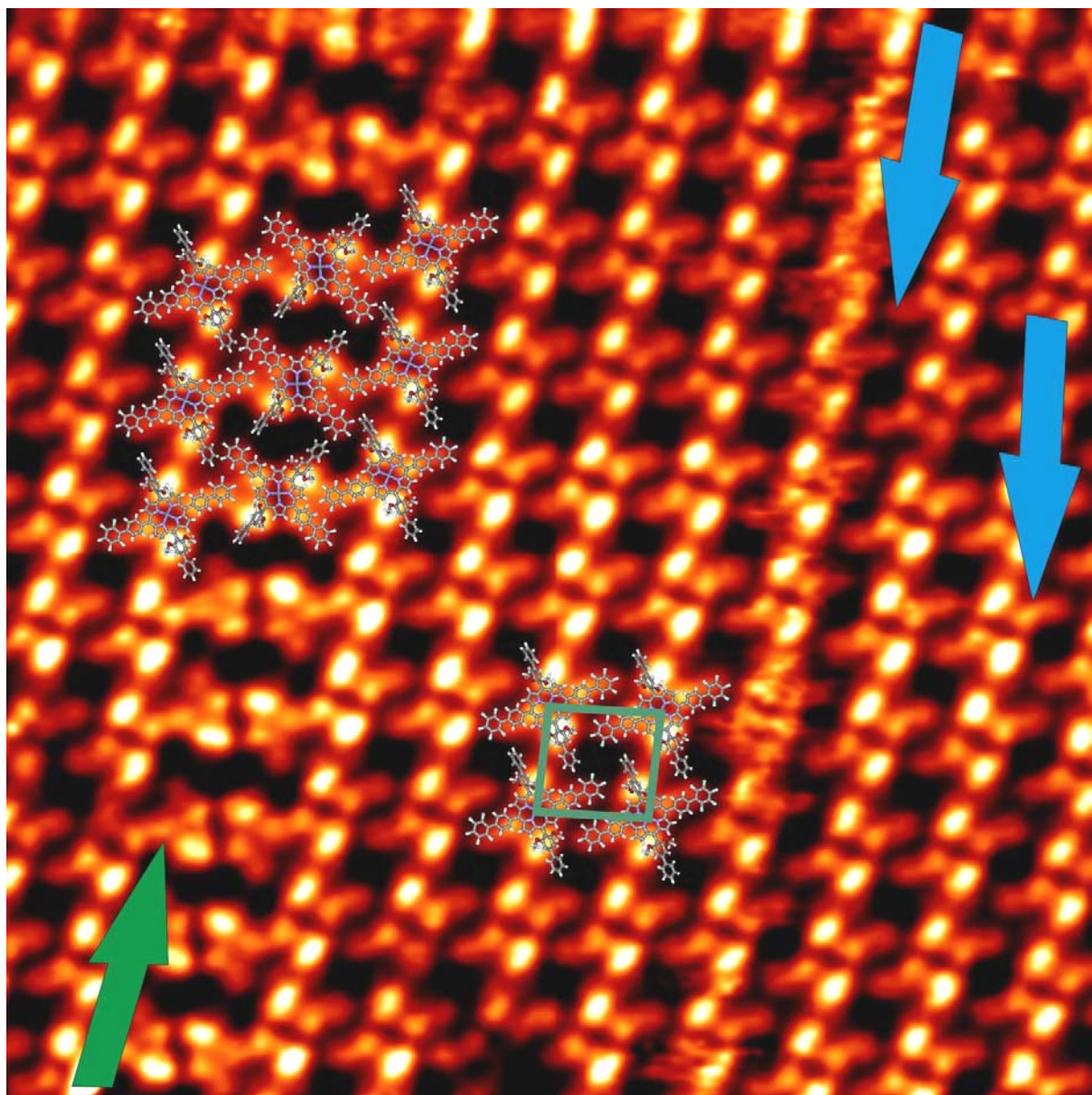


Figure 21: STM-image (20nm\*20nm, I=30pA, U=1.8V, 0.6ML of 1+0.05ML SubPc, Sample 11b) showing the close packed assembly caused by the presence of SubPc. Bright dots are identified as the methoxy groups similar as in imaging modes observed without the presence of SubPc. The porphyrin bending line [refs. 15,16] which can be seen too supports the orientation of the molecules in the model. Blue arrows mark the lines where one can see that the rows in the assembly are not connected always in the same way. Further the green arrow points out a row where the molecules have a different orientation; tilted by  $60^\circ$  from the molecules in the other rows.

To conclude, on Ag(111) we observed 3 different assemblies without SubPc. Probably the close packed assembly observed after annealing at 300°C corresponds to the Ag3 assembly. However this is not confirmed since the resolution was not sufficient for an undoubted identification. Furthermore one assembly was observed with an addition of a certain amount of SubPc. The hexagonal network looks exactly the same with and without SubPc on the surface. The close packed assemblies seem to be affected by substrate-molecule interactions and a mismatch with the substrate lattice in case of the simplest close packed assembly (Ag3). This mismatch would then be compensated by the slightly different architecture of the unit cell in the alternating close packed assembly (Ag2) and compensated by defects in the case of the SubPc induced close packed assembly (AgSub). The arms of the molecule **1** seem to be quite flexible which can be seen on different assemblies and especially in the high-resolution images (see *figures 13,21*).

In the overview (*table 1*) one can see that the porous network has a lower molecule density than the different close packed assemblies which have roughly the same molecule density. So since the hexagonal network is not the densest phase it must be energetically favoured and is not just appearing because of an optimal packing of the molecules.

### 3.1.3. Molecule 1 on Cu(111)

On Cu(111) samples were prepared with a coverage between 0.15 and 1.2ML. Three different types of close packed assembly were found. These 3 assemblies are labelled Cu1a, Cu1b and Cu2 to prevent confusion since especially Cu1a and Cu1b assemblies are described in a very similar way (*table 2*). It might even be that Cu1a and Cu1b are the same assembly, further experiments would be required to confirm or refute this conjecture. We see that the molecular density of Cu2 is much higher than the ones of Cu1a and Cu1b. However, for Cu2 we were only able to determine the unit cell, but we were not able to find a molecular model. So it would be possible that in this assembly even more than 1 molecule per unit cell is present. But this would somehow contradict the observation that Cu2 appeared already below a full monolayer coverage.

		Unit cell vectors		$\sigma$					
		a[nm]	b[nm]	Angle a-b [°]					
Cu1a	Close packed 80°	2.03	2.03	81.8		0.25	0.25	-	0.25
Cu1b	Close packed 90°	1.86	2.01	87.4		0.11	0.07	1.6	0.27
Cu2	High close packed	1.32	2.06	86.5		0.09	0.09	1.8	0.37

Table 2: Assemblies of molecule 1 found on Cu(111). Cu1a parameters were found by LEED measurements and have an error which is much smaller than for the other assemblies. Cu2 Molecule Density corresponds to the assumption of 1 molecule per unit cell.

The most common assembly (Cu1a) was found under nearly all conditions (except for the samples where Cu1b and Cu2 were found) and was in most cases prevalent over the whole surface (*figure 22a*). When the coverage was then increased on the sample a new assembly appeared (Cu2, *figure 22b*) together with a close packed assembly that looked similar (Cu1b) to the assembly which was observed before (*figure 22a*). *Figure 22b* shows now an image of the two assemblies together. Cu2 is clearly higher than Cu1b and first it was not clear if Cu2 is already part of the second layer or not. A further increase of the coverage led to a disorder on the surface except for some small islands of close packed assemblies (*figures 23*). But since the resolution of these images was not good enough, we could not say if this assembly was Cu1a, Cu1b or even Cu2. However when we reached the full monolayer in one shot (and not in several depositions) we saw the second layer without any doubt (*figure 24*).

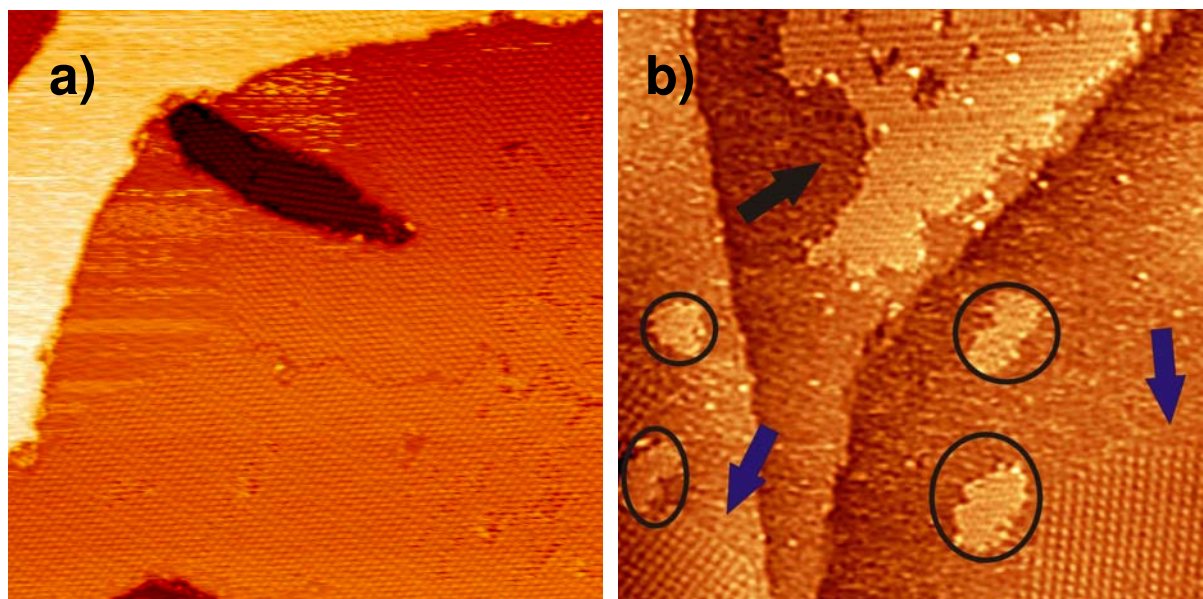


Figure 22: a) Close packed assembly (Cu1a, 150nm\*150nm, I=10pA, U=-1.1V, 0.55ML, Sample 1b) on Cu(111) without a full monolayer. b) Right Image (150nm\*150nm, I=20pA, -1.6V, 0.7ML, Sample 1c) shows coexistence of assemblies Cu1b (pointed out with blue arrows) and Cu2 (black arrow and black circles).

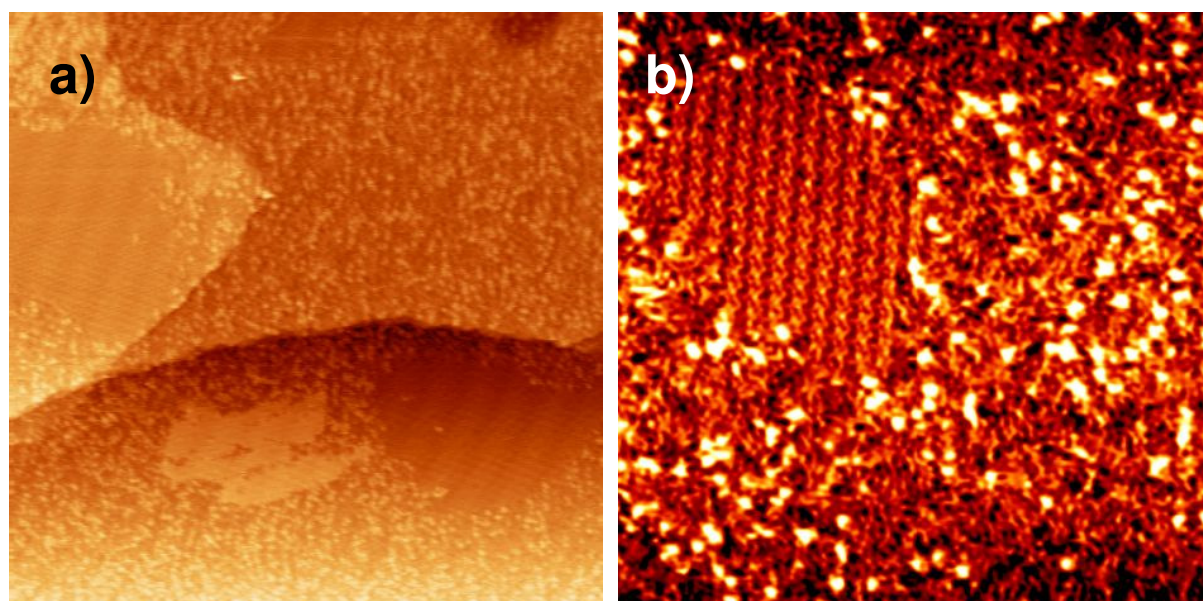


Figure 23: a) Overview (200nm\*200nm, I=22pA, U=-0.9V, 1.2ML, Sample 1e) showing ordered and disordered regions. b) STM-image (50nm\*50nm, I=22pA, U=-0.9V, 1.2ML, Sample 1e): Zoom into a typical ordered region eventually with the Cu1a or Cu1b phase.

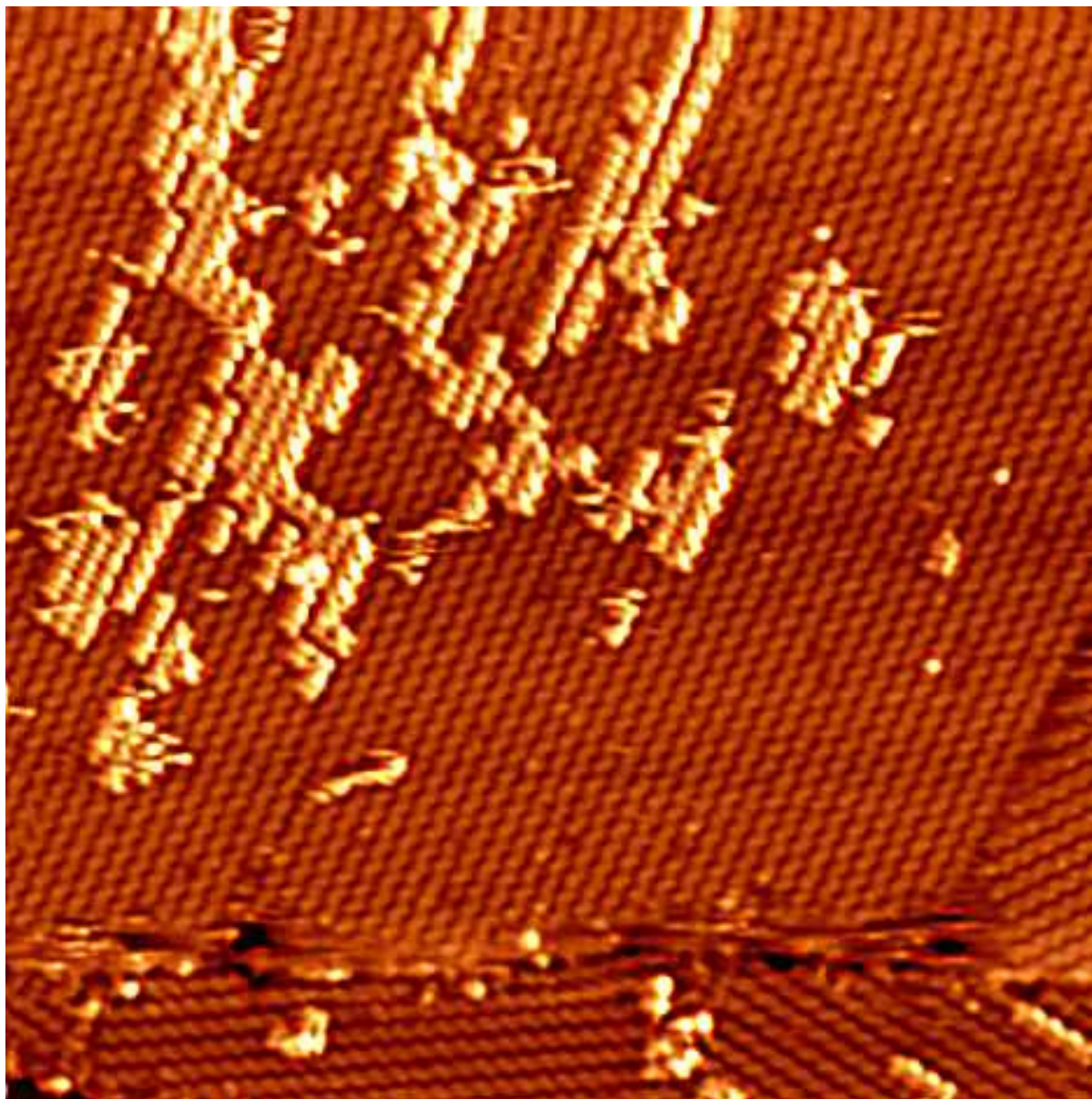


Figure 24: STM overview (100nm\*100nm, I=15pA, U=1.1V, 1.05ML, Sample 5a) with a step edge showing the second layer on Cu1a.

The statistical analysis of STM images indicated the unit cell vectors of Cu1a to be  $a=1.94\pm 0.07\text{nm}$ ,  $b=2.06\pm 0.08\text{nm}$  with an angle of  $80.9\pm 2.2^\circ$ . Results from LEED-measurements ended in a slight difference of the unit cell vectors with  $a=b=2.03\text{nm}$  with an angle of  $81.8^\circ$  (figure 25a; detailed LEED results following in the specific sub-chapter). The model fits well into the high resolution images (figure 26a). We were also able to resolve the structure of the second layer which seems to be slightly displaced with respect to the first layer while having the same structure as the first layer (figure 26b).

One remarkable thing with the LEED result for the unit cell is that the unit cell vectors are the same even if the molecule itself is not a square, having a length of  $\sim 2.7\text{nm}$  and a width of  $\sim 2.6\text{nm}$ . The commensurability of the first layer with the substrate, in combination with the fact that the unit cell doesn't match the asymmetry of the molecule, indicates a strong influence of the substrate on the assembly.

The difference of the assembly Cu1b from Cu1a was only minimal with unit cell vectors  $a=1.86\pm 0.11\text{nm}$ ,  $b=2.01\pm 0.07\text{nm}$  with an angle of  $87.4\pm 1.6^\circ$  (figure 25b). But we think that in the case of Cu1b the two vectors  $a$  and  $b$  are indeed different. In analogy to Cu1a also Cu1b should probably be commensurate with the substrate. The identification of Cu1b was very

difficult and it is not clear if it is coexisting with Cu1a in some cases or only present together with Cu2.

However just by theoretical considerations we were able to construct the difference between Cu1a and Cu1b but it was difficult to confirm this exactly since better images especially of Cu1b were missing. Basically there is only one image of Cu1b in a useful resolution (figure 27).

The difference between Cu1a and Cu1b seems to be that in Cu1a the pentafluoro-groups interact mostly with each other due to hydrogen bonds which results in a very small pore in the centre of the unit cell. Cu1b seems to have stronger interactions between the pentafluoro-group and the neighbouring peripheral phenyl groups of the methoxy arm. Probably they are also of an H-Bonding kind with nearly no space in the centre of the unit cell.

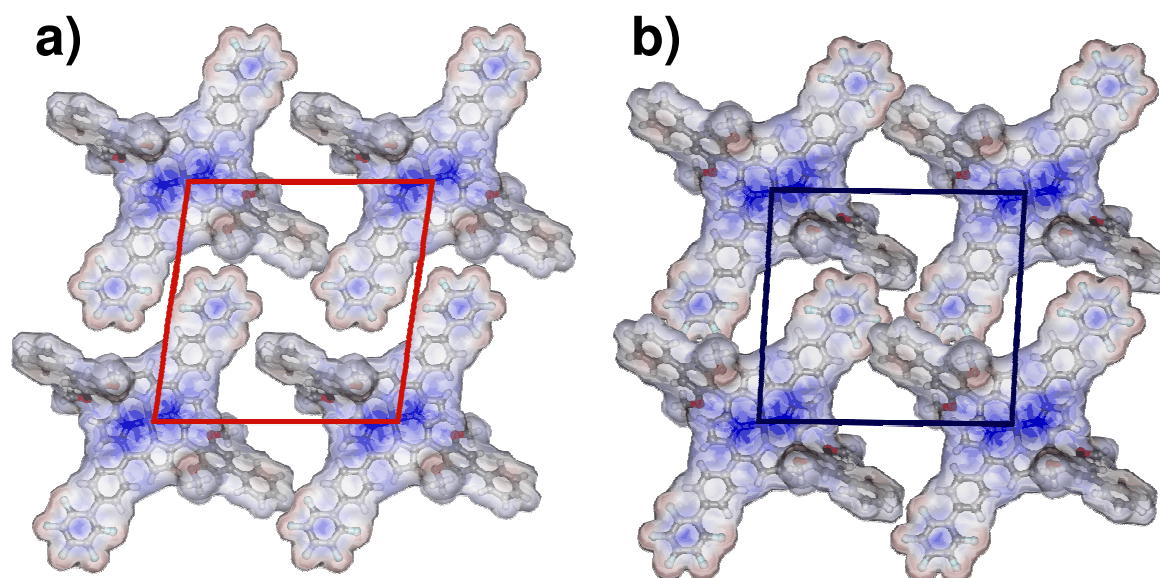


Figure 25: a) Model of close packed assembly Cu1a. The arms of the pentafluoro-group come quite close together and form H-Bonds together. Unit Cell vectors:  $a=1.94\pm 0.07\text{nm}$ ,  $b=2.06\pm 0.08\text{nm}$ ; Angle= $80.9\pm 2.2^\circ$ . b) Model of close packed assembly Cu1b. The arms of the pentafluoro-group have more distance here between each other. Unit Cell vectors:  $a=1.86\pm 0.11\text{nm}$ ,  $b=2.01\pm 0.07\text{nm}$ ; Angle= $87.4\pm 1.6^\circ$ .

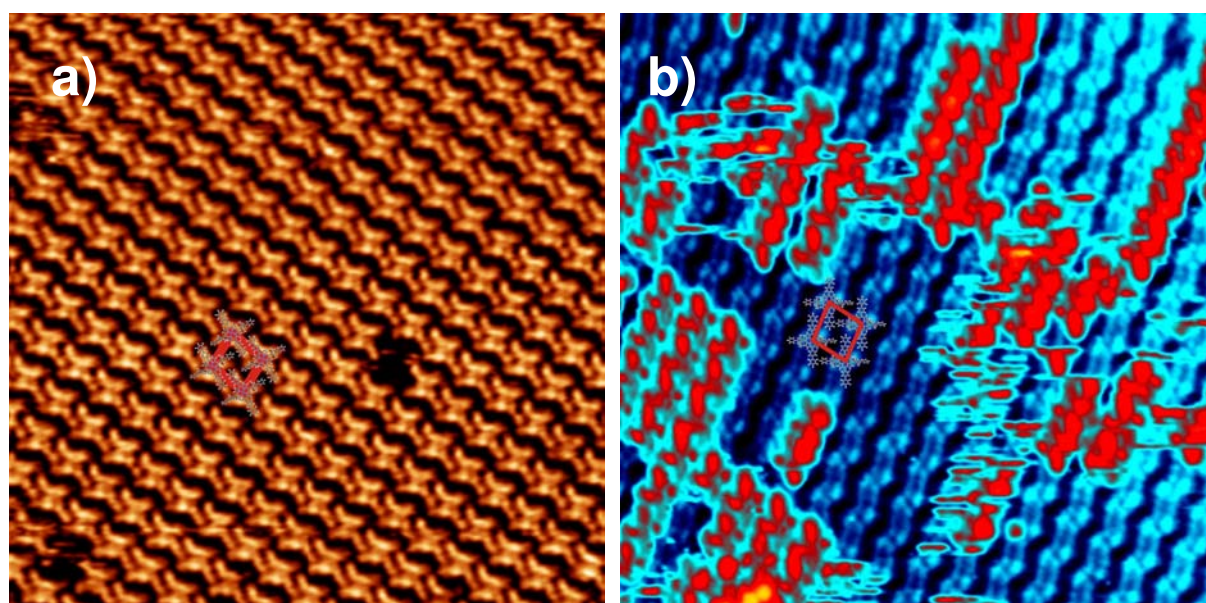


Figure 26: a) High-resolution STM-image of Cu1a (30nm\*30nm,  $I=20\text{pA}$ ,  $U=1.4\text{V}$ , 0.7ML, Sample 2b) assembly on Cu(111). b) High-resolution STM-image of Cu1a (30nm\*30nm,  $I=15\text{pA}$ ,  $U=1.1\text{V}$ , 1.05ML, Sample 5a) where the second layer is already observed.

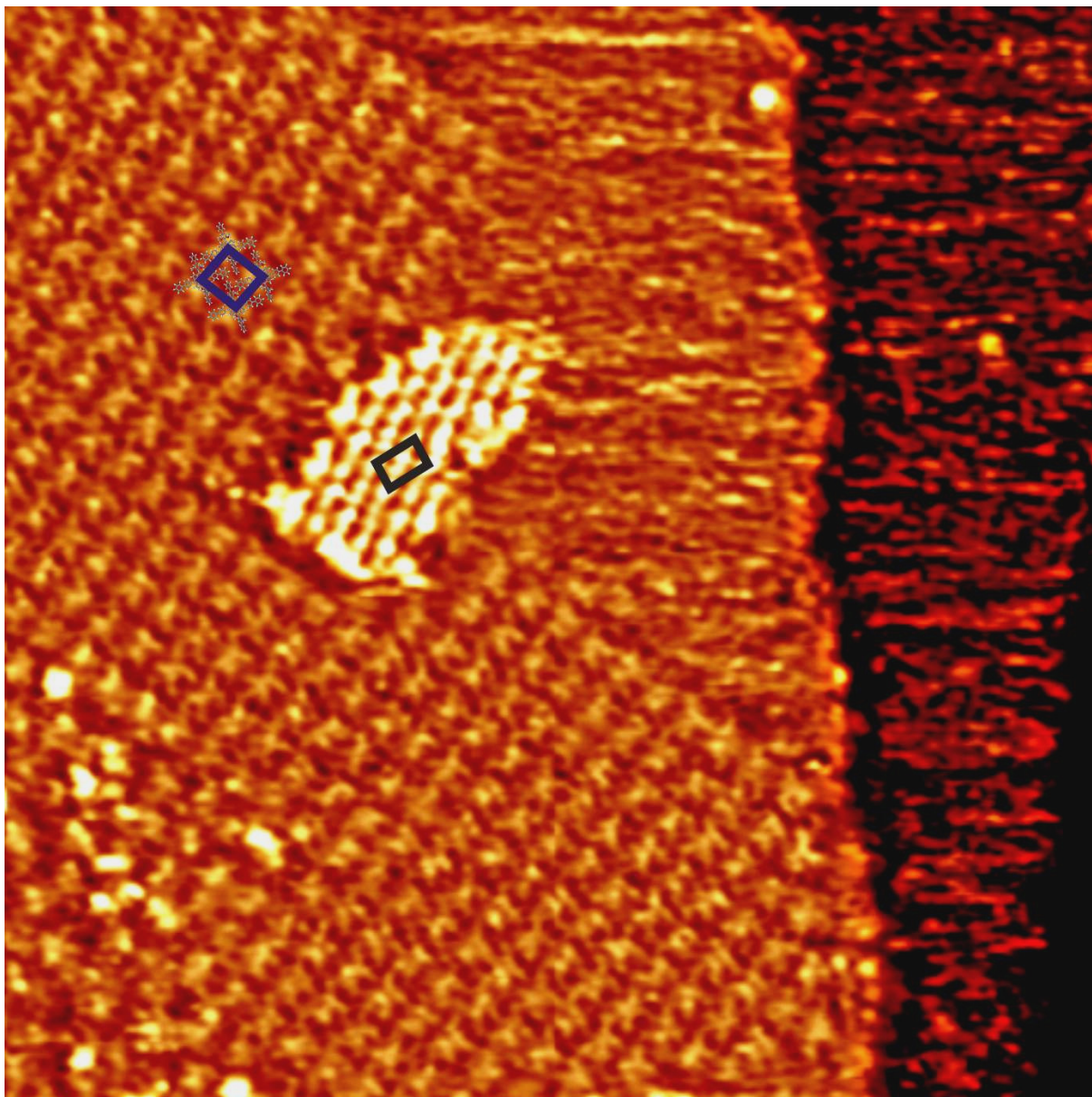


Figure 27: Detailed STM image (50nm\*50nm, I=20pA, U=-1.6V, 0.7ML, Sample 1c) showing Cu1b and Cu2 close to a step edge. The unit cell of Cu1b is shown in blue, the unit cell of Cu2 is shown in black. Unfortunately one cannot see the exact orientation of the molecules in Cu1b and Cu2.

For the last assembly Cu2 we couldn't find a model where the molecules lie flat on the surface without any overlap. The vectors for the unit cell were  $a=1.32\pm 0.09\text{nm}$ ,  $b=2.06\pm 0.09\text{nm}$  with an angle of  $86.6\pm 1.8^\circ$ . Since this assembly was only observed on 1 sample where the molecules were added sequentially it could be also more complicated to understand how this assembly is formed. At least we can say that the molecules are probably standing upright, stabilizing each other. The assembly also has a higher density than the close packed assemblies Cu1a and Cu1b. We see (*figures 28*) that the pattern is quite regular and has a lot of defects. It was also not possible to identify a single molecule at the borders of the assembly.

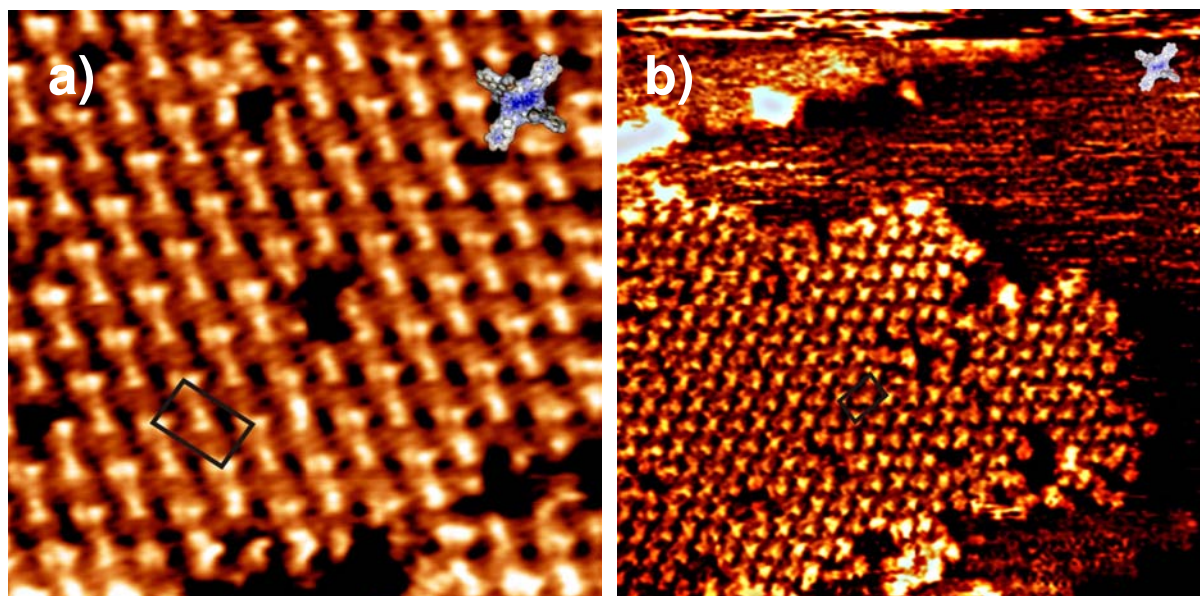


Figure 28: High resolution STM-images of Cu<sub>2</sub>. The unit cell of Cu<sub>2</sub> is denoted in black for both images. A model of molecule **1** is placed in the top right corner to visualize the dimensions. a) STM-image (15nm\*15nm, I=20pA, U=-1.6V, 0.7ML, Sample 1c) of Cu<sub>2</sub> assembly. b) Another STM-image (30nm\*30nm, I=20pA, U=-1V, 0.7ML, Sample 1c) with different imaging mode of the Cu<sub>2</sub> assembly. The unit cell of Cu<sub>2</sub> is denoted in black for both images.

In conclusion, three assemblies were identified on Cu(111), where especially between Cu1a and Cu1b it's very difficult to decide because they are easy to mix up. Cu<sub>2</sub> is also difficult to interpret since it was observed only on one sample. The conditions to get the Cu<sub>2</sub> assembly might be important.

### 3.1.4. LEED Results for molecule **1**

As already mentioned, the close packed assembly Cu1a which we observed on Cu(111) was also investigated by LEED-measurements. We were able to relate the surface structure to the molecular superstructure. The obtained matrix for the superstructure is the following:

$$\begin{pmatrix} 9 & 3 \\ 3 & 9 \end{pmatrix}$$

From the fact that the unit cell vectors *a* and *b* in Cu(111) have a length of 0.256nm we were able to determine the unit cell vectors of the molecular superstructure. The vectors for the superstructure were *a*=*b*=2.03 nm with an angle of 81.8°. The lattice of the superstructure has an angle against the surface lattice of 19.1°. Unfortunately we were not able to observe the molecule lattice and the substrate lattice at the same energy on the LEED-screen. But by simulating the LEED-pattern (*figure 29a*) we were able to determine the relationship between the molecule lattice which was observed between 5eV and 25eV on the fluorescent LEED-screen (*figures 30,31*) and the substrate lattice which appeared between 60eV and 80eV

(figure 29b). The reason for this large energy difference between the appearances of these two structures on the LEED-screen lies in the large dimension difference of the substrate lattice and the superstructure.

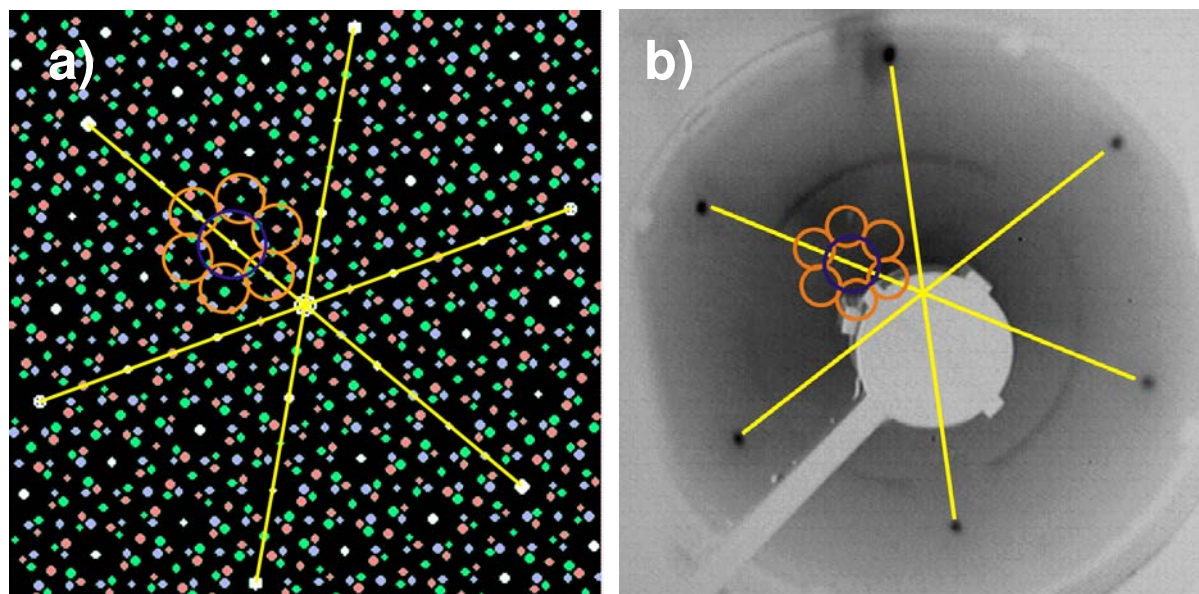


Figure 29: LEED patterns of Cu<sub>1</sub>a assembly from **1** on Cu(111). Different colours refer to different domains of the molecule assembly. White dots refer to all domains and big bright dots refer to the substrate. Yellow lines indicate the principle directions of the substrate. Blue and yellow lines highlight symmetries of the pattern. a) Simulated LEED-pattern. b) LEED-pattern taken with energy of 65eV where only substrate spots could be observed (Sample 5a).

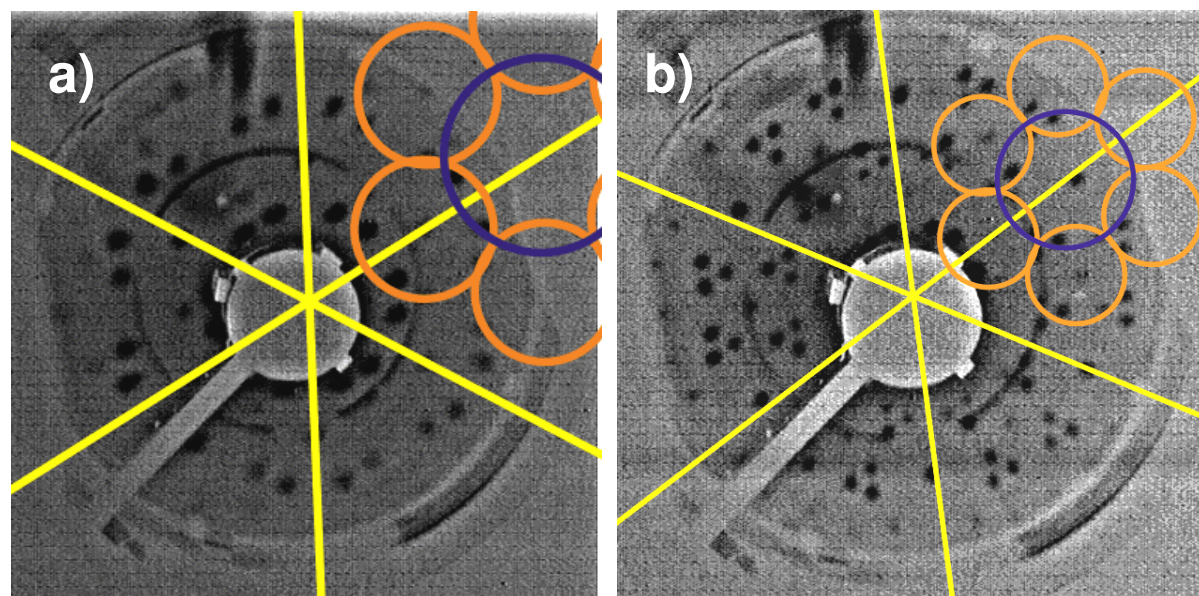


Figure 30: Results from LEED-measurements using the same lines and circles to highlight symmetries of the assembly Cu<sub>1</sub>a from **1** on Cu(111) (Sample 5a). a) LEED-pattern taken with energy of 4eV. b) LEED-pattern taken with energy of 10eV.

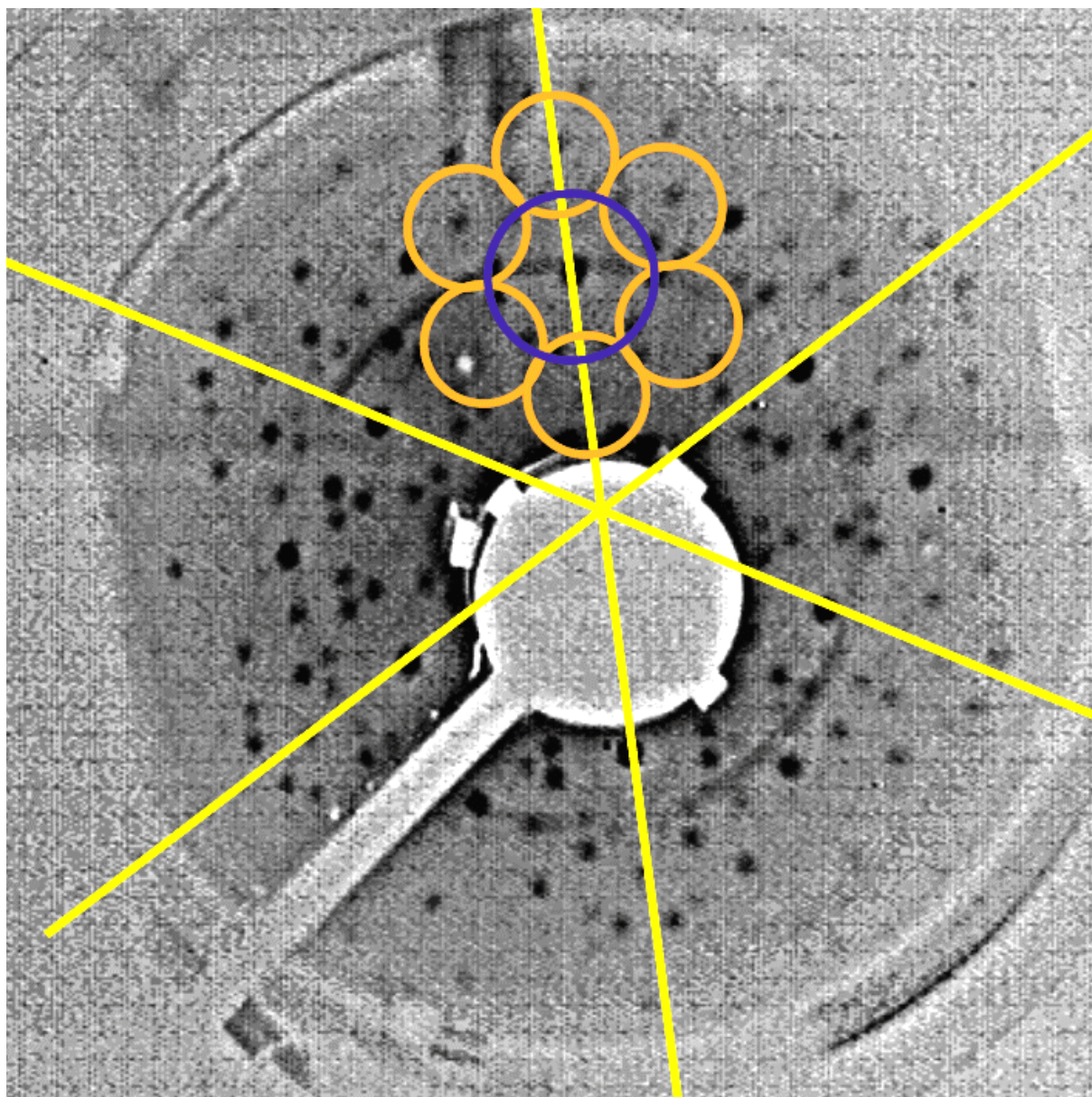


Figure 31: LEED-pattern of the same experiment with energy of 20eV (Sample 5a).

### 3.2. Porphyrin derivative 2

Molecule **2** was deposited by evaporation at temperatures around 650K. The deposition rates were between 0.1 and 0.5ML/min. It was difficult for this molecule to determine the real coverage since on Ag(111) as well as on Cu(111) problems appeared when we scanned with a coverage close to a full monolayer. So the determined coverages for this molecule could have an error of about  $\pm 50\%$ .

#### 3.2.1. Molecule 2 on Ag(111)

On Ag(111) two different samples were prepared with a coverage of 0.35ML and 0.55ML. The STM measurements revealed only a close packed assembly.

On a larger scale we didn't get a lot of good images but one could see clearly that at the lower coverage of 0.35ML only the close packed assembly was present (*figure 32a*). At the higher coverage of 0.55ML the scanning conditions were much worse but still some close packed assembly was detected (*figure 32b*). The rest of the surface had no more observable ordering. Fortunately we were able to compare the close packed assembly which we see at 0.55ML to the ones we see at 0.35ML and we were able to classify them as the same assembly since the unit cell parameters were equal.

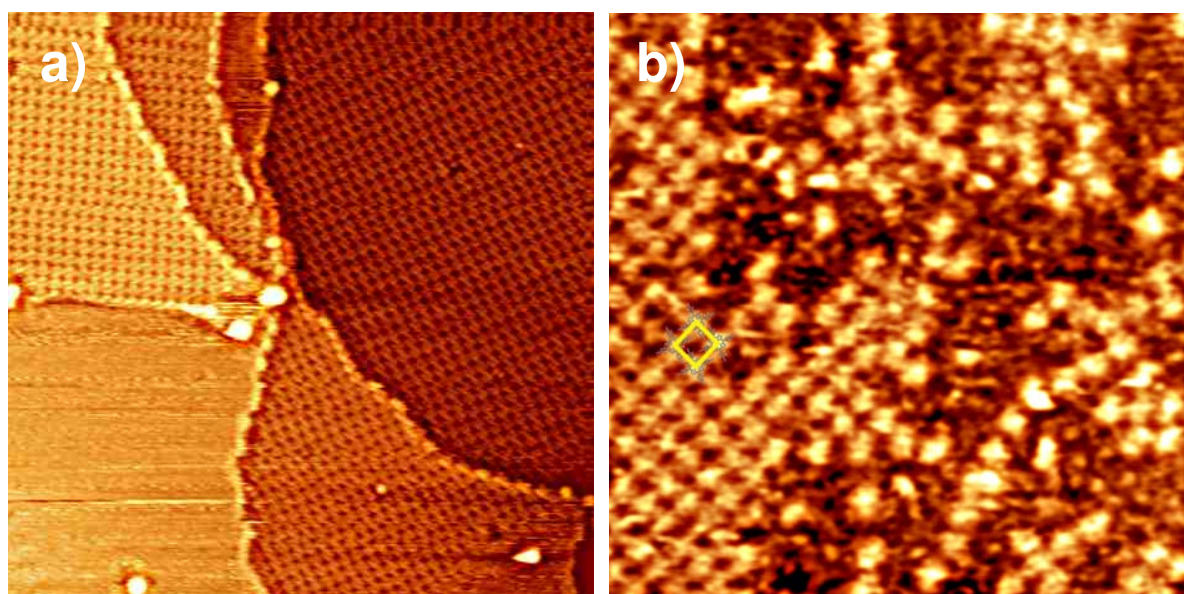


Figure 32: a) STM-image (70nm\*70nm, I=14pA, U=1.4V, 0.35ML, Sample 4a) of the close packed assembly at a low coverage. b) STM-image (30nm\*30nm, I=20pA, U=0.8V, 0.55ML, Sample 1b) of the close packed assembly at a higher coverage. The unit cell is denoted in yellow.

The unit cell vectors of the close packed assembly are  $a=1.54\pm 0.06\text{nm}$ ,  $b=1.63\pm 0.07\text{nm}$  with an angle of  $87.5\pm 1.9^\circ$  (*figure 33a*). Since molecule **2** has a 4-fold symmetry one could think of a square lattice model based on the values that we got from the statistical analysis. And indeed, a square lattice model would fit into the statistical results for the unit cell if we also consider the standard deviation. Nevertheless, the difference between the unit cell vectors could also depend on the lattice mismatch between the molecules and the substrate. The four peripheral nitrogen residues each pointing directly to a peripheral phenyl-ring of the neighbouring molecules stabilize the structure, most probably by H-bonding. The H-bonding occurs probably between the nitrogen residue and one of the two closest hydrogen residues on the neighbouring phenyl-ring. The other possibility would be an H-bonding between the nitrogen residues and the next hydrogen that is part of the porphyrin core. It is difficult to

decide where this H-bonding occurs, since the resolution of the acquired images is insufficient.

On the high resolution STM-image (*figure 33b*) one can see that the model fits quite nicely. However, turning the molecules by  $45^\circ$  also fits the image. We chose the former version because we assign the bright dots to the phenyl-rings and not to the porphyrin core since the distance between the dots of one molecule fits better to the distance between phenyl-rings.

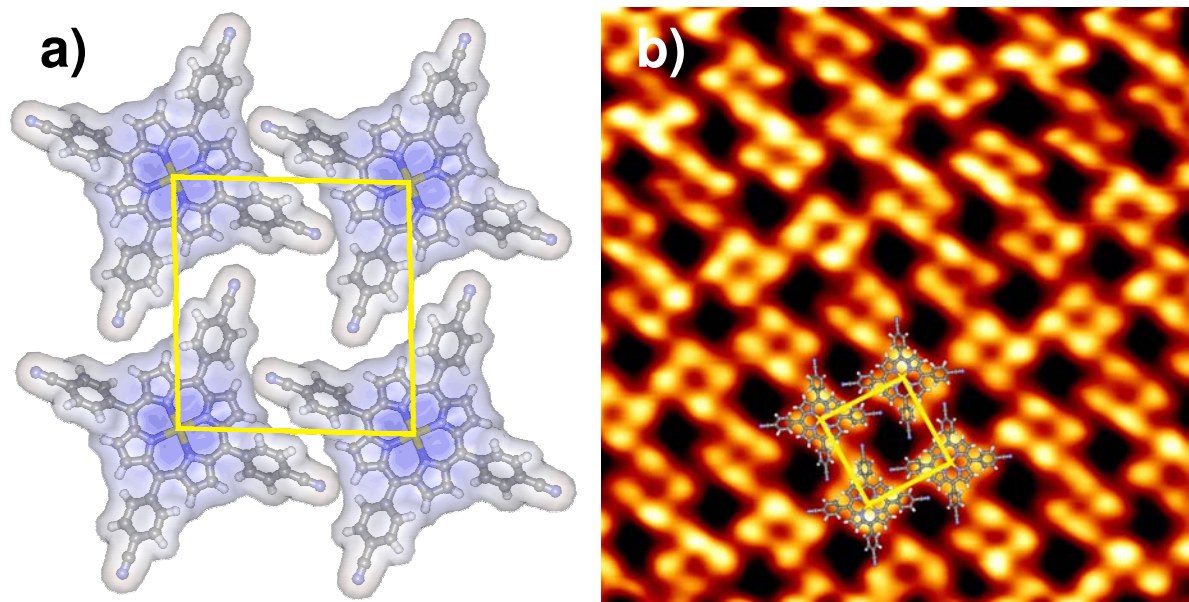


Figure 33: a) Model of molecule **2** close packed assembly on Ag(111). Unit cell vectors:  $a=1.54\pm 0.06\text{nm}$ ,  $b=1.63\pm 0.07\text{nm}$ ; Angle= $87.5\pm 1.9^\circ$ . b) High resolution STM-image ( $10\text{nm}\times 10\text{nm}$ ,  $I=14\text{pA}$ ,  $U=1.4\text{V}$ ,  $0.35\text{ML}$ , Sample 4a) of close packed assembly on Ag(111). Bright dots are assigned to the peripheral phenyl-rings.

### 3.2.2. Molecule 2 on Cu(111)

On Cu(111) four different samples were prepared and investigated with coverages between 0.45ML and 1 ML. Three different types of assemblies were observed. *Table 3* shows an overview of the assemblies of molecule 2 which were found on Cu(111) including the standard deviations  $\sigma$  from the statistics which were done on the available STM data.

	Unit cell vectors		$\sigma$ Angle a-b [°]	a [nm]	b [nm]	Angle a-b [°]	Molecule Density [molecules/nm <sup>2</sup> ]
	a[nm]	b[nm]					
Porous network (triangles)	2.90	2.90	60	-	-	-	0.41
Close packed low coverage	1.56	2.16	69.4	0.08	0.08	2.6	0.32
Close packed high coverage	1.31	1.53	85.5	0.07	0.08	3.1	0.50

Table 3: Assemblies of molecule 2 found on Cu(111).

At a coverage far below a ML, a porous network was predominant (*figure 34a*). Moreover, there were also some very small areas covered with a close packed assembly (*figure 34b*). Annealing at 150°C didn't change the structures on the surface.

When the coverage was increased the sample lost some of its ordering. The porous network was still observed but there were also areas without any observable ordering. At a coverage above 0.6ML a new type of close packed assembly appeared (*figure 35*). Finally at a coverage of 1ML, large areas were covered with a mobile gas phase (*figure 36a*). Annealing up to 300°C resulted into a less ordered structure (*figure 36b*). One can see in this example that there are still small areas having a close packed order. However these regions did not exceed over 10 by 10 molecules and had usually only dimensions in the region of something like 3 by 3 molecules or 2 by 5 molecules. We were not able to determine if these ordered regions are all of the same type. It seems that these structures do not correspond to any of the 3 assemblies which are described in *table 3*.

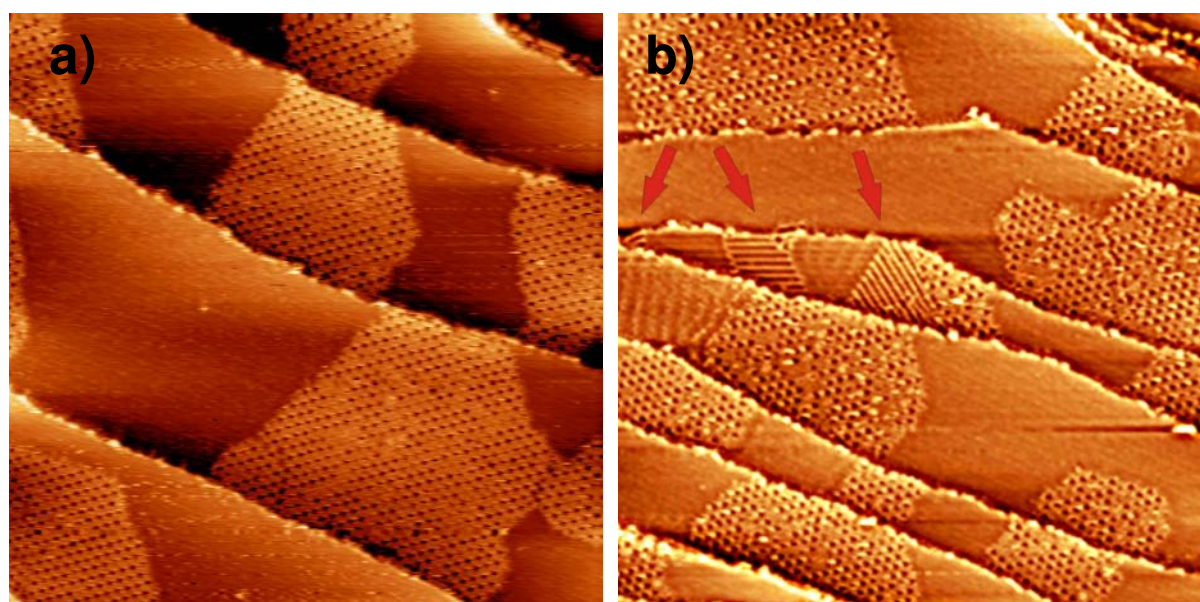


Figure 34: a) STM-overview at lower coverage (160nm\*160nm, I=20pA, U=2.2V, 0.55ML, Sample 5b). b) Another STM-overview (160nm\*160nm, I=20pA, U=2.2V, 0.55ML, Sample 5b) showing some of the rare close packed assemblies which were observed (pointed out by red arrows). The close packed assembly pointed out by the right red arrow was next to the porous network and it built an island together with this close packed assembly.

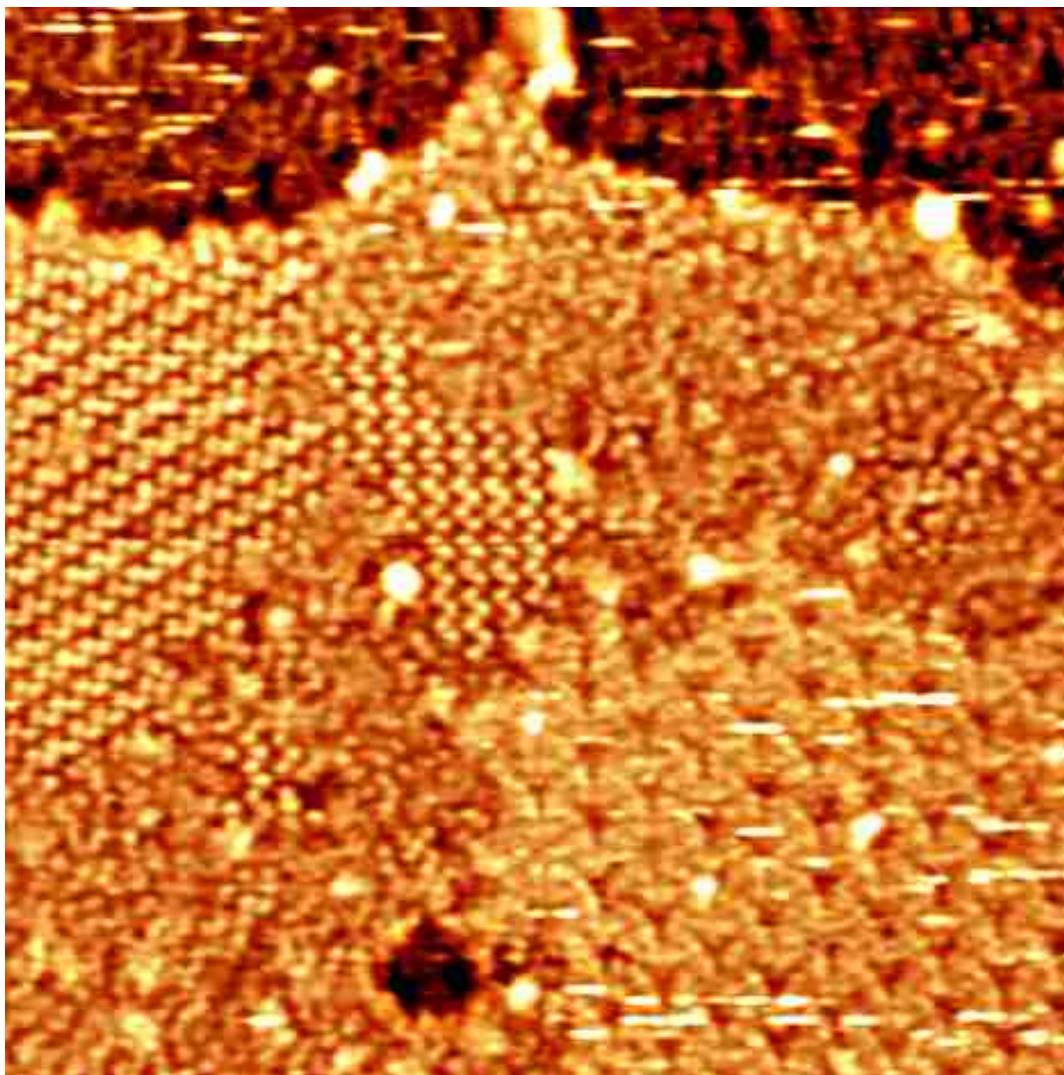


Figure 35: Overview at higher coverage (40nm\*40nm, I=10pA, U=1.6V, 0.7ML, Sample 3b) showing a coexistence of the triangular pores with the new close packed assembly.

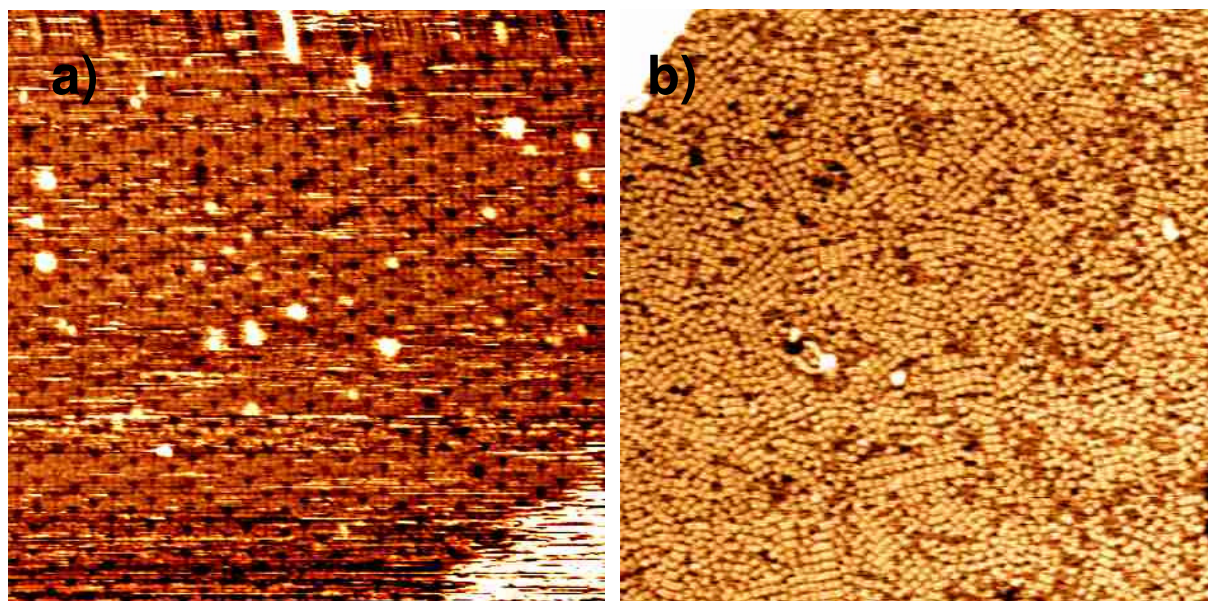


Figure 36: a) STM-overview after annealing at 150°C with higher coverage (80nm\*80nm, I=14pA, U=1.6V, 1ML, Sample 2c). One can see that also some pores are probably filled by molecule **2** itself (like in [ref. 14]). b) Overview (100nm\*100nm, I=11pA, U=-1.5V, 1ML, Sample 2d) after annealing up to 300°C. The triangular pores are not observed anymore.

After statistical analysis the unit cell vectors of the porous network were determined to be  $a=2.78\pm 0.25\text{nm}$ ,  $b=3.02\pm 0.15\text{nm}$  with an angle of  $61.4\pm 3.0^\circ$ . Like in the case of the hexagonal network of molecule **1** on Ag(111) we chose the unit cell vectors to be  $a=b$  with an angle of  $60^\circ$  and a value of  $a=b=2.9\pm 0.25\text{nm}$  because of symmetrical reasons (*figure 37*). Like in the case of the hexagonal network of molecule **1** on Ag(111) we also had to estimate the error based on the statistics and the Van der Waals surface of the molecules. The model also indicates that the molecules are not lying completely flat on the surface because the Van der Waals surfaces overlap. Probably the core of the molecules is bent slightly, which leads to a more compact assembly than one would expect from the molecule dimensions.

Probably substrate-molecule interactions are the reason for the formation of this assembly with a 3-fold symmetry. The molecules around the pore are tilted against each other by  $30^\circ$ . The network might be stabilized by hydrogen-nitrogen interactions between peripheral nitrogen residues and hydrogen residues of the porphyrin core. Unfortunately there is some distortion in the high resolution images caused by drift, but it is still possible to superimpose the molecular model onto the images (*figure 38*). Further it can be seen that the pores have a triangular shape. There is additionally a small pore observed in these high resolution images. Since the pores have shape of an equilateral triangle we will describe the pore dimension as the distance from vertex to the midpoint of the opposite side and call it "pore diameter". The pore diameter of the big pore in the centre of the unit cell is  $\sim 1-1.5\text{nm}$ , the diameter of the 6 small pores which surround one big pore is  $\sim 0.5-0.7\text{nm}$ . At all 3 edges of the big pore there are two cyano-groups close together. The size of the big pore was difficult to determine from the STM data since the cyano-groups are probably not seen there. The big pore might have some flexibility allowing molecules with a diameter of more than  $1.5\text{nm}$  fit inside (like e.g. molecule **2** itself).

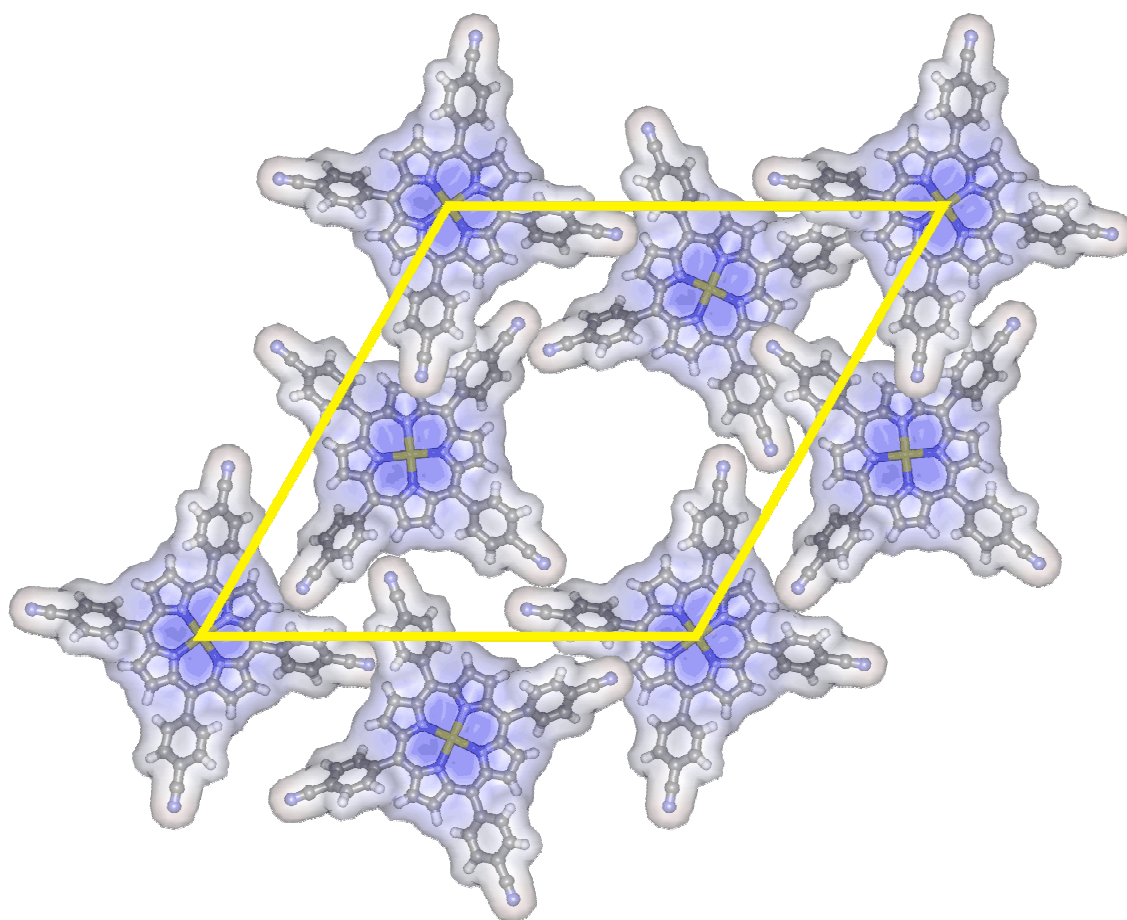


Figure 37: Model of the porous network on Cu(111). Unit cell vectors:  $a=b=2.9\pm 0.25\text{nm}$ ; Angle= $60^\circ$ . The Van der Waals surfaces are slightly overlapping which indicate that the porphyrin core might be a bit tilted.

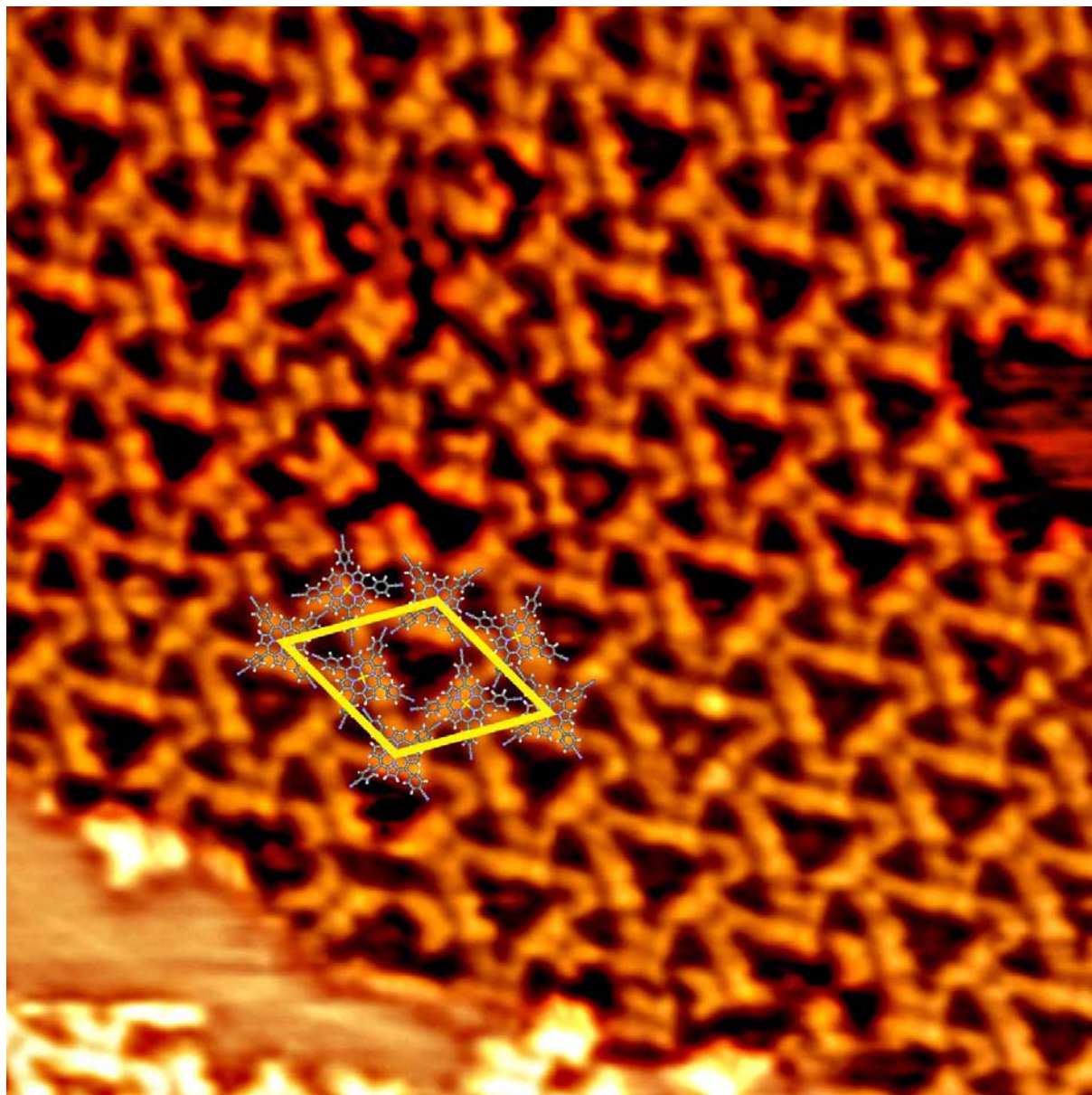


Figure 38: High-resolution image (20nm\*20nm, I=20pA, U=2V, 0.55ML, Sample 5b) of the porous network with triangular pores. Small defects are visible like e.g. above the position where the molecular model is placed.

The normal close packed assembly on Cu(111) was a bit different from the one seen on Ag(111). It didn't exhibit a 4-fold symmetry one would expect not considering the substrate influence. One can see clearly ordering into parallel rows. The reason was probably substrate-molecule interactions which were stronger than molecule-molecule interactions. The unit cell vectors were  $a=1.56\pm 0.08\text{nm}$ ,  $b=2.16\pm 0.08\text{nm}$  with an angle of  $69.4\pm 2.6^\circ$  (figure 39a). The high resolution images also indicate that probably only in the rows the molecular interaction plays a role (figure 39b).

The third assembly which also looks like a close packed we could not really understand. It looks like the molecules are much closer together in that case but on the other hand the apparent height is the same or even lower than in the porous network (as can be roughly seen already on figures 35). It might be that the porous network which is seen aside that special close packed assembly is already a second layer. In that case the special close packed assembly would consist of molecules which stand up from the surface (like in [ref. 5] with a similar molecule). Unfortunately we were not able to observe pure metal next to these assemblies (figures 40). It was also not possible to determine the structure of these special

close packed assemblies. The unit cell vectors for this assembly were  $a=1.31\pm 0.07\text{nm}$ ,  $b=1.53\pm 0.08\text{nm}$  and the angle was  $85.5\pm 3.1^\circ$ .

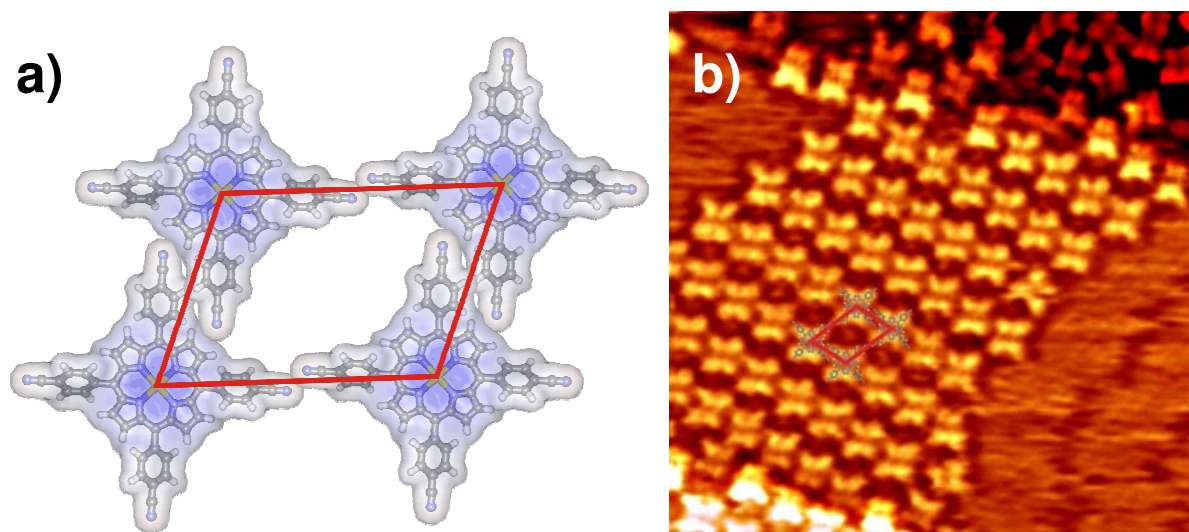


Figure 39: a) Model of the close packed assembly of molecule **2** on Cu(111). Unit cell vectors:  $a=1.56\pm 0.08\text{nm}$ ,  $b=2.16\pm 0.08\text{nm}$ ; Angle= $69.4\pm 2.6^\circ$ . b) High-resolution STM-image ( $20\text{nm}\times 20\text{nm}$ ,  $I=20\text{pA}$ ,  $U=2.2\text{V}$ ,  $0.55\text{ML}$ , Sample 5b) of close packed assembly on Cu(111).

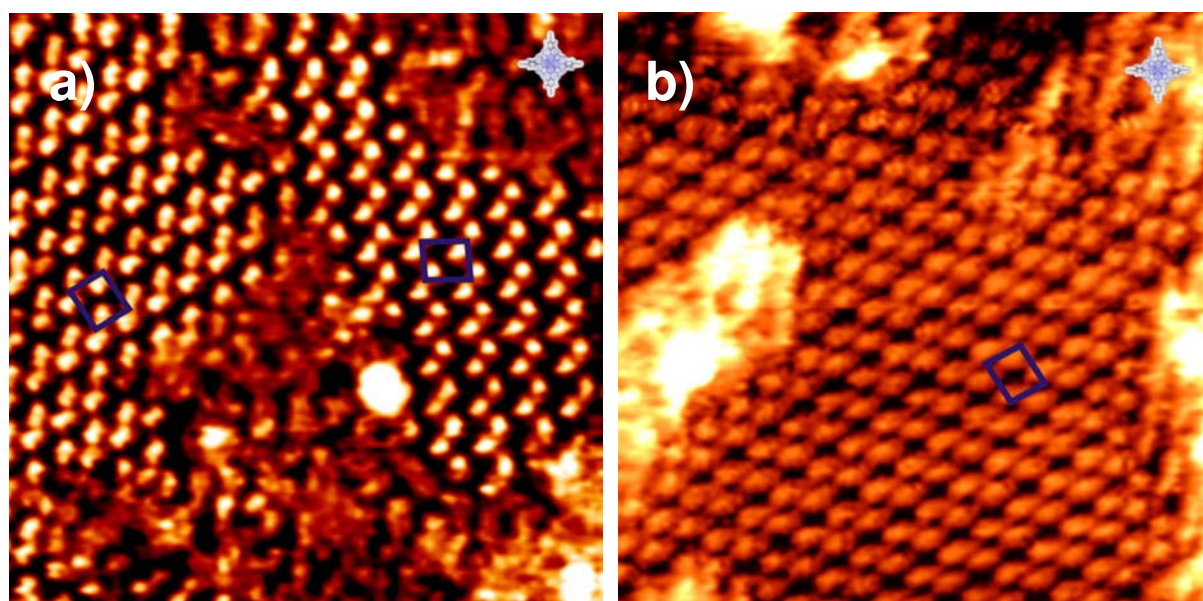


Figure 40: Detailed images of the third assembly which is close packed. A model of molecule of **2** is placed top right to illustrate the dimensions of that assembly. a) STM-image ( $20\text{nm}\times 20\text{nm}$ ,  $I=10\text{pA}$ ,  $U=1.6\text{V}$ ,  $0.7\text{ML}$ , Sample 3b) showing two island of the assembly. b) Another STM-image of the special close packed assembly ( $20\text{nm}\times 20\text{nm}$ ,  $I=14\text{pA}$ ,  $U=1.6\text{V}$ ,  $0.7\text{ML}$ , Sample 3b) distorted by drift.

We conclude that for molecule **2** on Cu(111) we observed 3 different assemblies. The close packed assembly seems to be less favoured because of a lattice mismatch between molecule and substrate lattice, since the packing is much denser on Ag(111). The molecule density is even lower on Cu(111) than for the porous network (see *table 3*). There are probably nearly no interactions between the single molecule rows of the close packed assembly which may also explain why the close packed assembly is so rare. The third assembly was impossible to resolve. Higher quality images or other studies would be needed to understand what is going on at the surface of the sample in this case.

### 3.2.3. Molecule 2 with SubPc on Cu(111)

Finally, we tried to fill the triangular pores of the porous network of molecule **2** with SubPc. The SubPc molecules were evaporated at temperatures of about 500K and deposited at a rate between 0.05 and 0.2ML/min. Like in the case of molecule **2** there might be an error of a factor 2 since we didn't make a reference sample to calibrate the monolayer coverage. Instead we took reference data measured with an old QMB which might have been calibrated a bit different.

We deposited a low amount of ~0.12ML SubPc onto a surface covered with less than a ML of **2** (0.55ML, see *figures 34* for images before SubPc deposition on the same sample) since the ordering of the assemblies of molecule **2** was better below the full monolayer coverage. The porous network with the triangular pores looked the same with and without SubPc on the surface. But we also obtained at least one new phase which was most probably a mixed layer of SubPc with molecule **2** (*figure 41a*). The other SubPc molecules coordinated with the pores of the network of molecule **2** (*figure 41b*).

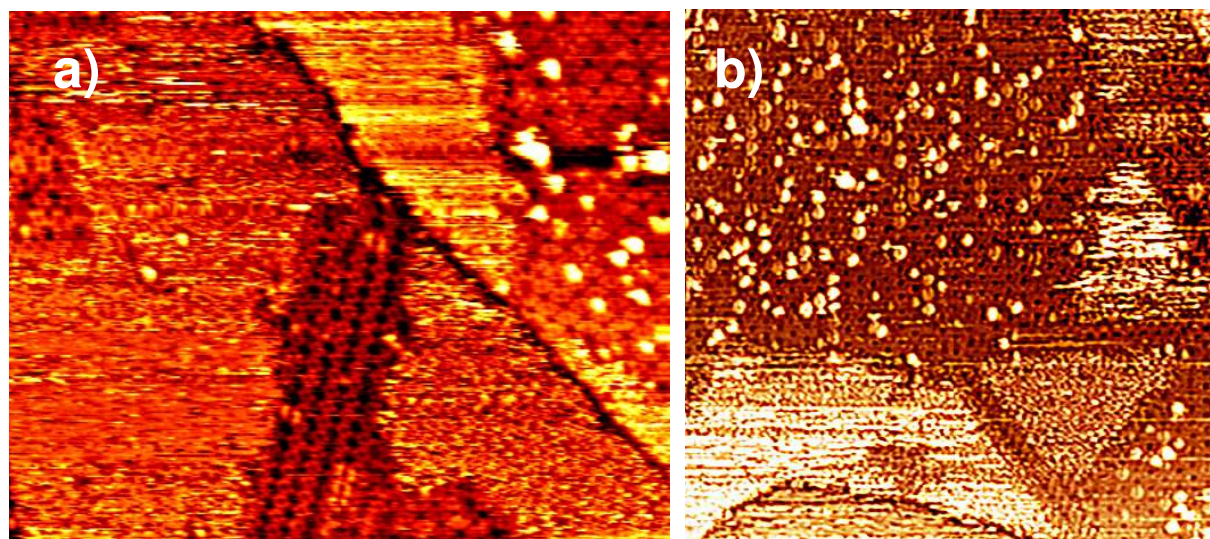


Figure 41: a) STM-overview (100nm\*80nm, I=20pA, U=1.5V, 0.55ML of **2**+0.12ML SubPc, Sample 5c) after addition of SubPc. In the center is the new assembly. Top right, the porous network with SubPc coordinating and top left might be another new assembly but this is hard to tell since it is only seen on this image. b) STM-overview (100nm\*100nm, I=20pA, U=1.8V, 0.55ML of **2**+0.12ML SubPc, Sample 5c) on the same sample illustrating how high the SubPc coverage was. One can also see that the major assembly was still the porous network of molecule **2** on which the SubPc molecules coordinated.

## 4. Discussion

The results of the STM experiments show a big variety of assemblies formed by the investigated two molecules, depending on different parameters like the substrate, the coverage, the deposition rate and the post deposition annealing. Some differences between the two porphyrins are also a bit surprising. One example is the formation of porous networks which occurs for both porphyrin derivatives on only one of the two substrates but not on the same substrate. However, it is already quite well known that the side groups can have a big influence onto the self-assembly of porphyrin derivatives [refs. 4,17]. While molecule **1** assembles in close packed structures on Cu(111) and creates a porous network on Ag(111) it is exactly vice versa for molecule **2**. Further, the assemblies of molecule **1** are quite stable at a full coverage while the assemblies of **2** loose some of their ordering at a higher coverage. Also the stability differs what demonstrates again the big influence of the chemistry and the geometry of the side groups of the porphyrins.

Molecule **1** is especially interesting because it contains the halogenated fluorine groups and forms the detected porous network. The conformation of the molecule on the surface is not really known. STM-images indicate that for most assemblies the molecule is quite flat on the surface having more or less the same conformation. However, the distance from the porphyrin core to the surface should be increased because of the methoxy-groups that lift up the core because of steric hindrance compared to other porphyrin derivatives like e.g. also molecule **2**. Theoretical calculations estimating the energy barrier for different rotational conformations between the porphyrin core and the inner phenyl ring as for the conformation between two phenyl rings have been done without considering the influence of the surface [ref. 18]. The conclusion was that the phenyl ring attached to the porphyrin core is perpendicular and that the attachment of a methoxy group increases the energy barrier between 0° angle and 90°. Inner and outer rings were free to rotate at room temperature. However, since these calculations were not done with surface influence and also the interaction between the pentafluoro-phenyl and the inner phenyl of molecule **1** might be quite different to the case of that study one cannot devolve the results of that study one by one. Other experimental STM-studies further found that the phenyl-rings attached to the porphyrin core can be also tilted with respect to the core in addition to the rotation [refs. 15,16,20,21]. The next important factor for the surface-molecule interaction as for the intermolecular interactions is the influence of the fluorine residues. According to the literature we expect that the fluorine residues have a larger distance from the surface than the porphyrin core, indicating that the fluorine residues are not really attracted to the surface even if the molecules are difficult to compare because they are quite different from **1** [refs. 22-24]. A good example has been also found with the phthalocyanines ZnPcF<sub>8</sub> and ZnPcCl<sub>8</sub> [ref. 25]. In that case ZnPcF<sub>8</sub> molecules create on Ag(111) a close packed assembly which is not distorted by the surface, while the close packed assembly of ZnPcCl<sub>8</sub> adapts to the surface by the formation of a striped structure which is commensurate to the substrate. The explanation is that attractive interaction between the fluorine residues and the surface is weaker than the interaction between chlorine residues and the surface. Next the intermolecular interactions in the fluorine case can be stronger because of the H-Bonding which can be much stronger from fluorine to hydrogen than from chlorine to hydrogen. Perhaps the most investigated highly fluorinated aromatic molecule is F<sub>16</sub>CuPc which self-assembles on Cu(111), Ag(111) and Au(111) [refs. 26-28] into close packed structures. It was interesting that F<sub>16</sub>CoPc, having just a different central metal, did not self-assemble on Au(111) [ref. 29]. Further a Tris(thieno)hexaazatri-phenylene derivative was observed to self-assemble on Ag(110) but again in a close packed assembly [ref. 30]. The only other molecules which were reported to self-assemble in a porous network were also conjugated but completely different in their structure [ref. 31]. Furthermore these structures

were observed at the solid/liquid interface on HOPG and the assembly had a structure where the pentafluoro-phenyls interacted with neighbouring phenyl-rings of the neighbouring molecule. Next, the distance between the fluorine residues was quite large as expected in contrast with the case we observed with molecule **1** on Ag(111).

The hexagonal network (Ag1) of molecule **1** on Ag(111) has a density of 0.2 molecules/nm<sup>2</sup> which is lower than the comparable close packed assemblies with ~0.25 molecules/nm<sup>2</sup> (see *table 1*). Following our argumentation, the lattice mismatch would especially explain the small amount of assembly Ag3. It would also explain why Ag3 was interrupted always after something like 10 rows. Further it would describe why the close packed assembly induced by SubPc (AgSub) has such a high amount of defects. The most appearing close packed assembly with an alternating pattern Ag2 should then be energetically quite close to the hexagonal network since both assemblies are able to co-exist in a stable way with clear borders and no gas phase in between (see *figure 8*). Maybe the hexagonal network is preferred due to stronger molecule-molecule interactions. It may also help to the stability of the hexagonal network that additional molecules of **1** can jump into the pores of the hexagonal network (see *figure 8*). If one calculates the density of the hexagonal network with all pores filled by **1** itself, one even gets a similar density like for the close packed assemblies, i.e. 0.27 molecules/nm<sup>2</sup>. One can also see from the images that the structure of the alternating close packed assembly and the hexagonal network are related to each other. So while the molecules in the hexagonal network have 3 different orientations with a 60° angle between each other there are only 2 different positions in the alternating close packed assembly. But the molecules have also an angle of 60° between the two different orientations. The angle of 60° is one more indication that the substrate plays an important role in the formation of all these assemblies. Comparing to the literature, this substrate dependence should then be driven most probably by the porphyrin core. This is also quite surprising together with the fact that the porphyrin core should be lifted up much more in molecule **1** than in other porphyrin derivatives because of the methoxy-groups. Furthermore with the molecules ZnPcF<sub>8</sub> and F<sub>16</sub>CuPc which do not have such methoxy-groups lifting up the core, it seemed that the substrate influence was quite weak. It was further observed in some rare situations that in the hexagonal network single rows of alternating assembly were appearing (*figure 42*). It seems that these two assemblies have the same periodicity along one direction. However, the repetition length is slightly different for the two assemblies and is only about 3.9nm for the alternating close packed assembly. This is still within the statistical error limits and could be compatible with the 4.2nm repetition length of the hexagonal network. Since we also observed a high tolerance of the alternating close packed assembly to defects (see *figure 8*) we suppose that the alternating close packed assembly is just adapting to the hexagonal network in the neighbourhood if possible. We have also observed the case of a gas phase appearing at the border between the two assemblies (*figure 10a*). We would then consider that in this situation the alternating close packed assembly was unable to adapt to the hexagonal network which resulted in the gas phase dividing the assemblies. Unfortunately, we observed the clean border between hexagonal network and alternating close packed assembly only in one image, in a resolution good enough to determine the exact orientation of the molecules (*figure 8*). So we do not know if this interesting orientation change of 90° of the molecules at the border between hexagonal network and alternating close packed assembly had a systematic reason or if this orientation change was not needed. The overall conclusion is that the alternating assembly could adapt to the hexagonal network in some situations by tolerating some defects. Therefore it could also appear just as single rows within the hexagonal network adapting to the repetition length of the hexagonal network. But without the influence of the hexagonal network the repetition length of the alternating close packed assembly (3.9nm on the long axis) is slightly different compared to the one of the hexagonal network (4.2nm). Since we observed the appearance of the alternating close packed assembly only when we deposited at

high rates we think that the alternating close packed assembly is more kinetically favoured while the hexagonal network is thermodynamically favoured.

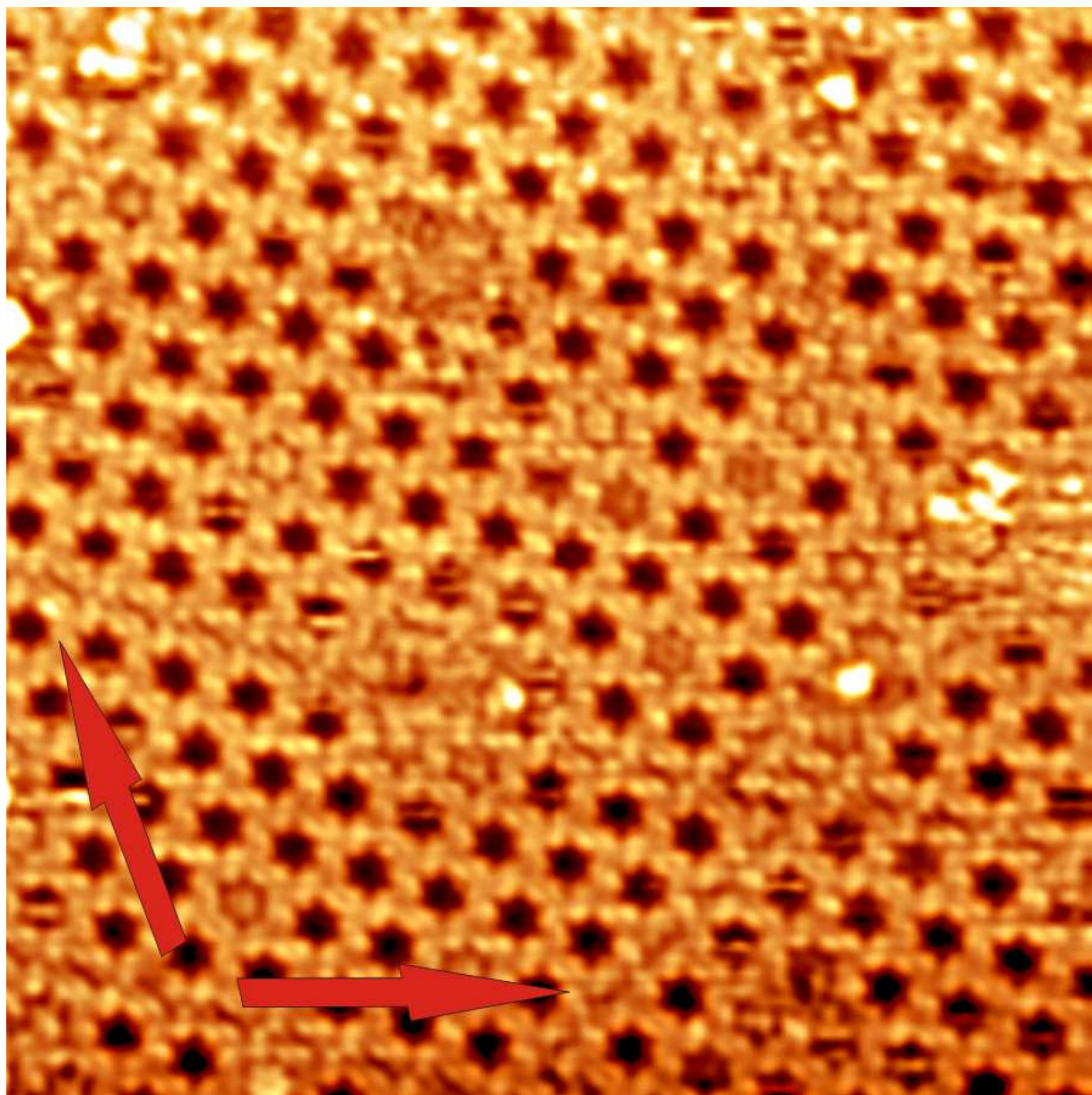


Figure 42: STM-image (60nm\*60nm, I=14pA, U=1.5V, 0.95ML of **1**, Sample 3b): Hexagonal network of molecule **1** on Ag(111) separated by single rows of alternating close packed assembly (pointed out by the red arrows).

The next interesting topic with molecule **1** on Ag(111) is that the codeposition of SubPc leads at a certain point to a collapse of the hexagonal network that was otherwise stable. Since the SubPc molecules were observed to enter the pores this does probably not destabilize the network. Maybe the molecules rarely bind to another site on the network like e.g. the place where the pentafluoro-phenyls are close together. The assembly was stable over days if no additional molecules were added. The big question is - why the situation can then be stabilized in equilibrium of SubPc close packed assembly (AgSub) and porous network (Ag1)? This equilibrium is especially surprising since the SubPc molecules were only rarely seen in the AgSub islands with the STM. It might be that the SubPc molecules are not observed by the STM because they are somewhere hidden in this structure; however this is not very probable. The second possibility would be that the SubPc close packed assembly could also develop back to the hexagonal network. However no movement of the assembly

islands was observed during STM-measurements. The only other possibility, if we assume that SubPc is really not present in AgSub, would be that the SubPc molecules are somehow stabilized in the gas phase which separated the porous network and the close packed assembly (AgSub, see *figure 43*) leading to the observed equilibrium. It could be that the SubPc molecules destroy the network leading to free space filled by a 2D gas-phase where the SubPc molecules have a better access to the Ag substrate. This would also explain why the hexagonal network is not completely destroyed from the beginning because the SubPc molecules would then not destroy anymore hexagonal network if there would be enough 2D gas-phase with enough access to the substrate.

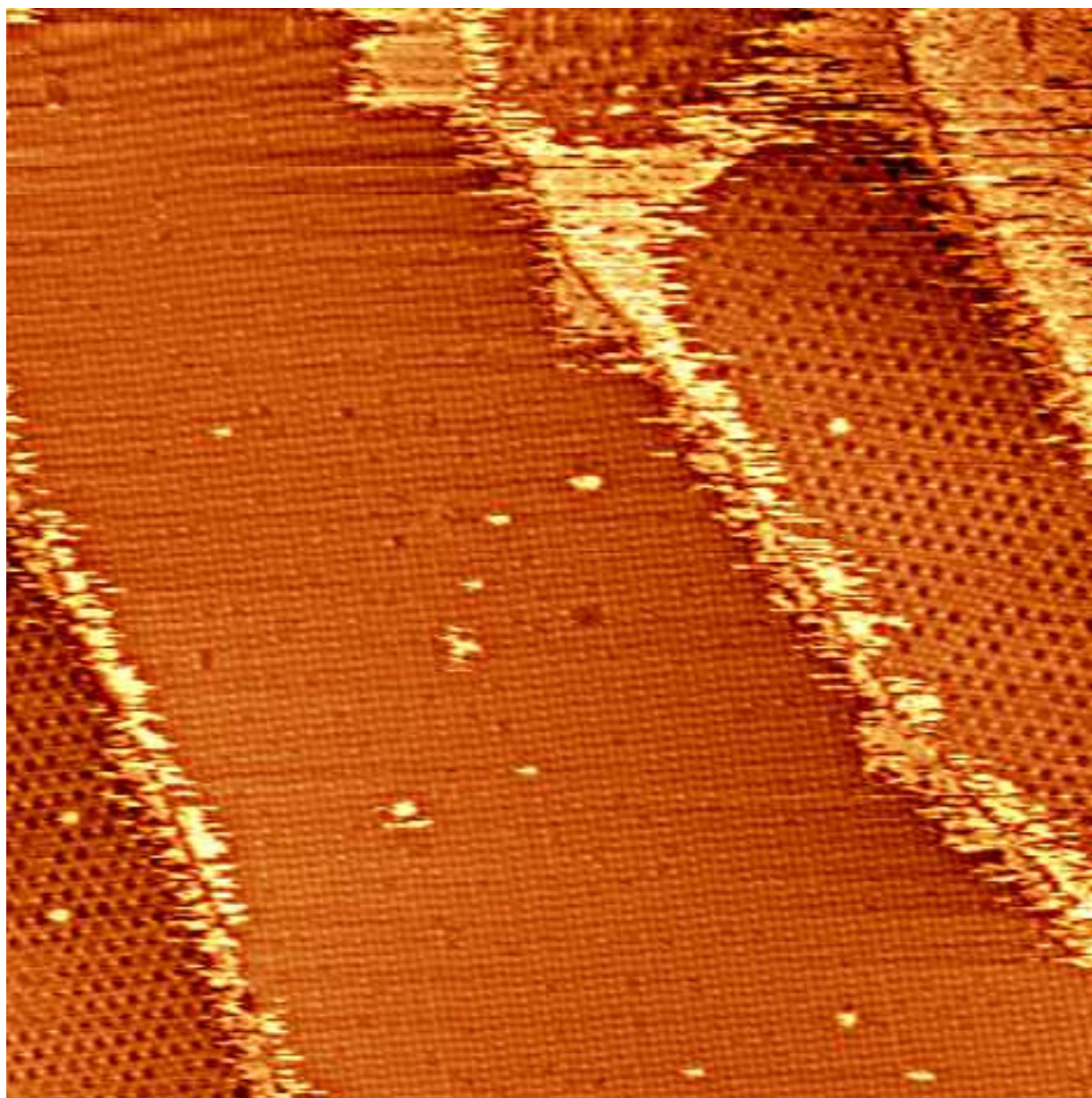


Figure 43: STM-overview (200nm\*200nm, I=20pA, U=1.6V, 0.6ML of **1**+0.05ML SubPc, Sample 11b) showing the gas phases between the different assemblies Ag1 and AgSub of molecule **1** on Ag(111).

In case of molecule **1** on Cu(111), the first problem was the topic with Cu1a and Cu1b. There was some STM evidence that both assemblies are occurring on the same sample at the same time. On the other hand LEED-measurements which were done on the same sample confirmed that only Cu1a was present on the surface. This fact led also to the question if Cu1b is not only an artefact of thermal drift which affects the STM-images. But the problem

with this assumption is that in some measurements only Cu1b was observed. Next we think that the assembly AgSub which we observed on Ag(111) contained the same binding motives as Cu1a and Cu1b structures together interconnecting the rows in two different ways (see *figures 25 and 21*). Then Cu1b was especially found together with the Cu2 assembly and maybe Cu1b is really only corresponding to Cu2. The model of Cu1b is just a theoretical assumption and for Cu2 it is even less clear how the molecule could lie on the surface. For the Cu2 assembly one possible explanation for the observed STM-images might be that the porphyrin cores are still in contact with the substrate while the peripheral groups are pointing away from the substrate having some intermolecular interactions without any substrate influence. If this would be true the porphyrin cores would have two different angles corresponding to the best STM-images where two differently oriented objects can be observed (see *figures 28*). These differently oriented objects would then correspond to the porphyrin cores having two orientations. The space would be sufficient only for the porphyrin cores. But this would lead to two molecules per unit cell in Cu2 giving a molecule density which is about 3 times higher than for Cu1a and Cu1b. And exactly because of this high density, such a structure is quite unlikely. Therefore this assembly has to be reproduced and investigated more to find more new and more precise solutions for the orientation of the molecules. At least it is clear that the solution will not be simply the molecules lying parallel to the surface because the unit cell is too small. Some parts of the molecules or even whole molecules will be not in contact with the surface for this assembly. Some more STM-images on samples where no LEED-data was taken even indicate an unknown number of further assemblies. So the next problem on Cu(111) is that only Cu1a is a completely confirmed assembly. We still keep Cu1b and Cu2 assemblies since they were observed not only in a single region or on a single day. The other unsorted images which are not shown in this thesis were not really possible to be categorized and had much less different positions. This was the reason to sort out all these images. But just because of that it wouldn't be surprising if more assemblies would be found in further experiments. Then one would have to clarify the exact phase behaviour of molecule **1** on Cu(111) by finding parameters which really determine the obtained assemblies.

On molecule **2** other things are remarkable. For example the interactions between cyanophenyls are already quite known [*refs. 17,32,33*]. However it was interesting to find out that the binding motives in the porous network on Cu(111) were a bit different. It seems that the nitrogen residues interact with hydrogen of the porphyrin core and not with hydrogen of a neighbouring phenyl-ring. Further, especially the 3 central molecules which create the big pore of the network do not interact too much in the model. Next, it seems that the phenyl-rings are not perpendicular to the core what is also the reason why they would be observed on Cu(111) as on Ag(111) (see *figures 38 and 33b*). The other binding motives [*ref. 32*] were partly observed, especially the one of the close packed assembly on Cu(111) which seems to be distorted (*figure 39b*). This might be also the reason why the porous network on Cu(111) with triangular pores is the densest phase and the dominating phase at lower coverages. But for the other close packed assembly on Cu(111) where we could not resolve the structure we also did not find a candidate in the literature. Another interesting topic is molecule **2** with SubPc on Cu(111). A closer view of the STM-images of the sample allowed us to approximately determine the structure of the mixed layer containing SubPc and molecule **2** (*figure 44*). But one big problem is to understand why in this assembly the SubPc molecules do not appear higher in this assembly compared to molecule **2**. However, since we can clearly identify molecule **2** because of the porphyrin bending line that is observed (*in figure 44 mixed layer assembly*) we should assign the remaining dots to SubPc. Also the size of these dots matches the dimensions of SubPc. It might be that SubPc has a different conformation with respect to the surface compared to the pores because of the interactions with molecule **2**. We assume that the conformation of SubPc on the pores might be such that the chlorine residue of

SubPc is pointing towards the surface when the molecule appears as a bright ring (red arrows on *figure 44*). And exactly the opposite conformation would then be observed as 3 single bright dots (blue arrows on *figure 44*). Multiple SubPc molecules on a single pore or maybe a molecule of **2** itself on the pores would then be observed as big bright dot (green arrow on *figure 44*).

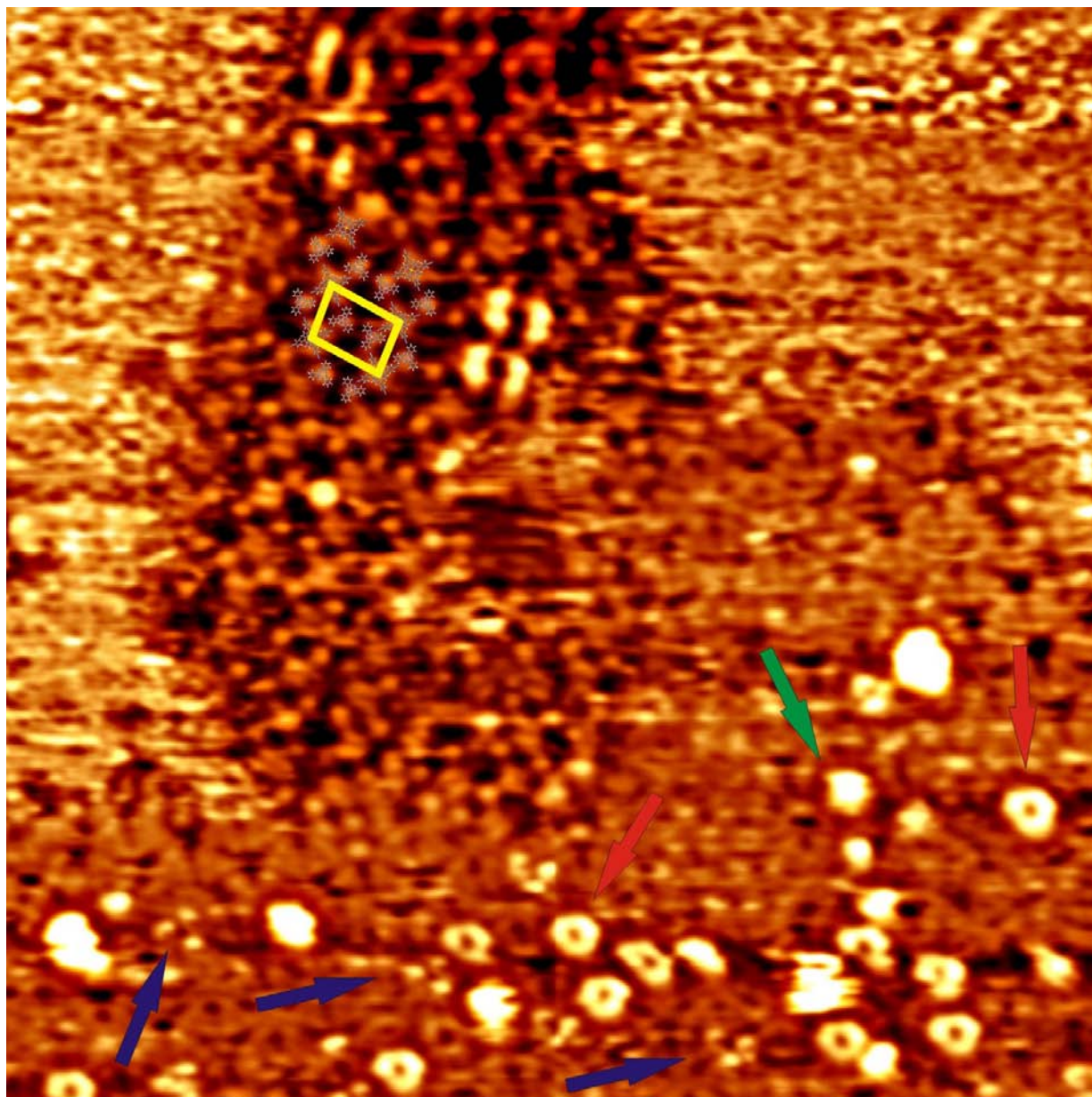


Figure 44: STM-image (50nm\*50nm, I=15pA, U=1.8V, 0.55ML of **2**+0.12ML SubPc, Sample 5c) of molecule **2** and SubPc together on Cu(111). Apparent is the mixed layer phase of molecule **2** and SubPc on top (unit cell denoted in yellow, molecules are placed there too but especially SubPc only to show the dimensions). On bottom the porous network of molecule **2** where some pores are filled by SubPc molecules which correspond to the bright spots (different types marked with arrows of different colours, see text). Further on the left and top right a 2D gas phase is observed.

Finally the unit cell of the mixed layer of SubPc and molecule **2** was measured. The unit cell had the vectors  $a \sim 2.5\text{nm}$ ,  $b \sim 3.5\text{nm}$  and an angle of  $\sim 80^\circ$  containing one molecule of **2** and two molecules SubPc. But there are a lot of uncertainties since that specific experiment of adding SubPc to molecule **2** on Cu(111) was only done once. Further the mixed layer phase was only observed on a single position in this resolution (*figure 44*) which was not optimal. It might be that this mixed layer evolves from the rare close packed assembly of **2** when adding

SubPc. However, the mixed layer phase is very interesting but would need many more experiments to be validated and is therefore mentioned here only as a first impression. But the coordination of the SubPc molecules to the porous network of molecule **2** is observed. It depends on the real diameter of the pores, on the attractive forces between the Cu(111) surface and the SubPc and on the flexibility of the big pores if the molecules really enter the pores. The fact that somehow two states for the SubPc on the pores were observed agrees with experiments done with pure SubPc [*ref. 13*].

In comparison to the porous network of molecule **1** on Ag(111) the porous network of molecule **2** on Cu(111) is much less stable. One reason might be weaker intermolecular interactions since a hydrogen-bond between hydrogen and nitrogen is much weaker than between hydrogen and fluorine. The network is also destabilized if the coverage is increased close to a full monolayer. On the other hand, it is interesting that the addition of SubPc had much less influence onto the porous network than in the case of molecule **1** on Ag(111). There are two possible reasons why the effect is so much weaker. First the substrate was Cu(111) in the case of molecule **2** and second the charge distribution of molecule **2** at the surface might be more homogeneous. Because of that, the interaction between the porous network of molecule **2** and SubPc molecules might be weaker and less repulsive. It was also interesting to observe that SubPc appeared on the porous networks of **1** and **2** in two different states. In the hexagonal network of **1** on Ag(111) the second state was only found very rarely (*figure 45*). On the porous network of **2** on Cu(111) the second state was observed more often (blue arrows *figure 44*). We think that these two states correspond to the orientation of the SubPc molecule against the surface. The normal state would correspond to a case where the chlorine residue points down to the surface (like in [*ref. 13*]). The second state would correspond to the opposite case. The reason for these different ratios between first state and second state for molecule **1** and **2** might be the different substrates. While for Ag(111) it is already well known that the SubPc molecule likes to stick to the surface with the chlorine residue pointing down, on Cu(111) the situation might be a bit different, as indicated by the ratio how the pores of **2** are filled.

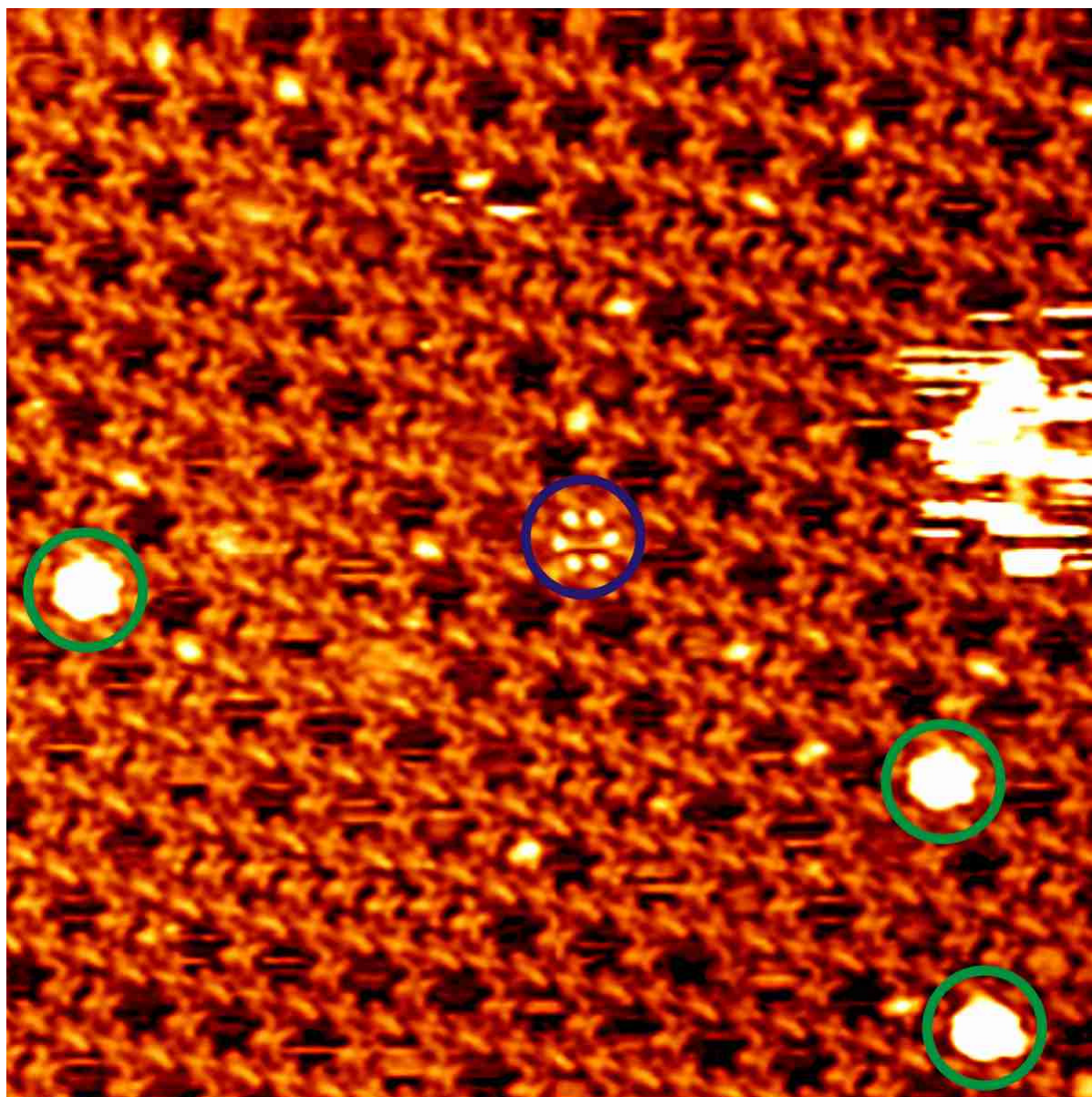


Figure 45: STM image (50nm\*50nm, I=20pA, U=-1.5V, 0.6ML of **1**+0.05ML SubPc, Sample 11b) where probably the two different states of SubPc are observed. One can see the normal state which was observed very often (green circles) and the state that was observed very rarely (blue circle).

So if we compare in total the two molecules from a geometrical point of view (4-fold axis on **2** versus 2-fold axis on **1**) the differences can be understood since the peripheral groups of **1** and **2** are totally different. This further influences also the electronic state which is for sure important for molecule-molecule as for molecule-substrate interactions. The sizes of the molecules are also different with a diameter of  $\sim 2.1\text{nm}$  for molecule **2** and  $\sim 2.7\text{nm}$  respectively  $\sim 2.6\text{nm}$  for molecule **1**. But on the other side both molecules have a porphyrin core with a  $\text{Zn}^{2+}$  as a co-factor. And probably the porphyrin core will not play a very important role in intermolecular interactions because it is too much in the centre of the respective molecules. But for substrate-molecule interactions the porphyrin core will be an important factor since it is an aromatic system [ref. 3]. Looking onto STM-images, we can say that it is further likely that the porphyrin cores of both molecules are lying roughly in the same conformation on the surfaces for most assemblies. It seems that for the well understood assemblies the porphyrin core is not tilted away too much from the surface and also the whole molecules seem to be more or less parallel to the surface. For the compact assemblies we do not understand the situation. The porphyrin core might be bent much more leading to a

conformation of the molecules where the side-groups point away from the surface. The probability that the non-understood assemblies are induced by contaminations is quite low. Also a partial decomposition of the molecules is not very likely because for both molecules the compact assemblies were observed in some cases already before annealing. There are further similarities between the molecules like the possibility of creating hydrogen-bonds. Especially for molecule **1** the hydrogen-bonds between fluorine residues and hydrogen residues might be quite strong with energies of up to 150kJ/mol per hydrogen-bond. The strength of these bonds influences the self-assembly a lot and is a further reason for the stability of the assemblies.

Since we see differences in the assemblies between different substrates we know that substrate-molecule interactions are stronger on one substrate than on the other, leading to substrate influenced assemblies. However since the molecules lie on the surface in a defined position, the self-assembly still works because the molecules are free to rotate and to move on the surface leading to assemblies which are at least commensurate with the substrate. The example is Cu1a assembly of molecule **1** which is a commensurate close-packed assembly. All molecules of **1** are oriented in the same way in that assembly and the vectors of the unit cell are equal even if the arms of the molecule do not have the same length. Further the close packed assemblies of molecule **1** on Cu(111) were not dominating on Ag(111). On Ag(111) the porous network was dominating even though it was not observed on Cu(111) at all, having a 6-fold symmetry like the substrate. So the explanation would be that molecule-molecule interactions would prefer a close packed assembly which could be established on Cu(111) but is commensurate since the substrate-molecule interactions are also strong in that case. But on Ag(111) this simple assembly was hindered by a mismatch between molecule- and substrate-lattice leading to different assemblies. These different assemblies were then mainly the porous network (Ag1) and the alternating close packed assembly (Ag2) which were compatible with the substrate lattice of Ag(111). We cannot confirm this hypothesis completely since we would need to find the relation of Ag1 or Ag2 with the substrate. Therefore it's only an assumption based on the LEED results, the 6-fold symmetry of Ag1 and the 60° angle between differently oriented molecules which also corresponds to a strong substrate influence. In summary, it was possible to plot a map of the phase behaviour of these two molecules on Cu(111) and Ag(111). But of course several things remain unclear. Especially things that were not observed very often like e.g. rare assemblies that were found for both molecules. Also the particular binding motives of the different assemblies were only characterized roughly by determining the positions of the molecules with respect to each other. The locations of possible H-Bonds and their strength were not characterized. One consequence was that it was difficult to compare the two molecules. The similarities between molecule **1** and molecule **2** like e.g. the existence of a porous network and differences like e.g. the different stability of the porous networks or the different interactions with the substrate could be explained in a qualitative way. Also the interaction with SubPc was quite different for each molecule which is probably related to the charge distribution of SubPc which is known to be inhomogeneous [*ref. 13*]. Considering symmetry, we see for example the important difference between the 4 equal arms of molecule **2** and the two different types of arms of molecule **1** which could also explain some differences in a qualitative way. The qualitative arguments are based on comparisons with the literature or on the symmetry. One example would be the strength of the H-Bonds which was measured for simpler molecules and used as a scale in our case.

## 5. Conclusion

During this master project two different molecules (**1** and **2**) were studied on two crystal surfaces (Copper and Silver) with a (111) orientation. With STM experiments 3 different assemblies of molecule **1** were found on Ag(111) and the assemblies observed were depending on the deposition rate of **1**. Of special interest was the porous network Ag1 with hexagonal pores which was stable up to temperatures of 300°C. A pore of the network had a diameter of about ~2nm at its closest point and of about ~3.2nm at its furthest point. SubPc molecules were added to the porous network and some molecules adsorbed into the pores while the majority of the molecules probably remained in gas phase at the surface. If a certain amount of SubPc (~0.05ML) was added the porous network started to collapse and changed into a new close packed assembly. It was further observed that the new close packed assembly (AgSub) and the porous network (Ag1) phase could co-exist in equilibrium. If the collapse of the porous network was interrupted in that state or if the close packed assembly could also develop back into porous network was not clear. STM-observations indicated that the phases were stable over days after the close packed assembly (AgSub) was formed on the surface. The same molecule on Cu(111) formed 3 different assemblies from which none was porous. LEED experiments on Cu(111) helped to characterize the unit cell parameters of the most prevalent assembly with high precision.

Molecule **2** formed a close packed assembly on Ag(111) and 3 different assemblies on Cu(111). This molecule formed a porous network on Cu(111). It contained two types of triangular pores. The bigger one had a diameter of ~1-1.5nm and the smaller one had a diameter of ~0.5-0.7nm. This porous network was not observed to cover the whole surface in contrary to the porous network of molecule **1**. At lower coverages, molecule **2** formed islands of the porous network. At such a low coverage SubPc molecules were added onto the surface. SubPc molecules coordinated to the islands of porous network without influencing the stability of the porous network too much.

The formation of porous networks of both molecules is an indication that substrate-molecule interactions are stronger than molecule-molecule interactions, since the symmetry of these networks are 3-fold and 6-fold, respectively - compatible to the (111) substrate symmetries. The molecules themselves had a 2-fold and a 4-fold symmetry, respectively.

Molecule **1** is the first example of a highly fluorinated porphyrin derivative which arranges on a surface in a porous network. Furthermore, it creates a surprising arrangement of the molecules with the fluorine residues quite close to each other. Quantifying the stabilizing factors for the structure might be very interesting and help to understand other interactions where fluorine residues are involved. It is also shown in this thesis that SubPc can be coordinated to a porous network. Unfortunately the molecules seem to destroy the porous network of molecule **1**. Molecule **2** has probably pores too small for the SubPc molecules. However, the SubPc molecules can still be coordinated to the pores while the porous network is not being affected too much.

The phase behaviour for both molecules on both substrates is explained to a certain extent. The topic seems to get quite more complicated if SubPc is added and for that case much less is understood. Understanding the interactions between molecules in a more detailed way is crucial for any type of molecular engineering. Only if the principles are understood in a better way it will be possible to design systems with properties that can be accurately predicted.

## 6. Acknowledgements

I want to thank to the group of Thomas Jung at the University of Basel that gave me the possibility to make these STM experiments under UHV conditions. In particular I want to thank Meike Stöhr for being the supervisor of my project and also Tomas Samuely who helped me with a lot of experiments and for his corrections on my thesis. Next I want to thank all the other group members in Basel: Mihaela Enache, Manfred Matena, Serpil Boz, Jorge Lobo-Checa, Saranyan Vijayaraghavan, Nicholas Reynolds and the technician Stefan Schnell. Everybody of them helped me in a very kindly way on particular practical problems and taught me how to interpret the results.

Then I want to thank Jens Hornung and Tobias Voigt from the collaborating chemistry group of François Diederich at ETH Zurich for synthesising and nomenclature of the molecules **1** and **2**.

Finally I want to thank Professor Ernst Meyer for the project work I could do in his group and for being assessor of my master thesis.

## 7. References

1. Binnig, G. and Rohrer, H. *Scanning Tunnelling Microscopy*, Helvetica Physica Acta **1982**, 55, 726.
2. Binnig, G., Rohrer, H., Gerber, C. and Weibel, E. *Tunnelling through a Controllable Vacuum Gap*, Appl. Phys. Lett. **1982**, 40, 178.
3. Tautz, F.S. *Structure and bonding of large aromatic molecules on noble metal surfaces: The example of PTCDA*, Progress in Surface Science, **2007**, 82, 479
4. Wintjes, N., Hornung, J., Lobo-Checa, J., Voigt, T., Samuely, T., Thilgen, C., Stöhr, M., Diederich, F., Jung, T.A. *Supramolecular Synthons on Surfaces: Controlling Dimensionality and Periodicity of Tetraarylporphyrin Assemblies by the Interplay of Cyano and Alkoxy Substituents*, Chem. Eur. J., **2008**, 14, 5794
5. Maier, S., Fendt, L.-A., Zimmerli, L., Glatzel, T., Pfeiffer, O., Diederich, F., Meyer, E. *Nanoscale Engineering of Molecular Porphyrin Wires on Insulating Surfaces*, small, **2008**, 8, 1115
6. Bonifazi, D., Spillmann, H., Kiebele, A., de Wild, M. Seiler, P., Cheng, F., Güntherodt, H.-J., Jung, T.A., Diederich, F. *Supramolecular Patterned Surfaces Driven by Cooperative Assembly of C<sub>60</sub> and Porphyrins on Metal Substrates*, Angew. Chem. Int. Ed., **2004**, 43, 4759
7. Spillmann, H., Kiebele, A., Stöhr, M., Jung, T.A., Bonifazi, D., Cheng, F., Diederich, F. *A Two-Dimensional Porphyrin-Based Porous Network Featuring Communicating Cavities for the Templated Complexation of Fullerenes*, Adv. Mater. **2006**, 18, 275

8. Kiebele, A., Bonifazi, D., Cheng, F., Stöhr, M., Diederich, F., Jung, T.A., Spillmann, H. *Adsorption and Dynamics of Long-Range Interacting Fullerenes in a Flexible, Two-Dimensional, Nanoporous Porphyrin Network*, ChemPhysChem, **2006**, 7, 1462
9. Meyer, E.A., Castellano, R.K., Diederich, F. *Interactions with Aromatic Rings in Chemical and Biological Recognition*, Angew. Chem. Inter. Ed., **2003**, 42, 1210
10. Stroschio, J.A., Feenstra, R.M., Fein, A.P. *Electronic Structure of the Si(111) 2x1 Surface by Scanning-Tunneling Microscopy*, Phys. Rev. Lett., **1986**, 57(20), 2579
11. Horcas, I., Fernandez, R., Gomez-Rodriguez, J.M., Colchero, J., Gomez-Herrero, J., Baro, A.M. *WSXM: A software for scanning probe microscopy and a tool for nanotechnology*, Rev. Sci. Instrum. **2007**, 78, 013705
12. Berner, S., Brunner, M., Ramoino, L., Suzuki, H., Güntherodt, H.-J., Jung, T.A. *Time evolution analysis of a 2D solid-gas equilibrium: a model system for molecular adsorption and diffusion*, Chem. Phys. Lett., **2001**, 348, 175
13. Berner, S., de Wild, M., Ramoino, L., Ivan, S., Baratoff, A., Güntherodt, H.-J., Suzuki, H., Schlettwein, D., Jung, T.A. *Adsorption and two-dimensional phases of a large polar molecule: Sub-phthalocyanine on Ag(111)*, Phys. Rev. B, **2003**, 68, 115410
14. Wintjes, N., Bonifazi, D., Cheng, F., Kiebele, A., Stöhr, M., Jung, T.A., Spillmann, H., Diederich, F. *A Supramolecular Multiposition Rotary Device*, Angew. Chem. Int. Ed., **2007**, 46, 4089
15. Yokoyama, T., Yokoyama, S., Kamikado, T., Mashiko, S. *Nonplanar adsorption and orientational ordering of porphyrin molecules on Au(111)*, J. Chem. Phys., **2001**, 115 (8), 3814
16. Yokoyama, T., Kamikado, T., Yokoyama, S., Mashiko, S. *Conformation selective assembly of carboxyphenyl substituted porphyrins on Au(111)*, J. Chem. Phys., **2004**, 121(23), 11993
17. Yokoyama, T., Yokoyama, S., Kamikado, T., Okuno, Y., Mashiko, S. *Selective assembly on a surface of supramolecular aggregates with controlled size and shape*, Nature, **2001**, 413, 619
18. Okuno, Y., Kamikado, T., Yokoyama, S., Mashiko, S. *Theoretical study of aryl-ring rotation in arylporphyrins*, Journal of Molecular Structure (Theochem), **2002**, 594, 55
19. Auwärter, W., Weber-Bargioni, A., Riemann, A., Schiffrin, A., Gröning, O., Fasel, R., Barth, J.V. *Self-assembly and conformation of tetrapyrrolyl-porphyrin molecules on Ag(111)*, J. Chem Phys. **2006**, 124, 194708
20. Auwärter, W., Klappenberger, F., Weber-Bargioni, A., Schiffrin, A., Strunskus, T., Wöll, C., Pennec, Y., Riemann, A., Barth, J.V. *Conformational Adaptation and Selective Adatom Capturing of Tetrapyrrolyl-porphyrin Molecules on a Copper (111) Surface*, JACS, **2007**, 129, 11279

21. Buchner, F., Comanici, K., Jux, N., Steinrück, H.-P., Marbach, H. *Polymorphism of Porphyrin Molecules on Ag(111) and How to Weave a Rigid Monolayer*, J. Phys Chem. C, **2007**, *111*, 13531
22. Jones, R.G., Chan, A.S.Y., Turton, S, Jackson, G.J., Singh, N.K., Woodruff, D.P., Cowie, B.C.C. *1-Chloro-2-fluoroethane Adsorption on Cu(111): Structure and Bonding*, J. Phys. Chem B, **2001**, *105*, 10600
23. Gerlach, A., Schreiber, F., Sellner, S. Dosch, H., Vartanyatns, I.A., Cowie, B.C.C., Lee, T.-L., Zegenhagen J. *Adsorption-induced distortion of F<sub>16</sub>CuPc on Cu(111) and Ag(111): A x-ray standing wave study*, Phys. Rev. B, **2005**, *71*, 205425
24. Koch, N., Gerlach, A., Duhm, S., Glowatzki, H., Heimel, G., Vollmer, A., Sakamoto, Y., Suzuki, T., Zegenhagen, J., Rabe, J.P., Schreiber, F. *Adsorption-Induced Intramolecular Dipole: Correlating Molecular Conformation and Interface Electronic Structure*, JACS, **2008**, *130*, 7300
25. Oison, V., Koudia, M., Abel, M., Porte, L. *Influence of stress on hydrogen-bond formation in a halogenated phthalocyanine network*. Phys. Rev. B, **2007**, *75*, 035428
26. Wakayama, Y. *Assembly Process and Epitaxy of the F<sub>16</sub>CuPc Monolayer on Cu(111)*. J. Phys. Chem. C, **2007**, *111*, 2675
27. Barrena, E., de Oteyza, D.G., Dosch, H., Wakayama, Y. *2D Supramolecular Self-Assembly of Binary Organic Monolayers*, ChemPhysChem, **2007**, *8*, 1915
28. Huang, H., Chen, W., Wee, A.T.S. *Low-Temperature Scanning Tunnelling Microscopy Investigation of Epitaxial Growth of F<sub>16</sub>CuPc Thin Films on Ag (111)*. J. Phys. Chem. C, **2008**, *112*, 14913
29. Scudiero, L., Hipps, K.W., Barlow, D.E. *A Self-Organized Two-Dimensional Bimolecular Structure*. J. Phys. Chem. B, **2003**, *107*, 2903
30. Salomon, E., Zhang, Q., Barlow, S., Marder, S.R., Kahn, A. *Quasi-epitaxy of a Tris(thieno)hexaazatriphenylene Derivative Adsorbed on Ag(110): Structural and Electronic Properties Probed by Scanning Tunnelling Microscopy*, J. Phys. Chem. C, **2008**, *112*, 9803
31. Mu, Z., Shu, L., Fuchs, H., Mayor, M., Chi, L. *Two Dimensional Chiral Networks Emerging from the Aryl-F...H Hydrogen-Bond-Driven Self-Assembly of Partially Fluorinated Rigid Molecular Structures*, JACS, **2008**, *130*, 10840
32. Kumar, R.K., Balasubramanian, S., Goldberg, I. *Self-assembly of Functionalized Metalloporphyrins into Microporous Polymeric Networks*, Mol. Cryst. Liq. Cryst., **1998**, *313*, 105
33. Okuno, Y., Yokoyama, T., Yokoyama, S., Kamikado, T., Mashiko, S. *Theoretical Study of Benzonitrile Clusters in the Gas Phase and Their Adsorption onto a Au(111) surface*, JACS, **2002**, *124*, 7218
34. [www.wikipedia.org](http://www.wikipedia.org)

## Appendix

In the appendix there is an overview presentation over all identified assemblies (*table 4*). Further all samples that were measured with the STM are listed here too (*table 5*).

### Overview of all identified assemblies

#### Molecule 1

#### Unit Cell vectors

Substrate			a[nm]	b[nm]	Angle a-b [°]	Molecules/ Unit Cell	Molecule Density [Molecules/nm <sup>2</sup> ]
Ag(111)	Ag1	Porous network (hexagons)	4.20±0.20	4.20±0.20	60.0	3	0.20
Ag(111)	Ag2	Alternating close packed assembly	2.02±0.15	3.92±0.19	80.6±1.6	2	0.26
Ag(111)	Ag3	Simple close packed assembly	1.84±0.04	2.04±0.06	88.5±0.5	1	0.27
Cu(111)	Cu1a	Close packed 80°	2.03	2.03	81.8	1	0.25
Cu(111)	Cu1b	Close packed 90°	1.86±0.11	2.01±0.07	87.4±1.6	1	0.27
Cu(111)	Cu2	High close packed	1.32±0.09	2.06±0.09	86.5±1.8	1	0.37

#### Molecule 1+SubPc

Substrate			a[nm]	b[nm]	Angle a-b [°]	Molecules/ Unit Cell	Molecule Density [Molecules/nm <sup>2</sup> ]
Ag(111)	AgSub	SubPc close packed (lots of defects)	1.93±0.02	2.05±0.07	86.5±2.9	1	0.25

#### Molecule 2

Substrate			a[nm]	b[nm]	Angle a-b [°]	Molecules/ Unit Cell	Molecule Density [Molecules/nm <sup>2</sup> ]
Ag(111)		Close packed	1.54±0.06	1.63±0.07	87.5±1.9	1	0.40
Cu(111)		Porous network (triangles)	2.90±0.25	2.90±0.25	60.0	3	0.41
Cu(111)		Close packed low coverage	1.56±0.08	2.16±0.08	69.4±2.6	1	0.32
Cu(111)		Close packed high coverage	1.31±0.07	1.53±0.08	85.5±3.1	1	0.50

#### Molecule 2+SubPc

Substrate			a[nm]	b[nm]	Angle a-b [°]	Molecules/ Unit Cell	Molecule Density [Molecules/nm <sup>2</sup> ]
Cu(111)		SubPc mixed layer	2.45±0.21	3.41±0.09	79.7±3.3	1 Molecule 2 +2 SubPc	0.12 Molecule 2 +0.24 SubPc

Table 4: Overview of all assemblies that were detected in the project.

## Overview of the prepared samples

### Molecule 1

Sample Nr.	Version	Substrate	rate[ML/min]	d[ML]	Comment	Structures
3	a	Ag(111)	0.16	0.95		Porous network (hexagons)
	b	Ag(111)	-	0.95	annealed@150°C	Porous network (hexagons)
	c	Ag(111)	-	0.95	annealed@250°C	Porous network (hexagons)
	d	Ag(111)	-	0.95	annealed@300°C	Porous network (hexagons), small minority close packed
6	a	Ag(111)	0.66	0.8		Porous network (hexagons), Close packed assemblies
7	a	Ag(111)	0.16	0.55		Porous network (hexagons)
8	a	Ag(111)	0.56	0.25		no molecules observed
	b	Ag(111)	0.44	0.45		Porous network (hexagons), Close packed
	c	Ag(111)	0.17 SubPc	0.45 1+0.08 SubPc	<b>add SubPc</b>	Close packed (AgSub)
9	a	Ag(111)	0.14	0.7		Porous network (hexagons)
10	a	Ag(111)	0.13	0.6		Porous network (hexagons)
	b	Ag(111)	0.08 SubPc	0.6 1+0.02 SubPc	<b>add SubPc</b>	Porous network (hexagons)
	c	Ag(111)	0.05 SubPc	0.6 1+0.03 SubPc	<b>add SubPc</b>	Porous network (hexagons), some filled pores
	d	Ag(111)	0.06 SubPc	0.6 1+0.05 SubPc	<b>add SubPc</b>	Porous network (hexagons), some filled pores
11	a	Ag(111)	0.13	0.6		Porous network (hexagons)
	b	Ag(111)	0.07 SubPc	0.6 1+0.03 SubPc	<b>add SubPc</b>	Porous network (hexagons), Close packed (AgSub), some filled pores
1	a	Cu(111)	0-0.14	0-0.35	lost rate during deposition	no molecules observed
	b	Cu(111)	0.23	~0.55		Close packed (Cu1a)
	c	Cu(111)	0.20	~0.7		Close packed structures (Cu1b+Cu2?)
	d	Cu(111)	0.13	~1.2		Disordered and close packed
	e	Cu(111)	-	~1.2	annealed@250°C	Disordered and close packed
2	a	Cu(111)	0.21	0.7		Close packed structures
	b	Cu(111)	-	0.7	annealed@150°C	Close packed structures
	c	Cu(111)	-	0.7	annealed@200°C	no molecules observed
4	a	Cu(111)	0.15	0.7		Close packed structures
5	a	Cu(111)	1.09	1.05	LEED-Probe	Close packed (Cu1a), traces of second layer

## Molecule 2

Sample Nr.	Version	Substrate	rate[ML/min]	d[ML]	Comment	Structures
1	a	Ag(111)	0.18	0.55		Close packed
	b	Ag(111)	-	0.55	annealed@150°C	Close packed
4	a	Ag(111)	0.40	0.35		Close packed
2	a	Cu(111)	0.11	0.45		Porous network (triangles), small minority Close packed
	b	Cu(111)	0.46	1		Porous network (triangles), small minority Close packed
	c	Cu(111)	-	1	annealed@150°C	Porous network (triangles), small minority Close packed
	d	Cu(111)	-	1	annealed@300°C	only small ordered regions, no Porous network anymore
3	a	Cu(111)	0.52	0.00		Porous network (triangles), small minority Close packed
	b	Cu(111)	-	0.70	annealed@150°C	Porous network (triangles), Close packed high coverage
5	a	Cu(111)	0.55	0.55		Porous network (triangles), small minority Close packed
	b	Cu(111)	-	0.55	annealed@150°C	Porous network (triangles), small minority Close packed
	c	Cu(111)	0.11 SubPc	0.55 2+0.1 SubPc	<b>add SubPc</b>	SubPc on triangle network, SubPc mixed layer
6	a	Cu(111)	0.36	0.65		Close packed high coverage

Table 5: Overview of all samples which were prepared in the project.